Atmos. Chem. Phys. Discuss., doi:10.5194/acp-2016-563, 2016
Manuscript under review for journal Atmos. Chem. Phys.
Published: 21 July 2016

Atmospheric Chemistry and Physics Discussions

Current Understanding of the Driving Mechanisms for Spatiotemporal Variations of Atmospheric Speciated Mercury: A Critical Review

Huiting Mao[1*], Irene Cheng[2], and Leiming Zhang[2]

[1]Department of Chemistry, State University of New York College of Environmental Science and Forestry, Syracuse, NY 13210
[2]Air Quality Research Division, Science and Technology Branch, Environment and Climate Change Canada, 4905 Dufferin Street, Toronto, Ontario, M3H 5T4, Canada

[*]Corresponding author: hmao@esf.edu

Atmos. Chem. Phys. Discuss., doi:10.5194/acp-2016-563, 2016
Manuscript under review for journal Atmos. Chem. Phys.
Published: 21 July 2016

Atmospheric Chemistry and Physics Discussions

Abstract

Understanding of spatial and temporal variations of atmospheric speciated mercury can advance our knowledge of mercury cycling in various environments. This review summarized spatiotemporal variations of total gaseous mercury or gaseous elemental mercury (TGM/GEM), gaseous oxidized mercury (GOM), and particulate-bound mercury (PBM) in various environments including oceans, continents, high elevation, the free troposphere, and low to high latitudes. In the marine boundary layer (MBL), the oxidation of GEM was generally thought to drive the diurnal and seasonal variations of TGM/GEM and GOM in most oceanic regions, leading to lower GEM and higher GOM from noon to afternoon and higher GEM during winter and higher GOM during spring-summer. At continental sites, the driving mechanisms of TGM/GEM diurnal patterns included surface and local emissions, boundary layer dynamics, GEM oxidation, and mountain-valley winds at high elevation sites. Oxidation of GEM and entrainment of GOM from the free troposphere influenced the diurnal patterns of GOM at continental sites. No pronounced diurnal variation was found for Tekran measured PBM at MBL and continental sites. Seasonal variations in TGM/GEM at continental sites were attributed to increased winter combustion, increased surface emissions during summer, and monsoons in Asia. GEM oxidation, free tropospheric transport, anthropogenic emissions, and wet deposition appeared to affect the seasonal pattern of GOM at continental sites. Since measurements were predominantly in the northern hemisphere (NH), increased PBM at continental sites during winter was primarily due to local/regional coal combustion and wood burning emissions. Long-term TGM measurements from the MBL and continental sites indicated an overall declining trend consistent with those of anthropogenic and natural emissions and potentially redox chemistry. The latitudinal gradient in TGM/GEM showed an increase from

Atmos. Chem. Phys. Discuss., doi:10.5194/acp-2016-563, 2016
Manuscript under review for journal Atmos. Chem. Phys.
Published: 21 July 2016

Atmospheric Chemistry and Physics Discussions

the southern to northern hemisphere due largely to the vast majority of Hg emissions in the NH. This gradient was insignificant during summer probably as a result of stronger meridional mixing. Aircraft measurements indicated no significant GEM gradient with altitude over the field campaign regions; however depletion of GEM was observed in air masses under stratospheric influence. Remaining questions and issues related to factors potentially contributing to the observed spatiotemporal variations were identified, and recommendations for future research needs were provided.

1. Introduction

Atmospheric mercury (Hg) is a pervasive toxic with comparable natural and anthropogenic sources (UNEP, 2013). It is operationally defined in three forms, gaseous elemental mercury (GEM), gaseous oxidized mercury (GOM), and particulate-bound mercury (PBM). In most environments GEM comprises >95% of total gaseous mercury (TGM = GEM+GOM) with lifetime of 0.5 – 1 year (Driscoll et al., 2013). Besides emissions, GOM and PBM are largely formed from oxidation of GEM, with lifetimes of hours to weeks (Cole et al., 2014). They are highly soluble, and their wet and dry deposition is a major input of Hg to ecosystems and oceans followed by bioaccumulation, where Hg can enter human bodies through the food chain. To ultimately regulate anthropogenic emissions of Hg in order to control the ambient atmospheric concentration of Hg, it is imperative to understand Hg cycling between the atmosphere, ecosystems, and oceans.

The pathways of Hg cycling include chemical transformation and transport via air and water in various systems as illustrated in Subir et al. (2011). Mercury can be chemically

Atmos. Chem. Phys. Discuss., doi:10.5194/acp-2016-563, 2016
Manuscript under review for journal Atmos. Chem. Phys.
Published: 21 July 2016

Atmospheric Chemistry and Physics Discussions

transformed from one species to another through oxidation/reduction reactions, complex formation, phase transitions, biodegradation, and surface and heterogeneous interactions with aerosols, clouds, snow, and ice. Mercury can also be redistributed between geographic locations and spheres through physical processes such as wind, water runoff, dry and wet deposition, and volatilization. In addition, natural and anthropogenic sources of Hg are distributed vastly uneven as a result of anthropogenic activities and land surface types. The eventual effect of all these processes, some of which are in fact sinks, and sources is manifested in the great heterogeneity of temporal and spatial variations of atmospheric Hg concentrations observed in numerous studies (Sprovieri et al, 2010b, references therein; references in Tables S1 – S7 in the supplementary information (SI)). Characterization and intercomparison of such variations for different geographic and chemical environments can provide a gateway to our understanding of Hg cycling.

Numerous measurement studies in the literature have shown distinctly different spatiotemporal variations of GEM, GOM, and PBM in the following environments:

- Marine boundary layer
- Land: urban, rural, and remote
- High elevation, high altitude
- Low, mid-, and high latitudes

owing to their respective atmospheric chemical composition, sources, and meteorological conditions. In spite of our nebulous understanding of chemical transformation of atmospheric Hg, it is commonly thought that GEM is oxidized by halogen radicals (e.g., Br, BrO, ClO, BrCl), ozone (O_3), and hydroxyl radicals (OH) in gas and/or solid phase (Hynes et al., 2009, references therein). A more recent quantum calculation study suggested that more abundant radicals such as

Atmos. Chem. Phys. Discuss., doi:10.5194/acp-2016-563, 2016
Manuscript under review for journal Atmos. Chem. Phys.
Published: 21 July 2016

Atmospheric Chemistry and Physics Discussions

NO, NO_2, HO_2, ClO, or BrO could more readily oxidize GEM (Dibble et al., 2012). In springtime Antarctic and Arctic regions, where there were relatively more abundant halogen radicals, it was observed that GEM was depleted to very low levels accompanied by hundreds of picograms GOM (e.g., Schroeder and Munthe, 1998; Lindberg et al., 2002). The diurnal and seasonal variation of GEM, GOM, and PBM appeared to be highly correlated with that of BrO leading to the hypothesis of GEM oxidation by Br and BrO. In the marine boundary layer (MBL) over the Dead Sea and Cape point, South Africa, similar GEM depletion was also observed (Brunke et al., 2010; Obrist et al., 2011), which was hypothesized to be associated with GEM oxidation by bromine-related species (Obrist et al., 2011). In most marine environments, however, GEM depletion events have not been observed.

Over land, spatiotemporal variations of GEM, GOM, and PBM exhibited different characteristics from over the ocean. Also, they appeared to differ greatly from urban to remote areas, from the surface to the free troposphere, from low to high latitudes, from the northern to southern hemisphere, and between different geographic locations of the same environment type. For example, GEM concentrations in urban locations were often observed to peak during the day and dip at night, and reached annual maximums/minimums in spring-summer/fall-winter (e.g., Zhu et al., 2012; Lan et al., 2012), while opposite variations were observed in rural and remote locations (e.g. Mao and Talbot 2012). Over land GOM concentrations appear to reach daily peaks during the day and mostly below the limit of detection (LOD) at night (Mao and Talbot, 2012), whereas in marine locations nighttime GOM concentrations were found often above LOD (Mao and Talbot, 2012). The spatiotemporal variation in PBM concentration and size distribution appeared to be quite elusive, without generalized patterns, although more often than not large concentrations were found in winter (e.g., Mao and Talbot, 2012).

Atmos. Chem. Phys. Discuss., doi:10.5194/acp-2016-563, 2016
Manuscript under review for journal Atmos. Chem. Phys.
Published: 21 July 2016

Atmospheric Chemistry and Physics Discussions

Airborne measurements have suggested latitudinal variation in TGM with on average ~50 ppqv (~0.45 ng m^{-3} in a standard atmosphere) lower in the tropics than in the polar region in spring based on tropospheric data covering surface to 12 km altitude (Talbot et al., 2007, 2008; Mao et al., 2010). While TGM concentrations remained fairly constant with increasing height in the troposphere (Banic et al., 2003; Radke et al., 2007; Ebinghaus et al., 2007; Talbot et al., 2007, 2008; Mao et al., 2010), TGM/GEM was found to be depleted in stratospheric intrusion (Talbot et al., 2007; Radke et al., 2007). On the contrary, it has been postulated and modeled that very high concentrations of GOM were in the free to upper troposphere (Holmes et al., 2006), which has been on occasion measured with values up to 680 pg m^{-3} (Lyman and Jaffe, 2011; Brooks et al., 2014; Gratz et al., 2015; Shah et al., 2016) compared to often below 1 pg m^{-3} over land.

Such differences in spatiotemporal variations of speciated Hg were attributed to natural and anthropogenic sources of not only Hg but also other reactive chemical compounds that are involved in Hg cycling, meteorological conditions, and chemistry, all of which were highly dependent on geographic locations and surrounding land surface types. Therefore, it is highly complex to delineate the effects of controlling factors determining observed spatiotemporal variations of Hg concentrations. Sprovieri et al. (2010b) reviewed the state of global mercury measurements focusing on instrumentation and techniques, and ranges of concentration levels in studies from different continents and oceanic regions up to 2009. Atmospheric Hg research has since continued to flourish, and in particular longer datasets accumulated in multiple regions have become available for temporal variability characterization so as to understand the driving mechanism for such variabilities. Also of importance is the efficacy of emission reductions that have been implemented in North America and Europe for nearly two decades and over shorter

Atmos. Chem. Phys. Discuss., doi:10.5194/acp-2016-563, 2016
Manuscript under review for journal Atmos. Chem. Phys.
Published: 21 July 2016

Atmospheric Chemistry and Physics Discussions

periods in East Asia. This paper is, different from Sprovieri et al. (2010b), aimed to provide a global picture of spatiotemporal variations of speciated Hg using measurement-based studies in the literature over ocean, over land, by altitude, and by latitude, and further glean insight on important factors that could potentially contribute to the observed variations.

It should be noted that ***units were converted for a standard atmosphere*** for comparison. One more cautionary note is that Hg data in earlier studies had coarser temporal resolution than in more recent studies, and hence the comparisons should be viewed with this caveat in mind. Though the earlier studies tended to have orders of magnitude larger concentrations, suggesting at higher temporal resolution those concentrations would have been even larger.

2. Marine Boundary Layer

Measured TGM/GEM, GOM, and PBM concentrations in the marine boundary layer globally were summarized in Tables S1 – S3 of the supplementary information (SI). The MBL studies providing these measurement data were discussed by ocean/sea. For each ocean/sea, spatiotemporal variations in speciated Hg and the potential causes for these variations were summarized with respect to their ambient concentration levels, continental (including anthropogenic) influence, hemispheric gradient, diurnal to annual cycles, and long term trends, accompanied by discussions on potential causal mechanisms.

2.1 TGM/GEM

TGM and GEM in the MBL atmosphere have been measured since the late 1960s. Near the surface in most environments, except polar springtime and Dead Sea mercury depletion events (MDEs) when strong GEM oxidation occurs, the difference between TGM and GEM was small to negligible (e.g., Temme et al., 2003a; Mao and Talbot, 2012). Concentrations were generally higher in near-coastal regions due largely to anthropogenic influence, which under

Atmos. Chem. Phys. Discuss., doi:10.5194/acp-2016-563, 2016
Manuscript under review for journal Atmos. Chem. Phys.
Published: 21 July 2016

153 certain meteorological conditions could extend to even open oceans. Natural emissions
154 including biomass burning, volcanic, and oceanic emissions were suggested to be of influence in
155 some studies. It was also found that meteorological conditions could play important roles in
156 determining ambient concentrations of TGM/GEM via transport, PBL dynamics, and solar
157 radiation, especially in regions nearing emission sources such as the Mediterranean, and in
158 springtime Polar Regions. Long term trends have varied over different time periods, speculated
159 to be associated with changing anthropogenic and natural emissions.

160 2.1.1 Concentration Metrics

161 The mean concentrations of TGM/GEM reported from various studies ranged from 1.05
162 ng m^{-3} over the Antarctic Ocean to 2.34 ng m^{-3} over the West Pacific seas, as shown in Table S1
163 (references therein). The concentration averaged for each oceanic region over values reported
164 from the studies was the lowest 1.53 ng m^{-3} over the Antarctic Ocean and the largest 2.36 ng m^{-3}
165 over the West Pacific seas (**Fig. 1a**). The range over the Atlantic 0.05 – 29 ng m^{-3} (**Fig. 1a**),
166 obtained from individual studies, appeared to be the largest, although the maximum
167 concentration was from a single event influenced by forest fires in Quebec, Canada at a long
168 term site in the MBL 20 km from the coast of southern New Hampshire, USA (Mao and Talbot,
169 2012). In fact, the TGM/GEM concentrations were much more variable in the MBL of the
170 Mediterranean Sea and its nearby seas (Table S1; references therein).

171 Atmospheric Hg over the *Atlantic* Ocean has been studied most extensively compared to
172 other oceans, largely via shipboard measurements. Over the four decades of 1973 – 2013 from
173 the near-coastal to open waters over the Atlantic Ocean, concentrations of TGM/GEM ranged
174 from 0.05 ng m^{-3} (15-minute average) in Cape Point, South Africa (Brunke et al., 2010) to 29 ng
175 m^{-3} (5-minute average) near the shore of southern New Hampshire, USA (Mao and Talbot, 2012).

Atmos. Chem. Phys. Discuss., doi:10.5194/acp-2016-563, 2016
Manuscript under review for journal Atmos. Chem. Phys.
Published: 21 July 2016

Atmospheric Chemistry and Physics Discussions

In the earliest shipboard global study of atmospheric Hg, Seiler et al. (1980) found highly variable TGM concentrations (1 – 10 ng m^{-3}, 2-4 h average) averaged at 2.8 ng m^{-3} between Hamburg (54°N, 10°E) and Santo Domingo (20°N, 67°W) across the Atlantic Ocean over 11 October - 1 November 1973. During the following 40 years, most studies reported TGM/GEM ranging from below LOD to a few ng m^{-3} and higher concentrations in near-coastal regions (Table S1; references therein). The *first* time Hg species measured was a one month shipboard study over the South Atlantic Ocean during polar summer (February) 2001 by Temme et al. (2003b). Their measurements (5-min – 15-min average data) exhibited very small variation with TGM averaged at 1.1(±0.2) ng m^{-3} and no significant difference between TGM and GEM during the cruise from Neumayer to Punta Arenas. The mean concentrations over the South *Atlantic* hovered around 1 ng m^{-3} with standard deviation <0.3 ng m^{-3} compared to larger mean values (1.3 – ~3 ng m^{-3}) over the North Atlantic. Relatively homogeneous distributions of TGM/GEM were observed over open waters in the South *Atlantic*.

Atmospheric Hg over the *Pacific* Ocean has been studied since the 1960s. The oldest data over the Pacific Ocean are from Williston (1968), in the San Francisco Bay area (Los Altos) over a 2-year period in the early 1960s, with concentrations from the Pacific varying over 1 – 2 ng m^{-3}. Over the following five decades of studies, 1 - 15-min TGM/GEM concentrations measured over the North and South *Pacific* Ocean ranged from 0.3 ng m^{-3} over 40° – 45°N in July – September 2008 (Kang and Xie, 2011) to 7.21 ng m^{-3} in the Los Angeles Port on 27 May 2010 (Weiss-Penzias et al., 2013), with generally higher concentrations near coasts and lower ones over open oceans (Table S1; reference therein). The distribution of TGM/GEM over the South *Pacific* appeared to be quite heterogeneous, where Xia et al. (2010) measured TGM

Atmos. Chem. Phys. Discuss., doi:10.5194/acp-2016-563, 2016
Manuscript under review for journal Atmos. Chem. Phys.
Published: 21 July 2016

198 averaged at 2.20±0.67 ng m^{-3}, a factor of 2 higher than those in Sorensen et al. (2010) that
199 measured a mean of 1.03 ±0.16 ng m^{-3}.

200 Over the *South China Sea, the Yellow Sea,* and other neighboring seas, located on the
201 Eastern Asian continental margin in the tropical-subtropical western North Pacific, adjacent to
202 major atmospheric Hg emission source regions, elevated concentrations of TGM/GEM were
203 observed with mean values varying over 2.08 – 2.62 ng m^{-3} (Fu et al., 2010; Nguyen et al., 2011;
204 Ci et al., 2011) (Table S1). TGM concentrations measured over the *Mediterranean Sea, Adriatic*
205 *Sea, Dead Sea, Augusta Basin,* and *Baltic Sea* ranged from 0.4 to 11 ng m^{-3} (Table S1; references
206 therein).

207 There were a few studies on Hg over the *Indian* Ocean (Soerensen et al., 2010; Xia et al.,
208 2010; Witt et al.; 2010; Angot et al., 2014), showing a concentration gradient of TGM with
209 increasing concentrations at more northern locations closer to the inter-tropical convergence
210 zone (ITCZ), with a mean concentration of 1.24±0.06 ng m^{-3} in the Indian Ocean at latitudes
211 ranging from 9°S to 21°S (Witt et al., 2010).

212 Studies on TGM/GEM over the *Arctic* Ocean showed fairly constant concentrations of
213 TGM/GEM in January and August – December, MDEs in spring, and summertime annual
214 maximums (Lindberg et al., 2002; Aspmo et al., 2006; Sommar et al., 2010; Steffen et al., 2013;
215 Yu et al., 2014) . During the 1998 – 2001 Barrow Atmospheric Mercury Study (BAMS), daily
216 average GEM concentrations ranged from <0.2 ng m^{-3} to ~3.7 ng m^{-3}, averaged between 1.5 – 2
217 ng m^{-3} in January and mid-August – December (Lindberg et al., 2002). In summer 2004, 2005,
218 and 2012, means and ranges, well within the 1999 summertime range of Lindberg et al. (2002),
219 were measured by Aspmo et al. (2006), Sommar et al. (2010), and Yu et al. (2014) (Table S1).

Atmos. Chem. Phys. Discuss., doi:10.5194/acp-2016-563, 2016
Manuscript under review for journal Atmos. Chem. Phys.
Published: 21 July 2016

Different concentrations of GEM over sea ice (1.81±0.43 ng m^{-3}) vs. ice-free (1.55±0.21 ng m^{-3}) Arctic Oceanic waters were measured by Sommar et al. (2010) in summer 2005. In spring 2009 (14 – 26 March) a mean 5-min GEM concentration of 0.59 ng m^{-3} was measured with a range of 0.01–1.51 ng m^{-3} over sea ice on the Beaufort Sea near Barrow, Alaska, which appeared to be depleted compared to annual Arctic ambient boundary layer concentrations (Steffen et al., 2013).

In the *Antarctica*, the first study, conducted by de More et al. (1993), reported a mean TGM concentration of 0.55 (±0.28) ng m^{-3} and a range of 0.02 - 1.85 ng m^{-3} (24-48 h) at Ross Island during 1987 – 1989. Over November 2000 – January 2001, Sprovieri et al. (2002) reported a similar range but a mean of 0.9 (±0.3) ng m^{-3}, twice larger than that of de More (1993) a decade earlier. Similar means and ranges of TGM/GEM concentrations were measured by Ebinghaus et al. (2002b), Temme et al. (2003b), Soerensen et al. (2010), and Xia at al. (2010). Similar mean values but a much wider range (0.02 – 3.07 ng m^{-3}) were found in the multi-year dataset in Pfaffhuber et al. (2012) (Table 1).

2.1.2 Hemispheric Difference

Hemispheric gradient over the *Atlantic* Ocean has been reported since the 1980s, with higher concentrations in the North Atlantic attributed to anthropogenic and biomass burning emissions (Seiler et al, 1980; Slemr et al., 1981, 1985, 1995; Slemr and Langer, 1992; Fitzgerald et al., 1996; Lamborg et al., 1999; Temme et al., 2003a; Soerensen et al., 2010; Müller et al., 2012). Average TGM concentrations of 1.45 and 1.08 ng m^{-3} were measured in the Northern and Southern Hemisphere (NH, SH), respectively, in October – November 1973 (Seiler et al., 1980). Measurements from the same cruise paths from Hamburg (54°N) and Buenos Aires (35°S) in 1977, 1978 – 1980, 1992, and 1994 consistently showed TGM hemispheric difference, 1.56±0.32

Atmos. Chem. Phys. Discuss., doi:10.5194/acp-2016-563, 2016
Manuscript under review for journal Atmos. Chem. Phys.
Published: 21 July 2016

Atmospheric Chemistry and Physics Discussions

and 1.05±0.22 ng m^{-3} in the NH and SH, respectively, in 1977, increased to 2.25±0.41 and 1.50±0.30 ng m^{-3} followed by significant decreases to 1.79±0.41 and 1.18±0.17 ng m^{-3} in 1994 (Slemr et al., 1981, 1985, 1995; Slemr and Langer, 1992). The hemispheric difference averaged over fall 2006 and spring 2007, documented by Soerensen et al. (2010), with a NH average of 1.32±0.16 ng m^{-3} in summer and 2.61±0.36 ng m^{-3} in spring, and a SH average of 1.27±0.2 ng m^{-3}, was close to the 1978 – 1980 hemispheric gradient in Slemr et al. (1985) but lower than the 1990 value in Slemr and Langer (1992).

Hemispheric gradient in TGM/GEM concentrations over the *Pacific* has been reported with higher values in the Northern Hemisphere, mostly ascribed to its larger anthropogenic emissions (Seiler et al., 1980; Chand et al., 2008; Xia et al., 2010; Soerensen et al., 2010). Seiler et al. (1980) found average TGM concentrations of 1.45 ng m^{-3} and 1.08 ng m^{-3} in NH and SH, respectively, at 6-8 km altitudes over the *Pacific* Ocean in fall 1973. A close hemispheric gradient was found in October 1980 shipboard measurements from Fitzgerald et al. (1984) with a constant concentration 1.5 ng m^{-3} north of 4°N, a decrease to ~1 ng m^{-3} south of 10°S. Higher concentrations but similar magnitude of hemispheric difference of TGM was measured 34 years later in December 2007 by Xia et al. (2010) with a mean of 1.746±0.513 ng m^{-3} over the North Pacific and 1.471±0.842 ng m^{-3} over the South *Indian* Ocean (Note: their cruise passed through the South Indian instead the South Pacific). Around the same time, Soerensen et al. (2010) measured nearly twice lower concentrations over the South *Pacific* (1.11±0.11 ng m^{-3} along the Chilean Coast and up to 1.33±0.24 ng m^{-3} near East Australia) than the North *Atlantic* concentrations (mean values of 2.26 and 2.86 ng m^{-3} over 23°N – 59°N; no measurements over the North *Pacific* in the study) from the same study.

Studies found higher TGM concentrations up to ~2.3 ng m^{-3} over *the equatorial Pacific*

Atmos. Chem. Phys. Discuss., doi:10.5194/acp-2016-563, 2016
Manuscript under review for journal Atmos. Chem. Phys.
Published: 21 July 2016

Atmospheric Chemistry and Physics Discussions

266 in October 1980, markedly higher (>0.5 ng m^{-3}) than those outside this region, demonstrated to
267 be caused by upwelling, biological production, and anthropogenic emissions (Fitzgerald et al.,
268 1984; Kim and Fitzgerald, 1988). However, Wang et al. (2014) found no sustained high GEM
269 concentrations indicative of persistently enhanced biotic mercury evasion from the upwelling
270 region over the Galápagos Islands in the equatorial Pacific during February – October 2011.
271 They found GEM concentrations averaged at 1.08±0.17 ng m^{-3}, twice lower than the earlier ones,
272 and significant correlation between GEM and sea surface temperature (SST).

273 2.1.3 Temporal Variations from Diurnal Cycle to Long-term Trend

274 2.1.3.1 Diurnal variation

275 Over the *Atlantic* Ocean, diurnal variation in TGM with daily peaks of 5 ng m^{-3} at noon
276 and amplitude of 2-3 ng m^{-3} was observed across the North and South Atlantic in Seiler et al.
277 (1980) whereas none in Slemr et al. (1981, 1985) and Slemr and Langer (1992). Measurements
278 of TGM at Cape Point, South Africa (Brunke et al., 2010) and GEM at Appledore Island, Maine,
279 USA (Mao and Talbot, 2012) exhibited pronounced diurnal variation in summer with daily peaks
280 (minimums) before sunrise (in the late afternoon) and amplitude of 0.8 ng m^{-3} and ~10 ppqv
281 (~0.09 ng m^{-3}), respectively.

282 Over the *Pacific*, significant diurnal variation in TGM/GEM concentrations have been
283 measured (Fitzgerald et al., 1984; Weiss-Penzias et al., 2003, 2013; Kang and Xie, 2011; Wang
284 et al., 2014) with daily peaks ranging from 0.7 ng m^{-3} (5-min) over the Japan Sea (Kang and Xie,
285 2011) to 2.25 ng m^{-3} (unknown time resolution) in the equatorial region (Fitzgerald et al., 1984).
286 The most pronounced diurnal variation in TGM was reported in Fitzgerald et al. (1984) with
287 daily amplitude of 0.7 ng m^{-3} in the equatorial region (4°N – 10°S). In contrast, Laurier et al.

Atmos. Chem. Phys. Discuss., doi:10.5194/acp-2016-563, 2016
Manuscript under review for journal Atmos. Chem. Phys.
Published: 21 July 2016

Atmospheric Chemistry and Physics Discussions

(2003) found no diurnal variation during a cruise from Osaka, Japan to Honolulu, Hawaii over 1 May 2002 – 4 June 2002.

Diurnal variation in GEM over the *South China Sea* was observed in the cruise study by Tseng et al. (2012) over May 2003 – December 2005, especially in warm seasons, exhibited minimums before sunrise and maximums around solar noon with daily peaks reaching > 4 ng m^{-3} and amplitude of ~1 ng m^{-3}, close to Seiler et al. (1980). Note that this diurnal pattern is in agreement with Fitzgerald et al. (1984) and Wang et al. (2014) but opposite of what was observed in Weiss-Penzias et al. (2003, 2013), Brunke et al. (2010), and Mao and Talbot (2012).

Over the *Arctic* diurnal variation of GEM was observed by Lindberg et al. (2002) with noontime minimums in spring and summer, diurnal amplitude ~2 ng m^{-3} on a typical day in January – June. On the other hand, the shipboard measurements from Sommar et al. (2010) suggested very small near none diurnal variation. Similarly, no diurnal variation was found over the *Antarctica* (Pfaffhuber et al., 2012), except one case with influence of in situ human activity.

2.1.3.2 Seasonal to Annual Variation

Annual cycles of TGM/GEM were reported over *the Atlantic* in the both hemispheres. Annual cycles with an annual maximum in January and February (austral summer) and a minimum in austral winter and average amplitude of 0.134 ng m^{-3} were observed at Cape Point, South Africa (Slemr et al., 2008; Brunke et al., 2010). Opposite annual variation with higher (lower) concentrations in winter (summer) was reported from measurements over the North Atlantic, such as Mace Head (amplitude 0.097 ng m^{-3}), a remote site on the west coast of Ireland adjacent to the North Atlantic (Ebinghaus et al., 2002a) and the Appledore Island (25 ppqv, i.e. ~0.2 ng m^{-3}) site in Mao and Talbot (2012). Significant seasonal variation in NH with an annual minimum in July and maximum in January – March and amplitude of 0.3 – 0.4 ng m^{-3},was

Atmos. Chem. Phys. Discuss., doi:10.5194/acp-2016-563, 2016
Manuscript under review for journal Atmos. Chem. Phys.
Published: 21 July 2016

311 measured in a global cruise (Soerensen et al., 2010), in close agreement with Ebinghaus et al.
312 (2002b; 2011), Sigler et al. (2009a), and Mao and Talbot (2012).

313 Average seasonal difference of 0.19 ng m^{-3} GEM concentrations over the *Pacific* were
314 observed by Wang et al. (2014) with the highest and most variable concentrations over February
315 – May 2011 and the lowest and least variable in October over the Galápagos Islands during 12
316 November 2011 – 11 December 2011. In contrast, a *lack* of seasonal variation in GEM was
317 reported by Weiss-Penzias et al. (2003) using a subset of data of marine origin extracted from
318 one year speciated Hg data (May 2001 – May 2002) at the Cheeka Peak Observatory on the east
319 coast of the Pacific. This was uncharacteristic of midlatitudinal northern hemispheric sites, but
320 significant interannual variation was noted in this study.

321 Distinct annual variation in GEM over the *South China Sea* was observed in the cruise
322 study by Tseng et al. (2012) over May 2003 – December 2005. The winter maximum was
323 5.7±0.2 ng m^{-3} and summer minimum 2.8±0.2 ng m^{-3}, 2-3 times higher than global background
324 levels. Difference of 0.4 ng m^{-3} in seasonal average GEM was quantified with higher
325 concentrations in the summer than in the autumn over the Adriatic Sea (Sprovieri et al., 2010)
326 and a factor of two less over the Augusta Basin (Bagnato et al., 2013). The study by Obrist et al.
327 (2011) was the first to show the occurrence of mercury depletion events (MDEs) in midlatitudes
328 most frequently in summer, with GEM down to 22 ppqv (0.2 ng m^{-3}) in the boundary layer of the
329 Dead Sea, as opposed to MDEs, as commonly known, occurring in the springtime Arctic and
330 Antarctic only.

331 Annual variation of GEM over the *Indian* Ocean were reported in Angot et al. (2014)
332 with higher concentrations in winter (1.06±0.09 ng m^{-3}) and lower in summer (1.04±0.07 ng m^{-3}),

Atmos. Chem. Phys. Discuss., doi:10.5194/acp-2016-563, 2016
Manuscript under review for journal Atmos. Chem. Phys.
Published: 21 July 2016

opposite of those at Cape Point (Slemr et al., 2008) and Galapagos Islands (Wang et al., 2014) with annual amplitude an order of magnitude smaller.

Annual maximum concentrations of GEM occurred in summer over the *Arctic* Ocean and frequent MDEs with GEM depleted to near zero in spring (Lindberg et al., 2002; Aspmo et al., 2006; Cole et al., 2013; Moore et al., 2013). Lindberg et al. (2002) observed GEM concentrations up to 4 ng m^{-3} in June 2000 compared to 1.82±0.24 ng m^{-3} in summer 2004 (Aspmo et al., 2006) and 1.23±0.61 ng m^{-3} in summer 2012 (Yu et al., 2014).

Seasonal variation in *Antarctic* Hg suggested large variation in TGM/GEM in spring due to the occurrence of MDEs. The longest continuous data record in the Antarctic started in February 2007 at the Norwegian Antarctic Troll Research Station (TRS) in Queen Maud Land near the Antarctic coast (Pfaffhuber et al., 2012). Concentrations were fairly constant hovering at ~1 (±0.07) ng m^{-3} in late fall through winter and highly variable ranging from 0.02 to 3.04 ng m^{-3} averaged at 0.86 (±0.24) ng m^{-3} in spring and summer (Pfaffhuber et al., 2012), close to the values from 6 years earlier in Sprovieri et al. (2002) and Temme et al. (2003b).

2.1.3.3 Long-term Trends

North *Atlantic* long-term trends in TGM varied during different time periods of the past decades. An increasing rate of 1.46±0.17% yr^{-1} in TGM concentrations from 1970 to 1990 (Slemr and Langer, 1992) was followed by a 22% decrease from 1990 to 1994 (Slemr et al., 1995) according to the measurements spanning latitudes over the Atlantic from Hamburg, Germany to Punta Arenas, Chile. In similar latitudinal coverage but over a wider longitudinal span during three cruises in September – November 1996, December 1999 – March 2000, and February 2001 (Temme et al., 2003a), TGM concentrations were averaged at 1.26 (±0.1) ng m^{-3} ranging from 0.76 to 1.84 ng m^{-3}, comparable to the 1977 – 1980 (Slemr et al., 1985) and 1994

Atmos. Chem. Phys. Discuss., doi:10.5194/acp-2016-563, 2016
Manuscript under review for journal Atmos. Chem. Phys.
Published: 21 July 2016

356 concentrations (Slemr et al., 1995) but lower than the 1990 ones (Slemr et al., 1992). Over
357 September 1995 – December 2001, a slight increase (4%) in TGM was observed at Mace Head
358 (Ebinghaus et al., 2002a). In the South Atlantic at Cape Point a small but significant decrease
359 was reported in TGM annual median from 1.29 ng m^{-3} in 1996 to 1.19 ng m^{-3} in 2004 (Slemr et
360 al., 2008).

361 As long-term continuous measurement data of Hg had been accumulated, studies
362 examined decadal trends in atmospheric TGM/GEM concentrations. A decreasing trend of -
363 0.034±0.005 ng m^{-3} yr^{-1} in TGM was measured at Cape Point, South Africa over 1996 – 2008
364 (Slemr et al., 2011). During the same time period, a statistically significant decreasing trend of -
365 0.028± 0.01 ng m^{-3} yr^{-1} (~1.6-2.0% yr^{-1}) in TGM over the North *Atlantic* was reported by
366 Ebinghaus et al. (2011) using data from Mace Head, Ireland. For the same site Weigelt et al.
367 (2015) presented a decreasing trend of -0.016 ± 0.002 ng m^{-3} yr^{-1} in monthly median marine
368 GEM concentrations over a longer period February 1996 to December 2013. A steep 1990–2009
369 decline of -0.046±0.010 ng m^{-3} yr^{-1} (-2.5% yr^{-1}) was found in TGM over the North Atlantic
370 (steeper than at NH land sites) but no significant decline over the South Atlantic (Soerensen et al.,
371 2012). A recent comparison by Slemr et al. (2015) found smaller trends during shorter time
372 periods and a possible increasing trend at Cape Point for the period 2007–2013, qualitatively
373 consistent with the trend changes observed at Mace Head (Weigelt et al., 2015).

374 Over the *Arctic* Ocean, weak or insignificant declines in TGM at rates of -0.007±0.019
375 and 0.003±0.012 ng m^{-3} yr^{-1} were found at Alert and Zeppelin, respectively, during 2000 – 2009,
376 significantly smaller than the trends at midlatitude sites (Cole et al., 2013; Berg et al., 2013;
377 Ebinghaus et al., 2011; Slemr et al., 2011; Soerensen et al., 2012; Weigelt et al., 2015).
378 TGM/GEM concentrations over the *Antarctic* Ocean appeared to have increased from the 1980s

Atmos. Chem. Phys. Discuss., doi:10.5194/acp-2016-563, 2016
Manuscript under review for journal Atmos. Chem. Phys.
Published: 21 July 2016

379 to the 2000s (Ebinghaus et al., 2002b; Temme et al., 2003b; Soerensen et al., 2010; Xia et al.,
380 2010; Pfaffhuber et al., 2012). However, no significant trend in the *Antarctic* Ocean could be
381 detected in mercury concentrations over 2007 – 2013 (Slemr et al., 2015).

382 2.1.4 Mechanisms Driving the Observed Temporal Variabilities

383 2.1.4.1 Causes for Episodic Higher Concentrations

384 It has been hypothesized that anthropogenic, biomass burning, and volcanic emissions
385 caused higher concentrations over open waters and near-coastal regions in many cases. Such
386 influences on the atmospheric concentration of Hg was demonstrated using backward trajectories
387 and correlations of TGM/GEM with carbon monoxide (CO), ^{222}Rn, black carbon, sulfur dioxide
388 (SO_2), and dimethylsulfide (DMS) (Williston, 1968; Seiler et al., 1980; Fitzgerald et al., 1981;
389 Fitzgerald et al., 1984; Kim and Fitzgerald, 1988; Slemr et al., 1981; Slemr et al., 1985; Slemr
390 and Langer, 1992; Slemr, 1996; Lamborg et al., 1998; Sheu and Mason, 2001; Laurier and
391 Mason, 2007; Soerensen et al., 2010; Mao and Talbot, 2012; Müller et al., 2012; Xia et al., 2010;
392 Chand et al., 2008; Kang and Xie, 2011; Weiss-Penzias et al., 2013; Fu et al., 2010; Nguyen et
393 al., 2011; Ci et al., 2011). Some studies also suggested that oceanic evasion was an important
394 source contributing to higher concentrations (Seiler et al., 1980; Sigler et al., 2009b), while
395 others thought otherwise (Slemr et al., 1981, 1985; Slemr and Langer, 1992). Strong
396 photoreduction could have caused higher TGM/GEM concentrations under favorable
397 meteorological conditions (Pirrone et al., 2003; Sprovieri et al., 2003; Sprovieri and Pirrone,
398 2008). These influences often occurred in multitude simultaneously leading to elevated ambient
399 Hg concentrations.

400 For instance, GEM concentrations averaged at 2.86 ng m^{-3} over the Sargasso Sea and the
401 Atlantic legs during March – April 2007 were speculated to be due to oceanic evasion and

Atmos. Chem. Phys. Discuss., doi:10.5194/acp-2016-563, 2016
Manuscript under review for journal Atmos. Chem. Phys.
Published: 21 July 2016

anthropogenic influence (Soerensen et al., 2010). Mainland, ship, and volcanic emissions appeared to elevate low concentrations of 5-min TGM in the northern Japan Sea, mostly <0.5 ng m^{-3}, to ~7 ng m^{-3} concurrent with peaks in CO and SO_2 at Nome Harbor of America (Kang and Xie, 2011). Higher TGM concentrations over the Mediterranean Sea, Adriatic Sea, Dead Sea, Augusta Basin, and Baltic Sea were suggested to have resulted from anthropogenic influence and oceanic evasion (Pirrone et al., 2003). The anthropogenic contribution was corroborated in Bagnato et al. (2013), who suggested that the basin was a receptor for Hg from intense industrial activity with an emission flux of 0.004 t yr^{-1}. The role of natural emissions was underscored in an overview of studies on Hg in the Mediterranean Sea region covering field campaigns from 2000 to 2007 (Kotnik et al., 2014). The sunny, warm and dry climate with lower amounts of precipitation in the region was conducive to photoreduction of oxidized Hg in water column leading to strong oceanic evasion contributing to higher TGM concentrations in the Mediterranean Sea Basin (Pirrone et al., 2003; Sprovieri et al., 2003; Sprovieri and Pirrone, 2008).

2.1.4.2 Diurnal Variation

Nearly in all studies diurnal variation was found to be most pronounced in warm seasons, i.e. spring and/or summer. Different combinations of oceanic emissions, photooxidation, biological production, and meteorology were suggested to work together shaping the observed patterns in different oceanic regions. While the pattern with daytime peaks was attributed to oceanic emissions and biological production in sea water (Seiler et al., 1980; Fitzgerald et al., 1984; Tseng et al.; 2012; Wang et al., 2014), the opposite pattern with daytime minimums was associated with photooxidation and meteorological conditions (Lindberg et al., 2002; Brunke et al., 2010; Mao and Talbot, 2012; Weiss-Penzias et al., 2003, 2013)

Atmos. Chem. Phys. Discuss., doi:10.5194/acp-2016-563, 2016
Manuscript under review for journal Atmos. Chem. Phys.
Published: 21 July 2016

Atmospheric Chemistry and Physics Discussions

425 Over the *Atlantic* Ocean, oceanic emissions, and photooxidation were speculated to shape
426 the diurnal variation of TGM/GEM (Seiler et al., 1980; Brunke et al., 2010). However, Mao et al.
427 (2012) suggested that the predominant effect of oceanic evasion on ambient GEM concentrations
428 was episodic, not necessarily diurnal, because they found, among all physical parameters, the
429 only significant correlation GEM had was with wind speed exceeding15 m s^{-1} at a marine
430 location, which occurred rather sparsely. This was corroborated by Sigler et al. (2009b)
431 suggesting enhanced oceanic evasion at a rate of ~7 ppqv hr^{-1} leading to 30 – 50 ppqv increases
432 in coastal and inland GEM concentrations in southern New Hampshire, USA during the April
433 2007 Nor'easter. Measurements of TGM at Cape Point, South Africa (Brunke et al., 2010) and
434 GEM at Appledore Island, Maine, USA (Mao and Talbot, 2012) exhibited pronounced
435 summertime diurnal variation with daily peaks (minimums) before sunrise (in the late
436 afternoon),which was speculated to be caused by daytime GEM oxidation by halogen radicals in
437 the marine environment.
438 Over the *Pacific*, significant diurnal variation in TGM/GEM concentrations have been
439 linked to biological production, photochemistry, and meteorology (Fitzgerald et al., 1984; Weiss-
440 Penzias et al., 2003, 2013; Wang et al., 2014). The most pronounced diurnal variation in TGM
441 in the equatorial area (4°N – 10°S) was demonstrated to be caused by biological production
442 (Fitzgerald et al., 1984). Diurnal variation with significantly higher nighttime concentrations
443 near the coast of Los Angeles was ascribed to the nighttime urban outflow (Weiss-Penzias et al.,
444 2013). Strong daytime photooxidation was speculated to have contributed to the marked diurnal
445 variation with nighttime maximums in summer and spring in Weiss-Penzias et al. (2003) and
446 Wang et al. (2014), respectively. In the study by Laurier et al. (2003) the lack of diurnal
447 variation was speculated to be caused by continuous evasion from surface water.

Atmos. Chem. Phys. Discuss., doi:10.5194/acp-2016-563, 2016
Manuscript under review for journal Atmos. Chem. Phys.
Published: 21 July 2016

GEM diurnal variation with minimums before sunrise and maximums around solar noon over the *South China Sea*, especially in warm seasons, was linked to oceanic evasion, which was supported by the concurrent measurements of dissolved elemental Hg (Tseng et al., 2012). The 100 m MBL height assumed for estimation appeared to be too low, indicating that other factors may have contributed to the diurnal pattern.

Noontime GEM minimums in spring and summer over the Summertime *Arctic* suggested photooxidation of GEM (Lindberg et al., 2002). On the other hand, the very small near none diurnal variation in GEM manifested in the shipboard measurements of Sommar et al. (2010) was speculated to result from low in situ oxidation of GEM. No diurnal variation was found over the *Antarctica* due possibly to lack of diurnally varying sources and sinks (Pfaffhuber et al., 2012), except one case with in situ human activity.

2.1.4.3 Seasonal to Annual Variation

Annual cycles of TGM/GEM in the MBL differed in various oceanic regions and were suggested to be driven predominantly by oceanic evasion, biomass burning, anthropogenic emissions, interhemispheric flux, and meteorological conditions (Slemr et al., 2008; Ebinghaus et al., 2002a,b; Sigler et al., 2009a; Brunke et al., 2010; Soerensen et al., 2010; Mao and Talbot, 2012; Angot et al., 2014; Wang et al., 2014). Over the Atlantic annual cycles of TGM/GEM with an annual maximum in summer and a minimum in winter at Cape Point, South Africa was hypothesized to be driven predominantly by the total emissions from oceans, biomass burning, and anthropogenic activities (Brunke et al., 2010), and the interhemispheric flux (Slemr et al., 2008; Brunke et al., 2010). *Opposite annual variation* with higher (lower) concentrations in winter (summer) was proposed to be largely determined by meteorology (Ebinghaus et al., 2002a, 2011) and photochemical oxidation of GEM (Mao and Talbot, 2012). The same annual cycle

Atmos. Chem. Phys. Discuss., doi:10.5194/acp-2016-563, 2016
Manuscript under review for journal Atmos. Chem. Phys.
Published: 21 July 2016

Atmospheric Chemistry and Physics Discussions

with higher concentrations in winter over the *Indian* Ocean (Angot et al., 2014), opposite of those at Cape Point (Slemr et al., 2008) and Galapagos Islands (Wang et al., 2014), was speculated to be a result of long range transport of air masses originated from biomass burning emissions in southern Africa during the winter months (July – September), and low GEM associated with southerly polar and marine air masses from the remote southern Indian Ocean. Higher concentrations of GEM in the summer over the *Adriatic Sea* (Sprovieri et al., 2010) and over the *Augusta Basin* (Bagnato et al., 2013) were suggested to be caused by the stagnant meteorological conditions in the former study and enhanced evasion from sea water in the latter.

Midlatitudinal MDEs were first reported by Obrist et al. (2011), which occurred in the MBL of the Dead Sea. The MDEs in the Dead Sea boundary layer were observed to be often concurrent with varying concentrations of bromine oxide (BrO) and high temperatures up to 45°C. Such high temperatures seemed to be contradictory to the general understanding that Br-initiated GEM oxidation tends to go forward under very cold conditions at temperature < -40°C. The authors suggested that Br species were the major oxidants of GEM during depletion events, in spite of constant high temperatures accompanied by sometimes low BrO concentrations.

Springtime large variation in *Arctic* and *Antarctic* TGM/GEM was suggested to be a result of the occurrence of MDEs. Polar MDEs have been generally linked to reactive Br-initiated GEM oxidation in spring when Br explosion occurs producing abundant reactive Br (Schroeder et al., 1998; Ebinghaus et al., 2002b; Lindberg et al., 2002; Temme et al., 2003b; Mao et al., 2010; Steffen et al., 2013; Moore et al., 2014). For Antarctic MDEs, Ebinghaus et al. (2002b) found a strong positive correlation between TGM and O_3 over August – October, accompanied by enhanced Global Ozone Monitoring Experiment (GOME) column BrO. Compared to Arctic MDEs, the first Antarctic MDE occurred about 1-2 months earlier, probably

Atmos. Chem. Phys. Discuss., doi:10.5194/acp-2016-563, 2016
Manuscript under review for journal Atmos. Chem. Phys.
Published: 21 July 2016

Atmospheric Chemistry and Physics Discussions

due to the lower latitude of the monitoring site and sea ice, the former allowing earlier sunrise and the latter conducive to Br/BrO formation. Temme et al. (2003b) found that the air masses reaching the station during MDEs had a maximum contact with sea ice (coverage >40%) over the South Atlantic Ocean, which was speculated to contain abundant reactive Br, released from sea salt associated with sea ice or sea salt aerosols.

Summertime annual maximums of GEM over the *Arctic* and *Antarctic* Ocean were generally associated with maximum exposed sea water after snow/ice melt (Lindberg et al., 2002; Aspmo et al., 2006; Soerensen et al., 2010; Cole et al., 2013; Moore et al., 2014) and were also in the Arctic with riverine input (Fischer et al., 2012) as well as with enhanced reduction by high chromophoric dissolved organic matter (CDOM) in river runoff (Yu et al., 2014). Soerensen et al. (2010) found a temperature decrease and wind coming along the Antarctica coast partly covered with sea ice corresponding to increases in GEM concentrations, which were speculated to be from reemission from snow covered surface or the release of dissolved gaseous mercury (DGM) in supersaturated environments exposed after ice melt. Lindberg et al. (2002) associated observed GEM concentrations up to 4 ng m^{-3} in June with enhanced evasion of GEM dissolved and from GOM reduction in snow. Aspmo et al. (2006) linked the summertime annual peak of GEM to >70% sea ice, possibly related to biotic reduction leading to higher concentrations of DGM in sea water binding more Hg and hence larger evasion in open leads in the sea ice. This hypothesis was further supported by Moore et al. (2014), who found coastal AMDEs in the springtime Arctic linked to sea-ice dynamics using backward trajectories, as well as by the model simulations of Dastoor and Durnford (2014). A different mechanism of riverine contribution was hypothesized in Fischer et al. (2012) using an atmosphere-ocean coupled model. Yu et al. (2014) observed high TGM concentrations concurrent with low salinity, CO, and high

Atmos. Chem. Phys. Discuss., doi:10.5194/acp-2016-563, 2016
Manuscript under review for journal Atmos. Chem. Phys.
Published: 21 July 2016

Atmospheric Chemistry and Physics Discussions

517 CDOM over the ice-covered central Arctic Ocean and speculated that the relatively high CDOM
518 concentrations associated with river runoff could enhance Hg^{2+} reduction. Moreover they related
519 the summer monthly variability in TGM concentrations to less chemical loss.

520 2.1.4.4 Long-term Trends

521 Varying trends in TGM/GEM different periods of the past decades were speculated to be
522 due largely to changes in anthropogenic emissions and at times natural emissions. A case in
523 point is the 1970 – 1990 1.46±0.17% yr^{-1} increasing rate of TGM concentrations (Slemr and
524 Langer, 1992) followed by a 1990 – 1994 22% decrease (Slemr et al., 1995) shown in the
525 measurements over the Atlantic from Hamburg, Germany to Punta Arenas, Chile. These trends
526 were attributed to changing anthropogenic emissions and possibly decreased natural emissions
527 associated with climate cooling in the wake of Pinatubo eruption. Ebinghaus et al. (2002a)
528 suggested that a slight increase (4%) in TGM at Mace Head over September 1995 – December
529 2001likely resulted from *increased* anthropogenic emissions. Soerensen et al. (2012) found that
530 sea surface water elemental Hg concentrations were decreasing at a rate of -5.7% yr^{-1} since 1999,
531 which might explain the steep 1990–2009 decline of -0.046±0.010 ng $m^{-}3$ yr^{-1} (-2.5% yr^{-1}) in
532 TGM over the North Atlantic. A recent comparison by Slemr et al. (2015) suggested that the
533 opposing trends over the periods of 1996–2004 (increasing) and 2004–2007 (possibly decreasing)
534 might have led to smaller trends at shorter time periods and an increasing trend at Cape Point for
535 the period 2007–2013.

536 Three *hypotheses* were made to explain these decadal decreasing trends. First, the global
537 decreasing trend was caused by decreased reemission of legacy mercury as a result of a
538 substantial shift in the biogeochemical cycle of Hg through the atmospheric, oceans, and soil
539 reservoirs, although exactly what may have caused this shift remained unexamined (Slemr et al.,

Atmos. Chem. Phys. Discuss., doi:10.5194/acp-2016-563, 2016
Manuscript under review for journal Atmos. Chem. Phys.
Published: 21 July 2016

2011). Conflicting evidence was found by Ebinghaus et al. (2011) for worldwide changing anthropogenic emissions, and hence the decreasing trends could not simply be attributed to decreasing anthropogenic emissions in some regions. They hypothesized that the decreasing trend was linked to increasing tropospheric O_3, and yet this speculation was negated by the plausibility of GEM oxidation by O_3 in the atmosphere. The third hypothesis, developed by Soerensen et al. (2012), was that, based on atmosphere-ocean coupled model simulations, the decreasing trend in TGM over the North Atlantic was caused by decreasing North Atlantic oceanic evasion driven by declining subsurface water Hg concentrations resulting from reduced Hg inputs from rivers and wastewater and from changes in the oxidant chemistry of the atmospheric MBL.

2.2 GOM and PBM

2.2.1 Concentration Metrics

The mean concentrations of GOM from individual studies varied from below LOD in several studies to 4018 pg m^{-3} (1-h) in the Dead Sea MBL from Obrist et al. (2011) and Moore et al. (2013), as shown in Table S2 (references therein). The GOM concentration averaged for each oceanic region based on values from the literature varied from 3 pg m^{-3} over the Atlantic to 40 pg m^{-3} over the Antarctic Ocean (**Fig. 1b**), and the largest range 0.1 – 4018 pg m^{-3} was over the Mediterranean Sea and its neighboring seas (**Fig. 1b**). Note that the small ranges in other oceanic MBL did not necessarily indicate less variability in GOM but merely a result of limited measurement data available (Table S2; references therein).

The mean concentrations of PBM from individual studies varied from below LOD in several regions to 394 pg m^{-3} (1-h) over the Beaufort Sea (Steffen et al., 2013) (Table S3; references therein). The PBM concentration averaged for each oceanic region based on values in

Atmos. Chem. Phys. Discuss., doi:10.5194/acp-2016-563, 2016
Manuscript under review for journal Atmos. Chem. Phys.
Published: 21 July 2016

Atmospheric Chemistry and Physics Discussions

the literature varied from 0.6 pg m^{-3} over the Indian to 394 pg m^{-3} over the Arctic Ocean (**Fig. 1c**). Due to limited numbers of studies in the Arctic, Antarctic and Indian Ocean MBL, no ranges were provided for each one of them. The ranges for the six oceans were not comparable as very few studies were available in some of them. However, the few studies available indicated that PBM concentrations were in most cases smaller and less variable than GOM.

The earliest shipboard measurements of GOM showed dimethyl mercury (DMM) concentrations of ≤0.1 ng m^{-3} comprising ≤10% of TGM in clean marine air as opposed to 0.4 – 15.3 ng m^{-3} in polluted air during the 1977 cruise (Slemr et al., 1981), and ranging between 0.02 and 0.12 ng m^{-3} (6-h) comprising <2% of TGM, during the 1978 – 1981 cruises across the *Atlantic* between Hamburg (50°N) and Buenos Aires (35°S) (Slemr et al., 1985). From the late 1990s to the 2010s generally GOM concentrations, instead of DMM, were measured and were mostly orders of magnitude smaller, except during MDEs when GOM concentrations could be on the order of magnitude of 10^2 pg m^{-3} (Table S2; references therein).

Same as GEM, GOM concentrations tended to be higher over the North than the South *Atlantic* and in near-coastal regions than open waters, and continental influence was detected at times over open waters (Temme et al., 2003b; Mason et al., 2001; Sheu and Mason, 2001; Mason and Sheu, 2002; Aspmo et al., 2006; Laurier and Mason, 2007; Sigler et al. 2009b; Mao and Talbot, 2012). 1-h GOM concentrations of 1 – 30 pg m^{-3} over the *South* Atlantic Ocean from Neumayer to Punta Arenas in February 2001 (Temme et al., 2003b) were 1 – 2 orders of magnitude smaller than the concentrations (1.38±1.30 pmol m^{-3}, i.e. ~300±280 pg m^{-3}) near Bermuda in September and December 1999 and March 2000 (Mason et al., 2001). However, at around the same time average values almost an order of magnitude smaller were reported at Bermuda (50±43 pg m^{-3}, a few pg m^{-3} to 128 pg m^{-3}) (Mason and Sheu, 2002) and at a US mid-

Atmos. Chem. Phys. Discuss., doi:10.5194/acp-2016-563, 2016
Manuscript under review for journal Atmos. Chem. Phys.
Published: 21 July 2016

586 Atlantic coastal site (40 pg m^{-3}) (Sheu and Mason, 2001). In comparison, at higher northern
587 latitudes (54°N – 85°N), GOM concentrations averaged at 2.5 pg m^{-3} varying from below LOD
588 to 22 pg m^{-3} were comparable to those over the South Atlantic. In the late 2000s at a North
589 Atlantic MBL site 25 km off the southern New Hampshire, US, GOM was averaged at 0.4 ppqv
590 (~3.6 pg m^{-3}) (0 – 22 ppqv, i.e. 0 – 196 pg m^{-3}, 2-h) for May – August 2007 (Sigler et al. 2009b)
591 and very close values from the 2007 –2010 dataset at the same site (Mao and Talbot, 2012).
592 These values were close to the open water and higher latitude concentrations (Aspmo et al., 2006;
593 Laurier and Mason, 2007), but one to two orders of magnitude lower than the early 2000s
594 measurements at close latitudes (Mason et al., 2001; Sheu and Mason, 2001; Mason and Sheu,
595 2002).

596 PBM concentrations (Table S3; references therein) of similar magnitude was measured
597 with an average of 1.9±0.2 pg m^{-3} over the May-June 1996 South and equatorial *Atlantic* cruise
598 (Lamborg et al., 1999) and 1.3 ± 1.7 pg m^{-3} (<0.5 pg m^{-3} (LOD) to 5.2 pg m^{-3}) in Bermuda, 30-40
599 times smaller than the concurrent weekly averaged GOM concentrations (Mason and Sheu, 2002;
600 Sheu, 2001). At higher North Atlantic latitudes, PBM concentrations were averaged at 2.4 pg m^{-3},
601 very close to the concurrent average GOM concentrations but with a factor of 4 smaller
602 varying range (below MDL to 6.3 pg m^{-3}) in summer 2004 (Aspmo et al., 2006). Mao and
603 Talbot (2012) reported PBM concentrations varying from 0.09 ppqv (0.8 pg m^{-3}) in winter 2010
604 to 0.52 ppqv (4.6 pg m^{-3}) in summer 2010 for the time period of spring 2009 to summer 2010.

605 During the 2000s decade, concentrations of GOM over the *Pacific* decreased by around a
606 factor of 2 from the mean value of 9.5 pg m^{-3} over open waters in 2002 (Laurier et al., 2003) to
607 around 4 pg m^{-3} at a remote Japanese site downwind of major Asian source regions in spring
608 2004 (Chand et al., 2008) and in the equatorial region in 2011 (Wang et al., 2014) (Table 2;

Atmos. Chem. Phys. Discuss., doi:10.5194/acp-2016-563, 2016
Manuscript under review for journal Atmos. Chem. Phys.
Published: 21 July 2016

609 references therein). The maximum concentration from a decade of studies was 700 pg m^{-3} (3-h), ,
610 measured in air masses originated from upper air over the Pacific (Timonen et al., 2013), about
611 two orders of magnitude larger than what Chand et al. (2008) and Laurier et al. (2003) reported.
612 PBM concentrations over the *Pacific* reached up to 17 pg m^{-3} and mean values were three
613 times larger downwind of East Asia (3.0±2.5 pg m^{-3}) than in the equatorial Pacific MBL (Chand
614 et al., 2008; Wang et al., 2014) (Table S3). Chand et al. (2008) found PBM concentrations
615 comparable to GOM.
616 In the southern *Indian* Ocean, very low GOM and PBM concentrations, averaged at 0.34
617 (<LOD (0.28 – 0.42 pg m^{-3}) – 4.07 pg m^{-3}) and 0.67 pg m^{-3} (<LOD – 12.67 pg m^{-3}), respectively,
618 were measured by Angot et al. (2014) over two years from a remote location, Amsterdam Island.
619 These concentrations were at the lower end of the range of MBL measurements from over the
620 Atlantic and the Pacific (Laurier et al., 2003; Temme et al., 2003b; Laurier and Mason, 2007).
621 Measurements over the *Mediterranean Sea and its neighboring seas* generally showed
622 much higher concentration levels than over the Atlantic, Pacific, and Indian Ocean, with GOM
623 ranging from 0.1 pg m^{-3} over the Adriatic (Sprovieri and Pirrone, 2008) to 4018 pg m^{-3} over the
624 Dead Sea (Obrist et al., 2011) (Tables S2 &S3; references therein). Frequency distributions of
625 24-hour average GOM and PBM concentrations from Palma de Mallorca, a site situated in the
626 Mediterranean MBL, exhibited log-normal distributions with the maximum frequency at around
627 59 and 48 pg m^{-3}, respectively (Pirrone et al., 2003). One of the major findings from Sprovieri et
628 al. (2003) was constant presence of GOM averaged at 7.9±0.8 pg m^{-3} in the MBL over a 6000
629 km long cruise path around the Mediterranean Sea. In a one year dataset of 2008, Beldowska et
630 al. (2012) showed 24-h PBM concentrations varied over 2 – 142 pg m^{-3} averaged at 20 (±18) pg
631 m^{-3} with 93% on average in the coarse fraction (>2 μm) over the southern *Baltic* Sea.

Atmos. Chem. Phys. Discuss., doi:10.5194/acp-2016-563, 2016
Manuscript under review for journal Atmos. Chem. Phys.
Published: 21 July 2016

In springtime *Arctic*, the highest concentrations of GOM at 900 – 950 pg m^{-3} were observed during the 1998 – 2001 Barrow Atmospheric Mercury Study (BAMS). Very high springtime PBM concentrations (mean 394 pg m^{-3}, 47 – 900 pg m^{-3}, 1-h) were reported over Beaufort Sea sea ice by Steffen et al. (2013). This was an order of magnitude higher than concurrent GOM concentrations (mean 30 pg m^{-3}, 3.5 – 104.5 pg m^{-3}) and even larger than those in temperate regions, where particle concentrations tended to be. In comparison, Sommar et al. (2010) found very low GOM and PBM over the summertime Arctic Ocean.

Two *Antarctic* DMM measurement studies conducted by de More et al. (1993) and Pongratz and Heumann (1999) differed by two orders of magnitude with a mean of 0.04 (±0.06) ng m^{-3} over a range of 0 – 0.63 ng m^{-3} (24-48 h) at Ross Island from the former, speculated to be under anthropogenic influence and a mean of 6 pg m^{-3} over a range of <4 – 9 pg m^{-3} over the Antarctic Ocean from the latter (Table 2). Total 2-h GOM concentrations ranged over 10.5 – 334 pg m^{-3} averaged at 116.2(±77.8) pg m^{-3} in 2000 spring – summertime in Terra Nova Bay (Sprovieri et al., 2002), and a similar range was also observed by Temme et al. (2003b) at the Neumayer Station in summer 2001 (Table 2). A range of 30 – 140 pg m^{-3} (80-min) for peaks of GOM over the Antarctic Ocean in summer 2007 (Soerensen et al., 2010) coincided with small peaks of GEM, unlike Sprovieri et al. (2002) and Temme et al. (2003b) who also saw high peaks of GOM from the Antarctic Ocean but were anti-correlated with GEM. Concentrations of 1-h PBM over the *Antarctic* Ocean from Temme et al. (2003b) varied over 15 – 120 pg m^{-3}, a range a factor of 3 smaller than that of concurrent GOM and tracking GOM well only at a lower level.

2.2.2 Hemispheric Difference

Hemispheric gradient has been measured in both GOM and PBM since the early 1980s (Slemr et al., 1985; Soerensen et al., 2010). In the first shipboard study, Slemr et al. (1985)

Atmos. Chem. Phys. Discuss., doi:10.5194/acp-2016-563, 2016
Manuscript under review for journal Atmos. Chem. Phys.
Published: 21 July 2016

655 derived PBM concentrations of 0.013 ± 0.018 and 0.007 ± 0.004 ng m^{-3} over the North and
656 South *Atlantic* Ocean, respectively, from the Hg concentrations in rain water. About three
657 decades later Soerensen et al. (2010) reported hemispheric difference of GOM with a NH
658 average of 0.3±3 pg m^{-3} in summer and 0.8±2 pg m^{-3} in spring, and a seasonally invariable SH
659 average of 4.3±0.14 pg m^{-3}.

660 2.2.3 Temporal Variations from Diurnal to Long-term Trend

661 2.2.3.1 Diurnal Variation

662 While some studies found a lack of diurnal variation in GOM (Sheu and Mason, 2001;
663 Aspmo et al., 2006; Temme et al., 2003b), many studies reported pronounced diurnal variation in
664 various oceanic regions (Mason et al., 2001; Mason and Sheu, 2002; Lindberg et al., 2002;
665 Laurie et al., 2003; Sprovieri et al., 2003, 2010; Laurier and Mason, 2007; Mao et al., 2008;
666 Chand et al., 2008; Sigler et al., 2009b; Soerensen et al., 2010; Mao and Talbot, 2012; Wang et
667 al., 2014). In only one out of seven 24-hr GOM sampling sessions did Sheu and Mason (2001)
668 find diurnal variation of GOM, with daily peaks at noon, below LOD at night and amplitude of
669 nearly 100 pg m^{-3}. The studies reporting distinct diurnal variation over the Atlantic showed
670 consistent daytime peaks and nighttime minimums, with amplitude values varying from 0.27 pg
671 m^{-3} in winter 2010 near the coast of southern New Hampshire, USA (Mao and Talbot, 2012)
672 to >80 pg m^{-3} from Barbados via Bermuda to Baltimore, Maryland, USA (Mason and Sheu, 2002;
673 Laurier and Mason, 2007). Distinct diurnal variation in GOM was also measured over the
674 *Pacific* Ocean with noon - afternoon maximums and nighttime minimums and amplitude > 80 pg
675 m^{-3} (Laurier et al., 2003; Chand et al., 2008; Wang et al., 2014). Over the *Mediterranean* Sea
676 and its neighboring seas diurnal variation of GOM concentrations was shown in most studies
677 with daily peaks at noon and amplitude up to 35 pg m^{-3} (Sprovieri et al., 2003; Sprovieri et al.,

Atmos. Chem. Phys. Discuss., doi:10.5194/acp-2016-563, 2016
Manuscript under review for journal Atmos. Chem. Phys.
Published: 21 July 2016

678 2010). For the springtime Arctic Lindberg et al. (2002) measured noontime maximums of GOM
679 up to 900 – 950 pg m^{-3} and near zero concentrations at night.
680 The diurnal pattern of PBM concentrations, measured using a Tekran speciation unit, at a
681 midlatitude North *Atlantic* MBL site close to southern New Hampshire, USA was in general not
682 consistent between seasons and years with seasonally averaged daily peaks 0.2 – 0.7 ppqv (1.7 –
683 6.2 pg m^{-3}) at varying time of a day (Mao and Talbot, 2012). The Tekran PBM instrument
684 measures PBM on particles < 2.5 μm, which is naturally a fraction of total atmospheric PBM.
685 Using a 10-stage impactor, Feddersen et al. (2012), perhaps the first to study the size distribution
686 of PBM in MBL, reported PBM concentrations (up to 0.25 ppqv, i.e. 2.2 pg m^{-3}, in 3.3 – 4.7 μm)
687 in ten size fractions (<0.4 μm to >10 μm) for the same MBL location from Mao and Talbot
688 (2012), and found a diurnal cycle with daily maximums at around 16:00 UTC (noon local time)
689 and minimums around sunrise.
690 2.2.3.2 Seasonal to Annual Variation
691 Several studies reported distinct seasonal variation in GOM with higher concentrations in
692 warmer months and lower in colder months (Mason et al., 2001; Mason and Sheu, 2002; Pirrone
693 et al., 2003; Laurier and Mason, 2007; Sigler et al., 2009a; Sprovieri et al., 2010; Soerensen et al.,
694 2010; Mao and Talbot, 2012; Angot et al., 2014). For instance, Mason et al. (2001) found GOM
695 concentrations elevated in September (2.54 – 6.86 pmol m^{-3}) compared to those in December and
696 March (0.23 – 2.68 pmol m^{-3}) near Bermuda. At the midlatitude North *Atlantic* MBL site near
697 southern New Hampshire, USA, a fairly flat baseline with negligible annual variation in GOM
698 was observed in a three year dataset, with more variability in higher mixing ratios and seasonal
699 median values ranging from 0.03 ppqv (~0.27 pg m^{-3}) in winter 2010 to 0.55 ppqv (~4.9 pg m^{-3})
700 in summer 2007 (Mao and Talbot, 2012). The PBM measurements using a 10-stage impactor

Atmos. Chem. Phys. Discuss., doi:10.5194/acp-2016-563, 2016
Manuscript under review for journal Atmos. Chem. Phys.
Published: 21 July 2016

Atmospheric Chemistry and Physics Discussions

701 from Feddersen et al. (2012) showed distinct seasonal variation with 50-60% of PBM in coarse
702 fractions, 1.1 – 5.8 μm, composing largely of sea salt aerosols at both sites in summer and 65%
703 in fine fractions at the coastal site in winter.

704 In the equatorial *Pacific*, seasonal variation in PBM concentrations was observed with an
705 average of 1.1±1.1 pg m^{-3} in October and below LOD (0.42 pg m^{-3}) in June (Wang et al., 2014).
706 In the southern *Indian* Ocean, a slight but significant seasonal variation was found in GOM
707 concentrations averaged at 1.34±0.45 pg m^{-3} in winter vs. 1.58±0.35 pg m^{-3} in summer, while a
708 seasonal trend in PBM with significantly higher concentrations in winter than in summer
709 (2.18±1.56 ng m^{-3} vs. 1.79±1.15 pg m^{-3}) (Angot et al., 2014).

710 Over the *Mediterranean* Sea and its neighboring seas, seasonal variation in GOM
711 concentrations was found, 31.5±39.2 pg m^{-3} in November, 40.4±43 pg m^{-3} in February,
712 52.3±43.9 pg m^{-3} in May, and 32.3±17.8 pg m^{-3} in July (Pirrone et al., 2003), and the fall 2004
713 and summer 2005 campaigns experienced no production of GOM and little variation in GOM in
714 the fall and very high concentrations varying over 21 – 40 pg m^{-3} in the summer (Sprovieri et al.,
715 2010a). In the *Dead* Sea MBL, AMDEs resulting in 1-h GOM up to 700 pg m^{-3}occurred more
716 frequently in the summer (20 of 29 days) than in winter (8 of 20 days), the majority of which
717 were not concurrent with ozone depletion events (ODEs) (Obrist et al., 2011; Moore et al., 2013).
718 Two studies observed seasonal variation in PBM. Sprovieri et al. (2010a) found PBM
719 concentrations on average more than a factor of 2 higher during high Hg episodes in the fall than
720 during the summertime ones over the Mediterranean Sea. Beldowska et al. (2012) measured an
721 average 24-h PBM of 15 pg m^{-3} and a 3 – 67 pg m^{-3} range in the non-heating season compared to
722 an average of 24 pg m^{-3} and a range of 2 – 142 pg m^{-3} in the heating season.

Atmos. Chem. Phys. Discuss., doi:10.5194/acp-2016-563, 2016
Manuscript under review for journal Atmos. Chem. Phys.
Published: 21 July 2016

723 In the Arctic MBL, several hundreds of pg m^{-3} GOM concentrations were observed in
724 spring (Lindberg et al., 2002; Steffen et al., 2013), while in summer very low GOM and PBM
725 concentrations were measured (Sommar et al., 2010). Different from the Arctic, summertime
726 GOM concentrations over the *Antarctic* seemed to be orders of magnitude larger (Sprovieri et al,
727 2002; Temme et al., 2003b; Soerensen et al., 2010).

728 2.2.4 Mechanisms Driving the Observed Temporal Variabilities

729 2.2.4.1 Factors Causing Episodic High and Low Concentrations

730 Long range transport of air masses with high PBM concentrations of terrestrial origin was
731 suggested due to elevated crustal enrichment factors in the PBM samples (Lamborg et al., 1999).
732 An episode of high GOM concentrations coincided with a passing hurricane, which led to
733 speculation that downward mixing of air aloft with higher GOM (Prestbo, 1997) might have
734 contributed to those high concentrations (Mason and Sheu, 2002). Mason and Sheu (2002)
735 found low GOM concentrations concurrent with high humidity (e.g., fog) and rainfall but highest
736 concentrations on the day after such events if temperatures were elevated. High nighttime
737 concentrations of GOM in the Mediterranean Basin were observed in anthropogenic plumes
738 identified using backward trajectories (Sprovieri et al., 2010). The GOM concentrations in air
739 masses of marine origin at a site on the East Pacific coast were unusually high ranging over 200
740 – 700 pg m^{-3} (Timonen et al., 2013). The high GOM concentrations were thought to be
741 partitioned back from the PBM that was accumulated on aqueous super-micron sea salt aerosols
742 in the MBL when being lofted above the MBL, and an anticorrelation between GOM and GEM
743 was found in air masses of marine origin indicating strong in-situ oxidation of GEM.

744 2.2.4.2 Diurnal Variation

745 The lack of diurnal variation observed at a US eastern seaboard coastal location was

Atmos. Chem. Phys. Discuss., doi:10.5194/acp-2016-563, 2016
Manuscript under review for journal Atmos. Chem. Phys.
Published: 21 July 2016

speculated to result from diverse air masses with different concentrations converging at the location leading to the removal of diurnal variation in GOM (Sheu and Mason, 2001). In another case at higher latitudes it was thought be due to low solar radiation (<200 W m^{-2}) (Aspmo et al., 2006). The majority of the studies reporting significant diurnal variation in GOM attributed the diurnal pattern with daytime peaks and nighttime minimums to photooxidation, loss via dry deposition, and oceanic evasion, which was backed up by modeling studies (Hedgecock et al., 2003, 2005; Laurier et al., 2003; Selin et al., 2007; Strode et al., 2007).

It was generally found that GOM concentrations were positively correlated with solar radiation flux and anticorrelated with relative humidity and at times with O_3 (Mason and Sheu, 2002; Laurier and Mason, 2007; Soerensen et al., 2010; Mao et al., 2012). Mason and Sheu (2002) and Laurier and Mason (2007) pointed out that the correlation between GOM and UV radiation flux indicated photochemical processes, and the anticorrelation between GOM and O_3 was caused by processes destroying O_3 and producing GOM, with an emphasis on oxidation reactions in the presence of deliquescent sea salt aerosols based on the laboratory experimental study by Sheu and Mason (2004). The fact that the daytime peaks in GOM over the *Pacific* increased with less wind speed, which was conducive to less dry depositional loss, and strong UV radiation suggested that GOM was produced in situ via photochemically driven oxidation (Laurier et al., 2003; Chand et al., 2008). Chand et al. (2008) estimated the magnitude of GOM close to the amount produced from the reaction of GEM + OH alone. Mao and Talbot (2012) speculated unknown production mechanism(s) of GOM in the nighttime MBL keeping the levels above the LOD. Positive correlation was found between GOM/PBM and temperature, indicating possible temperature dependence of certain oxidation reactions and gas-particle partitioning (Mao et al., 2012). Mao et al. (2012) also found anti-correlation between GOM/PBM and wind

Atmos. Chem. Phys. Discuss., doi:10.5194/acp-2016-563, 2016
Manuscript under review for journal Atmos. Chem. Phys.
Published: 21 July 2016

speed, which was not found at the coastal and inland locations, indicating enhanced loss via deposition caused by faster wind speed over water.

The diurnal pattern of PBM, measured using a Tekran speciation unit, in general was not consistent from season to season as found in Mao and Talbot (2012), which indicated more complicated processes than photochemistry involved in PBM budgets. However, for the same MBL location in Mao and Talbot (2012), Feddersen et al. (2012) found diurnal variation in 10-stage impactor PBM measurement data and speculated that GEM oxidation drove the PBM daytime maximum at around 16:00 UTC (noon local time) and deposition to aerosol surface without replenishment led to the minimum around sunrise. In the same study, the large peaks of PBM appeared to be of continental origin.

2.2.4.3 Seasonal to Annual Variation

Larger concentrations of GOM in spring and/or summer were generally associated with stronger photooxidation, biological activity, biomass burning, oceanic, and anthropogenic emissions, whereas low concentrations could be due to wet deposition in the MBL of various oceanic regions (Lindberg et al., 2002; Mason and Sheu, 2002; Temme et al., 2003b; Pirrone et al., 2003; Sprovieri et al., 2003; Hedgecock et al., 2004; Laurier and Mason, 2007; Sprovieri and Pirrone, 2008; Sprovieri et al., 2010; Soerensen et al., 2010; Obrist et al., 2011; Mao et al., 2012; Angot et al., 2014; Wang et al., 2014). The positive correlation between GOM concentrations and solar radiation was used to explain warm season maximums of GOM based on the same line of reasoning that was used to explain daytime peaks of GOM (Mason and Sheu, 2002; Pirrone et al., 2003; Mao et al., 2012).

To explain the annual maximum GOM concentration in October over the *equatorial Pacific*, Wang et al. (2014) included iodine in a two-step mercury oxidation mechanism, where

Atmos. Chem. Phys. Discuss., doi:10.5194/acp-2016-563, 2016
Manuscript under review for journal Atmos. Chem. Phys.
Published: 21 July 2016

BrHgI was hypothetically formed, helped to reconcile the modelled GOM with the observations. The authors mentioned that HO_2 and/or NO_2 aggregation with HgBr from Dibble et al. (2012) would be another possibility and further suggested that a major process in representing Hg oxidation is missing in current models.

In the southern *Indian* Ocean, Angot et al. (2014) speculated that very low levels of GOM and PBM were likely due to very frequent scavenging drizzle, whereas high GOM events in summer were associated with enhanced photochemistry and biological activity and high PBM events in winter were related to peaking southern African biomass burning.

Over the *Mediterranean* Sea and its neighboring seas, it was generally thought that meteorological conditions combined with anthropogenic, oceanic, and biomass emissions could affect GOM and PBM concentrations and subsequently their seasonal variation (e. g. Pirrone et al., 2003; Sprovieri et al., 2003; Hedgecock et al., 2004; Sprovieri and Pirrone, 2008). For instance, the seasonal contrast of no production and little variation in GOM in fall 2004 and very high concentrations in summer 2005 was due likely to weather conditions (e.g., large liquid water content, rainy, overcast) in fall 2004 and strong oxidation in summer 2005 under dry, sunny conditions associated with a prevailing stagnant high pressure system over the region (Sprovieri et al., 2010). Sensitivity box model simulations suggested that the Hg + Br controlled the production rate of GOM without contributions from the oxidation reactions by O_3 and OH and that HgBr was quickly converted to GOM. In the same study it was brought to attention that biomass burning and ship emissions in the region were not included in the emission inventory but could be important to ambient concentrations (Sprovieri et al., 2010).

In the Dead Sea MBL, more frequent occurrences of MDEs in the summer (20 of 29 days) than in winter (8 of 20 days) were linked to higher BrO concentrations in summer (Obrist et al.,

Atmos. Chem. Phys. Discuss., doi:10.5194/acp-2016-563, 2016
Manuscript under review for journal Atmos. Chem. Phys.
Published: 21 July 2016

2011). It was speculated that the strong MDEs, despite high temperature and sometimes low BrO concentrations, were caused by Br-initiated oxidation of GEM based on their box model results. There is apparent discrepancy between our theoretical understanding of the conditions required for Br-initiated GEM oxidation and the real atmospheric conditions in the summertime Dead Sea MBL.

Two studies observed seasonal variation in PBM. Sprovieri et al. (2010a) found that PBM concentrations on average were more than a factor of 2 higher during high Hg episodes in the fall than during the summertime ones over the Mediterranean Sea due to anthropogenic influence. Beldowska et al. (2012) suggested that the higher concentrations in winter were a result of mild temperatures and high relative humidity in winter being conducive to Hg adsorption on the surface of coarse particles as well as condensation and coagulation of fine particles, while during the warm season the strong influence of industrial sources led to higher PBM concentrations on working days than on weekends.

Lindberg et al. (2002) found that springtime *Arctic* maximum concentrations of GOM at 900 – 950 pg m^{-3} corresponded to open leads over sea ice and an extensive area of elevated BrO concentrations under the calmest conditions and strongest UV radiation. Over Beaufort Sea sea ice in spring 2009 lower GOM compared to PBM concentrations and larger PBM concentrations than those in temperate regions were speculated to be caused by low temperatures and the availability of sea salt and sulfate aerosols, as well as ice crystals around the sea ice, which enabled GOM formation followed by adsorption onto particles resulting in the unusually high PBM concentrations over the sea ice (Steffen et al., 2013). In contrast, summertime Arctic GOM and PBM were very low due possibly to low in situ oxidation of GEM and enhanced physical scavenging of GOM/PBM as a result of high relative humidity and low visibility (Sommar et al.,

Atmos. Chem. Phys. Discuss., doi:10.5194/acp-2016-563, 2016
Manuscript under review for journal Atmos. Chem. Phys.
Published: 21 July 2016

838 2010).

839 Higher concentrations of GOM over the *Antarctic* Ocean were proposed by Sprovieri et
840 al. (2002) to be produced from gas-phase oxidation of GEM by O_3, H_2O_2, and OH together with
841 favorable physical conditions such as planetary boundary layer height and perhaps more so by
842 the latter. The highest concentrations of GOM corresponding to the lowest concentration falling
843 below the LOD (0.3 pg m^{-3}) during MDEs in summer were associated with the air masses having
844 a maximum contact with sea ice (coverage >40%) over the South Atlantic Ocean, which was
845 speculated to contain abundant reactive bromine, Br, released from sea salt associated with sea
846 ice or sea salt aerosols (Temme et al., 2003b). Summertime GOM was found to be correlated
847 with GEM due to in situ oxidation and build-up (Soerensen et al., 2010), and was also observed
848 to be anti-correlated with GEM due likely to oxidation solely (Temme et al., 2003b; Sprovieri et
849 al., 2002). Similar to *Arctic* MDEs, air masses during *Antarctic* MDEs appeared to have contact
850 with sea ice potentially entraining abundant halogen radicals before arriving at the monitoring
851 location. Different from the Arctic, summertime GOM concentrations over the Antarctic seemed
852 to be orders of magnitude larger.

853 **3. Continental Boundary Layer**

854 In this section, continental sites are defined as inland sites located in non-polar regions
855 and exclude locations impacted by the MBL, e.g. coastal sites and the ocean.

856 ***3.1 TGM/GEM***

857 3.1.1 Concentration Metrics

858 Field measurements of TGM/GEM at continental sites were conducted mainly in Asia,
859 Canada, Europe, and USA. Very few TGM/GEM measurements have been made at inland sites
860 in the southern hemisphere. Of all the four regions, the median concentrations of TGM or GEM

Atmos. Chem. Phys. Discuss., doi:10.5194/acp-2016-563, 2016
Manuscript under review for journal Atmos. Chem. Phys.
Published: 21 July 2016

were 1.6 ng m^{-3} at remote and rural surface (low elevation) sites, 2.1 ng m^{-3} at urban surface sites, and 1.7 ng m^{-3} at high elevation sites (**Fig. 2a**). TGM/GEM ranged over 0.1-11.3 ng m^{-3} at remote sites, 0.2-18.7 ng m^{-3} at rural sites, 0.2-702 ng m^{-3} at urban sites, and 0.6-106 ng m^{-3} at high elevation sites. Overall these statistics indicate that TGM/GEM at continental urban sites were higher and had larger variability than rural and remote surface sites and high elevation sites in the northern hemisphere. By geographical region (**Fig. 2b**), the median TGM/GEM in Asia, comprising of sites predominantly in China and a few sites in Korea and Japan, were higher by 26-55% than those in Europe, Canada, and USA in this respective order. Although a higher median TGM/GEM was found in Asia, the maximum single 5-min concentration was recorded in the USA (324 ng m^{-3}, Engle et al., 2010). The 5-min maximum TGM/GEM among the four regions was the lowest in Europe (23 ng m^{-3}, Witt et al., 2010). It is important to note that most urban sites in the literature are located in North America and Europe, and hence the higher TGM/GEM at continental urban sites as shown in Figure 2b were predominantly driven by measurements at those sites (instead of Asian sites). A summary of the mean and the range of TGM/GEM at individual continental sites can be found in Table S4. Statistics from studies prior to 2009 are referred to Sprovieri et al. (2010b).

3.1.2 Temporal Variations from Diurnal Cycle to Long-term Trends

3.1.2.1 Diurnal Variation

At *remote* surface locations, the diurnal variation of TGM/GEM is characterized by a daytime increase reaching a maximum concentration in the afternoon and nighttime decrease (Manolopoulos et al., 2007; Cheng et al., 2012). The ratio of the daily standard deviation to the daily mean was 3% in one study (Cheng et al., 2012). Diurnal variations were stronger during spring than other seasons (Cheng et al., 2012).

Atmos. Chem. Phys. Discuss., doi:10.5194/acp-2016-563, 2016
Manuscript under review for journal Atmos. Chem. Phys.
Published: 21 July 2016

Atmospheric Chemistry and Physics Discussions

At *rural* surface and *high elevation* sites, several different diurnal patterns have been reported. The first pattern, similar to remote surface locations, is an early morning minimum, followed by midday to afternoon maximum and decrease at night (Swartzendruber et al., 2006; Yatavelli et al., 2006; Choi et al., 2008, 2013; Fu et al., 2008, 2009, 2010, 2012b; Lyman and Gustin, 2008; Mao et al., 2008; Obrist et al., 2008; Faïn et al., 2009; Sigler et al., 2009; Mazur et al., 2009; Nair et al. 2012; Mao and Talbot, 2012; Eckley et al., 2013; Parsons et al., 2013; Cole et al., 2014; Brown et al., 2015; Zhang et al., 2015). The daytime peak was narrower during winter/fall and broader during spring/summer, similar to the seasonal pattern of daylight hours (Eckley et al., 2013). At elevated sites, the magnitude of this diurnal variation varies with season and location. The diurnal variation was more pronounced during spring at Mt. Gongga, China (Fu et al., 2008, 2009), fall/winter at Storm Peak Laboratory, USA (Faïn et al., 2009), summer at Mt. Changbai, China (Fu et al., 2012b), and winter/spring at Mt. Lulin, Taiwan (Sheu et al., 2010). The diurnal amplitude at Mt. Lulin ranged from 0.34 ng m^{-3} (Fall) to 0.62 ng m^{-3} (winter) or from 17-31%. The second diurnal pattern typically observed is a higher nighttime TGM/GEM than daytime. This tends to occur in Asia and more polluted sites outside of Asia, e.g. abandoned Hg mines and cement plants (Lyman and Gustin, 2008; Wan et al., 2009a; Rothenberg et al., 2010; Li et al., 2011; Nguyen et al., 2011; Fu et al., 2012a; Gratz et al., 2013; Zhang et al., 2013; Cole et al., 2014). In one instance, this diurnal pattern only occurred during winter/fall (Zhang et al., 2013). The third pattern found at rural surface and elevated sites is a weak or lack of diurnal pattern in TGM/GEM (Choi et al., 2008, 2013; Mao et al., 2008; Sigler et al., 2009; Engle et al., 2010; Rothenberg et al., 2010; Mao and Talbot, 2012; Zhang et al., 2013; Han et al., 2014). This pattern was more prominent in specific seasons, e.g. winter (Choi et al., 2008) and spring/summer (Zhang et al., 2013).

Atmos. Chem. Phys. Discuss., doi:10.5194/acp-2016-563, 2016
Manuscript under review for journal Atmos. Chem. Phys.
Published: 21 July 2016

Atmospheric Chemistry and Physics Discussions

907 At *urban* surface sites, the predominant diurnal pattern is an increase in TGM/GEM
908 throughout the night that leads to a maximum in the early morning and a decrease in TGM/GEM
909 in the afternoon (Stamenkovic et al., 2007; Li et al., 2008; Choi et al., 2009; Lyman and Gustin,
910 2009; Song et al., 2009; Liu et al., 2010; Witt et al., 2010; Nguyen et al., 2011; Nair et al., 2012;
911 Zhu et al., 2012; Gratz et al., 2013; Kim et al., 2013; Civerolo et al. 2014; Cole et al., 2014; Han
912 et al., 2014; Lan et al., 2014; Xu et al., 2014; Xu et al., 2015). The higher nighttime than
913 daytime pattern was observed during spring, summer, and fall in one study (Civerolo et al. 2014).
914 The diurnal amplitude was 24% of the daily mean in one study (Song et al., 2009). The diurnal
915 amplitude can also vary by 9.2-17.8% depending on the location within an urban area (Kim et al.,
916 2013). The diurnal amplitude tends to be higher during summer compared to other seasons
917 (Stamenkovic et al., 2007; Peterson et al. 2009; Civerolo et al. 2014; Lan et al., 2014; Xu et al.,
918 2014). Zhu et al. (2012) found a larger diurnal amplitude in the spring (3.7 ng m^{-3}) than winter
919 (0.9 ng m^{-3}). The timing of the TGM/GEM peak also changes between seasons. TGM decreased
920 earlier in the day during spring than in other seasons (Xu et al., 2014), while the maximum TGM
921 occurred later in the morning during spring than in other seasons (Zhu et al., 2012). Diurnal
922 variations with daytime maximum and early morning minimum have also been observed at urban
923 surface sites (Fostier and Michelazzo, 2006; Rothenberg et al., 2010; Witt et al., 2010; Jiang et
924 al., 2013; Han et al., 2014). During winter, some studies observed a less pronounced diurnal
925 variation in TGM/GEM (Choi et al., 2013; Civerolo et al., 2014).

926 3.1.2.2 Seasonal Variation

927 The seasonal variation in TGM/GEM at some continental *remote* surface sites can be
928 characterized by a winter to early-spring maximum and lower summer/fall concentrations
929 (Manolopoulos et al., 2007; Cheng et al., 2012). At other *remote* sites, a completely opposite

Atmos. Chem. Phys. Discuss., doi:10.5194/acp-2016-563, 2016
Manuscript under review for journal Atmos. Chem. Phys.
Published: 21 July 2016

Atmospheric Chemistry and Physics Discussions

930 seasonal pattern was found with higher summer/fall concentrations than winter/spring (Abbott et
931 al., 2008; Cole et al., 2014). These two seasonal patterns were also reported at *rural surface* and
932 *elevated* sites. The predominant seasonal TGM/GEM trend at rural surface and elevated sites is
933 the winter to spring maximum and summer/fall minimum (Zielonka et al., 2005; Yatavelli et al.,
934 2006; Choi et al., 2008; Fu et al., 2008, 2009, 2010; Mao et al., 2008; Sigler et al., 2009a; Mazur
935 et al., 2009; Engle et al., 2010; Mao and Talbot, 2012; Nair et al., 2012; Chen et al., 2013; Parson
936 et al., 2013; Cole et al., 2014; Marumoto et al., 2015). Other studies conducted in *rural* sites and
937 *elevated* sites found higher TGM/GEM during warm seasons (spring/summer) than in the winter
938 (Weiss-Penzias et al., 2007; Obrist et al., 2008; Nguyen et al., 2011; Eckley et al., 2013; Zhang
939 et al., 2013; Zhang et al., 2015). Additional seasonal patterns were observed at *high elevation*
940 sites, including higher TGM in summer/fall than winter/spring (Fu et al., 2012a) and a spring
941 maximum and summer minimum in another study (Sheu et al., 2010). The seasonal patterns at
942 continental *urban* surface sites can by vastly different from each other. They can be summarized
943 into the following five seasonal patterns: The first pattern is a winter to spring maximum
944 (Fostier and Michelazzo, 2006; Stamenkovich et al. 2007; Choi et al., 2009; Peterson et al., 2009;
945 Civerolo et al., 2014; Xu et al., 2015). The second pattern is a summer TGM/GEM maximum
946 (Xu and Akhtar, 2010; Jiang et al., 2013). The third pattern is higher TGM during both winter
947 and summer (Xu et al., 2014). The fourth type is higher TGM/GEM during spring/summer than
948 winter/fall (Liu et al., 2007, 2010; Song et al., 2009; Nair et al., 2012; Zhu et al., 2012; Hall et al.,
949 2014). The last type reported is an absence of a clear seasonal trend (Kim et al., 2013; Civerolo
950 et al., 2014; Marumoto et al., 2015). Table 1 summarizes the predominant diurnal and seasonal
951 patterns observed at rural, urban and high elevation continental sites.

952 3.1.2.3 Long-term Trends

Atmos. Chem. Phys. Discuss., doi:10.5194/acp-2016-563, 2016
Manuscript under review for journal Atmos. Chem. Phys.
Published: 21 July 2016

Atmospheric Chemistry and Physics Discussions

At *rural* sites across Canada, TGM decreased at a rate of 0.9-3.3% per year between 1995 and 2011. Depending on the location, the trend was determined using 5-15 years of TGM data (Cole et al., 2014). A GEM decrease of 0.056 ng m^{-3} yr^{-1} from 2005-2010 was found at an *elevated* site in New Hampshire (Mao and Talbot, 2012). Widespread declines in GEM across North America between 1997 and 2007 have also been reported (Weiss-Penzias et al., 2016); however, the trends were not determined separately for rural and urban sites. No significant trends in TGM were found at *urban/industrial* sites in the UK from 2003-2013 (Brown et al., 2015) and at another urban site in Seoul, Korea from 2004-2011 (Kim et al., 2013). However, a short-term annual TGM decrease from 2.0 to 1.7 ng m^{-3} was recorded at an urban site in Windsor, Canada from 2007-2009 (Xu et al., 2014). At a chlor-alkali site in the UK, TGM declined by 1.36 ± 0.43 ng m^{-3} yr^{-1} from 2003-2012 (Brown et al., 2015). Weigelt et al. (2015) determined annual TGM trends for different air masses arriving at Mace Head, Ireland between 1996 and 2013. Specifically for continental airflows, TGM decreased by 0.0240 ± 0.0025 ng m^{-3} yr^{-1} for polluted air masses from Europe, which was a slightly faster decline compared to marine airflows from the North Atlantic Ocean (-0.0209 ± 0.0019 ng m^{-3} yr^{-1}) and southern hemisphere (-0.0161 ± 0.0020 ng m^{-3} yr^{-1}). In certain months, the TGM decreases associated with local and European airflows (0.047-0.051 ng m^{-3} yr^{-1}) were greater than other months (Weigelt et al., 2015).

3.1.3 Mechanisms Driving the Observed Temporal Variabilities

3.1.3.1 Diurnal Variation of TGM/GEM

TGM/GEM was higher during daytime than nighttime and often declined to a minimum in the early morning at remote, rural, high elevation, and some urban surface sites (Table 1). One of the mechanisms driving this diurnal pattern involves meteorological parameters, such as

Atmos. Chem. Phys. Discuss., doi:10.5194/acp-2016-563, 2016
Manuscript under review for journal Atmos. Chem. Phys.
Published: 21 July 2016

temperature, the increase of which enhances TGM/GEM volatilization (Manolopoulos et al., 2007; Mao et al., 2012; Jiang et al., 2013; Han et al., 2014). Surface emissions of TGM can occur during daytime from soil and snow as temperature and solar radiation increases (Mao et al., 2012; Cole et al. 2014). Solar radiation minimizes the activation energy required for Hg emissions (Zhu et al., 2012) and increases Hg photoreduction in soil and snow (Steffen et al., 2008; Zhu et al., 2012; Hall et al., 2014; Xu et al., 2014; Xu et al., 2015). This process is especially relevant at sites with elevated Hg in soil (Lyman and Gustin, 2008; Brown et al., 2015) because of a larger flux gradient. Dry deposition of GEM in the night might also play a role since deposition was typically observed in nighttime in contrast to emission during daytime (Zhang et al., 2009). Fog or dew formation occurring in the late summer was believed to have caused GEM depletion in the early morning hours by capturing GEM in fog or dew water (Manolopoulos et al., 2007; Mao and Talbot, 2012). Another driving mechanism of this TGM/GEM diurnal pattern is the change in the boundary layer mixing height. Lower TGM/GEM during nighttime is due to TGM/GEM deposition as the nocturnal inversion layer forms. In the morning, the nocturnal inversion breaks down and mixes with TGM/GEM-rich air in the residual layer and subsequently leads to increasing TGM/GEM during the day (Yatavelli et al., 2006; Mao et al., 2008; Mazur et al., 2009; Mao and Talbot, 2012; Nair et al. 2012; Choi et al., 2008, 2013; Jiang et al., 2013; Cole et al., 2014). At elevated sites, there is a transition from the sampling of boundary layer during daytime to free troposphere air at night which is driven by mountain/valley atmospheric patterns (Obrist et al., 2008). During daytime, mountain breezes causes moist air to ascend from the surface to higher altitudes carrying with it GEM from the boundary layer (Swartzendruber et al., 2006; Obrist et al., 2008; Fu et al., 2010, 2012b; Zhang et al., 2015). At night, drier free troposphere air impacts the elevated site leading to lower GEM

Atmos. Chem. Phys. Discuss., doi:10.5194/acp-2016-563, 2016
Manuscript under review for journal Atmos. Chem. Phys.
Published: 21 July 2016

and water vapor and higher GOM and ozone (Obrist et al., 2008). The shift in prevailing wind directions also contributed to this higher daytime TGM diurnal pattern in one study (Fu et al., 2008, 2009). A lack of diurnal variability was also reported at some rural surface locations, although the driving mechanism is not quite clear. At an elevated site, the sampling of air above the nocturnal boundary layer and lack of anthropogenic sources or GEM oxidants near the site led to constant GEM during most of the time except in the summer (Mao et al., 2008; Sigler et al., 2009a; Mao and Talbot, 2012). Thus this differs from other mountain sites, which were affected by surface emissions and local/regional transport of GEM from the boundary layer during daytime.

At most urban sites and some elevated and polluted rural sites, the nighttime TGM concentrations were higher than daytime, and the maximum concentration typically occurred in the early morning before sunrise (Table 1). This type of diurnal variation is driven by nighttime accumulation of TGM/GEM near the surface due to a shallow nocturnal boundary layer and dilution during the day initiated by convective mixing with cleaner air aloft as the mixing layer increases (Stamenkovic et al., 2007; Li et al., 2008; Lyman and Gustin, 2008, 2009; Choi et al., 2009; Wan et al., 2009a; Rothenberg et al., 2010; Witt et al., 2010; Li et al., 2011; Nguyen et al., 2011; Fu et al., 2012a; Nair et al., 2012; Zhu et al., 2012; Gratz et al., 2013; Kim et al., 2013; Zhang et al., 2013; Cole et al., 2014; Lan et al., 2014; Xu et al., 2014). The shallow nocturnal boundary layer is often associated with high TGM coinciding with low wind speeds at night (Li et al., 2008; Fu et al., 2012a; Lan et al., 2014). Increases in nighttime concentrations can also be driven by nighttime sources, such as emissions from mercury mining regions (Lyman and Gustin, 2008) and local emissions occurring at night (Song et al., 2009; Wan et al., 2009a; Rothenberg et al., 2010; Gratz et al., 2013; Kim et al., 2013). One study suggested that the evening TGM

Atmos. Chem. Phys. Discuss., doi:10.5194/acp-2016-563, 2016
Manuscript under review for journal Atmos. Chem. Phys.
Published: 21 July 2016

maximum was attributed to coal combustion and biofuel burning (e.g. wood/leaves) for cooking and coincided with winds travelling over residential areas in China (Wan et al., 2009a). The morning TGM/GEM maximum at a rural site after sunrise may be attributed to foliar emissions (Nguyen et al., 2011). At urban surface sites, studies suggested the driving mechanisms for the morning maximum were surface emissions (Zhu et al., 2012; Hall et al., 2014; Xu et al., 2014; Xu et al., 2015), volatilization of Hg from dew (Zhu et al., 2012), and vehicular traffic emissions evident by correlations between TGM/GEM and CO and NO_x (Zhu et al., 2012; Xu et al., 2015). However, there is little research suggesting significant amounts of Hg from vehicular emissions. The lower TGM/GEM observed in the afternoon was driven by GEM oxidation (Stamenkovic et al., 2007; Choi et al., 2009; Lyman and Gustin, 2009; Li et al., 2011; Nguyen et al., 2011; Kim et al., 2013; Zhang et al., 2013; Xu et al., 2014; Xu et al., 2015). Sea breeze also affected the diurnal pattern at an inland urban site (Lan et al., 2014). Sea breezes transported cleaner marine air 70 km inland to Houston, Texas leading to lower TGM in the afternoon on most days, similar to coastal sites (Cole et al., 2014). However on some days, the southerly sea breeze was intersected by northerly flows which led to a period of stagnant air. The lack of pollutant dispersion led to an increase in TGM (Lan et al., 2014).

Many studies conducted in urban areas found a larger diurnal amplitude during summer than other seasons. The major driving mechanism for this larger amplitude originated from higher solar radiation and temperature, which increased the boundary layer mixing height in the summer (Civerolo et al., 2014; Xu et al., 2014). Higher solar radiation during summer also increased photochemical reactions, like GEM oxidation. The larger diurnal variation was also attributed to increases in uptake and re-emissions by vegetation and power plant emissions from air conditioner use during summer nights (Xu et al., 2014). The shift in the timing of the

Atmos. Chem. Phys. Discuss., doi:10.5194/acp-2016-563, 2016
Manuscript under review for journal Atmos. Chem. Phys.
Published: 21 July 2016

TGM/GEM maximum varied with season at some urban sites as previously mentioned. During spring in Windsor, Canada, the decrease in TGM earlier in the afternoon was thought to be due to increase photochemical processes resulting from higher solar radiation and lower GEM emissions due to less vegetation coverage in the spring (Xu et al., 2014). In Nanjing, China, the peak concentration occurring later in the morning during spring was driven by prolonged sunlight hours (Zhu et al., 2012).

Site characteristics may have different impacts on the diurnal variation. During nighttime, GEM at an urban site was significantly higher than a rural site suggesting higher GEM fluxes from buildings and pavement than vegetation and soil (Liu et al., 2010). The diurnal amplitude at an urban site was greater than a suburban site in one study; however, the reason is not known (Civerolo et al., 2014). In the same study, nighttime GEM was 25-30% higher than daytime for the urban site close to the Atlantic Ocean, whereas the GEM difference between night and day was only 10% at an inland suburban site (Civerolo et al., 2014). The study suggested that the higher halogen concentrations in marine environments increased GEM oxidation and subsequently, the loss of GEM in the afternoon leading to larger diurnal variation. At a different coastal-urban location, nighttime GEM was only slightly higher than daytime because of the cleaner air transported from the marine environment (Nguyen et al., 2011). These studies suggested that MBL influence could lead to very different diurnal patterns. Sites continuously impacted by Hg point sources likely contributed to the large short-term fluctuations in the diurnal patterns at some urban sites (Rutter et al., 2008; Engle et al., 2010; Witt et al., 2010).

3.1.3.2 Seasonal Variation of TGM/GEM

The seasonal variation exhibiting a winter to spring maximum in remote, rural, urban and high elevation environments (Table 1) was suggested to be driven by multiple mechanisms,

Atmos. Chem. Phys. Discuss., doi:10.5194/acp-2016-563, 2016
Manuscript under review for journal Atmos. Chem. Phys.
Published: 21 July 2016

including anthropogenic emissions for winter heating (coal and wood combustion), reduced atmospheric mixing, decreased GEM oxidation, less scavenging, and emissions from soil, vegetation, and melting snow in the spring (Stamenkovic et al., 2007; Choi et al., 2008; Mao et al., 2008; Sigler et al., 2009a; Peterson et al., 2009; Wan et al., 2009a; Cheng et al., 2012; Mao and Talbot, 2012; Civerolo et al., 2014; Cole et al., 2014; Xu et al., 2015). The lower TGM/GEM during summer has been attributed to increased GEM oxidation, uptake by vegetation, and higher wet deposition of GOM (Yatavelli et al., 2006; Fu et al., 2008, 2009; Engle et al., 2010; Xu et al., 2015). While these were the predominant driving mechanisms of the seasonal variations in the northern hemisphere, the seasonal patterns could also be influenced by changes in the prevailing wind patterns (Fostier and Michelazzo, 2006; Fu et al., 2010, 2015; Sheu et al., 2010; Chen et al., 2013). The impact of combustion emissions from winter heating was ruled out at a subtropical site in the Pearl River Delta region of China (Chen et al., 2013). Chen et al. (2013) attributed the elevated TGM in the spring to monsoons, which advected southerly marine air masses during summer and northeasterly winds from Siberia during winter. The transition from cold dry air to warm moist air often led to strong temperature inversion and haze in the spring, which in turn inhibits pollutant dispersion. In Brazil, higher TGM in December than May was driven by airflow travelling over high traffic areas in December and then a switch to airflows travelling over vegetation in May (Fostier and Michelazzo, 2006).

Summer and spring maxima in TGM/GEM have also been found at remote, rural, and urban atmospheres. This pattern is predominantly driven by meteorology. Higher solar radiation and temperature during summer increased GEM emissions from Hg contaminated soil (Zhu et al., 2012; Eckley et al., 2013), from vegetation at a forested agricultural site (Nguyen et al., 2011), and from urban surfaces such as soil and pavement in Windsor, Canada (Xu and Akhtar, 2010).

Atmos. Chem. Phys. Discuss., doi:10.5194/acp-2016-563, 2016
Manuscript under review for journal Atmos. Chem. Phys.
Published: 21 July 2016

One study attributed the large difference in the mean TGM between summer and winter (4.4 ng m^{-3}) and frequent elevated TGM events (>12 ng m^{-3}) during summer to surface to air fluxes from Hg contaminated soil in Nanjing (Zhu et al., 2012). This was further supported by TGM correlation with temperature and solar radiation and weak correlation with CO during summer, in which the latter is a strong tracer of anthropogenic emissions. In addition to GEM emissions increasing in warm seasons, higher TGM during summer was attributed to lower wind speeds which prevent pollutant dilution, and increase power plant emissions resulting from higher energy consumption for cooling (Xu et al., 2014). Seasonal change in the prevailing wind direction was another mechanism contributing to this seasonal TGM pattern in China (Fu et al., 2012a,b, 2015; Zhang et al., 2013; Hall et al., 2014). During spring, summer and fall, the prevailing winds from the southwest transported Hg from polluted regions of China to Beijing, whereas cleaner air from the northwest arrived in Beijing during winter (Zhang et al., 2013). The summer monsoon advected biomass burning and industrial emissions from the Pearl River Delta, which also contributed to the summer TGM maximum in Nanjing, China (Hall et al., 2014) in addition to soil emissions discussed earlier.

3.1.3.3 Long-term Trends of TGM/GEM

Long-term trends of TGM/GEM over continental regions indicated a declining trend at some sites and no significant trend at others, particularly at urban sites. Previous studies partly attributed the long-term TGM trends to anthropogenic Hg emissions reductions. There has been a 60-70% decrease in anthropogenic Hg emissions from USA and Canada; however only up to 15% of those emissions reductions impacted TGM at Canadian sites (Cole et al., 2014). The more rapid decline in TGM measured at Mace Head, Ireland for local and European air masses compared to marine air masses was thought to be driven by Hg emissions reductions in Europe

Atmos. Chem. Phys. Discuss., doi:10.5194/acp-2016-563, 2016
Manuscript under review for journal Atmos. Chem. Phys.
Published: 21 July 2016

(Weigelt et al., 2015). The baseline TGM at Mace Head decreased at a larger rate in November than other months suggesting that it is related to lower Hg emissions from residential heating in Europe. The 21% decline in TGM from 2006-2012 in urban/industrial areas of the UK was also consistent with the 0.21 Mg yr^{-1} (24%) reduction in Hg emissions from the UK, even though the TGM trend from the 2003-2013 period was not statistically significant (Brown et al., 2015). In Seoul, Korea, no significant trend in TGM was found from 2004-2011, consistent with the slight decrease (1%) in coal consumption in Seoul over the same time frame (Kim et al., 2013). While TGM/GEM trends appear to be aligned with local/regional Hg emission trends, a discrepancy exists when the trend was compared to the increasing global anthropogenic Hg emissions (Sprovieri et al., 2010b; Ebinghaus et al., 2011; Cole et al., 2014). Alternative reasons for the decline in TGM could be due to faster cycling of Hg as ozone and other oxidants have been increasing or lower emissions of previously-deposited Hg (Sprovieri et al., 2010b; Ebinghaus et al., 2011). Modeling studies indicate global Hg emissions inventory have not accounted for the changes in Hg speciation emission profiles from coal combustion and reduced emissions from products containing Hg (Zhang et al., 2016).

3.2 GOM and PBM

3.2.1 Concentration Metrics

The highest median GOM and PBM were found at high elevation sites, while the lowest concentrations were found at rural surface sites. The median GOM from all locations were 12.1 pg m^{-3} at elevated sites, 9.9 pg m^{-3} at urban sites, 3.8 pg m^{-3}at remote sites, and 2.8 pg m^{-3} at rural sites (Fig. 2a), and correspondingly the median PBM concentration was 11.0, 10.0, 6.9, and 4.6 pg m^{-3}. The variabilities in GOM and PBM were greatest at urban locations. 2-3 hour GOM

Atmos. Chem. Phys. Discuss., doi:10.5194/acp-2016-563, 2016
Manuscript under review for journal Atmos. Chem. Phys.
Published: 21 July 2016

concentrations ranged from <LOD-880 pg m^{-3} at elevated sites, <LOD-8160 pg m^{-3} at urban sites, <LOD-224 pg m^{-3} at remote sites, and <LOD-462 pg m^{-3} at rural sites (see individual site statistics in Table S5). The large variability in GOM was also observed in PBM. 2-3 hour PBM concentrations ranged from <LOD-1001 pg m^{-3} at elevated sites, <LOD-11600 pg m^{-3} at urban sites, <LOD-404 pg m^{-3} at remote sites, and <LOD-205 pg m^{-3} at rural sites (Table S6). The large variability at remote sites is due to the presence of coal-fired power plants within 100 km of one of the sites. By geographical region, the median GOM in Asia was a factor of 1.4-5.1 higher than those in Canada and USA (Fig. 2b). Similarly, the median PBM in Asia was 1.8-8.1 times higher than those in Canada, Europe and USA. This is potentially because one-third of the elevated sites were in China. The GOM and PBM maxima of 8160 pg m^{-3} and 11600 pg m^{-3}, respectively, were both observed at an urban site in Illinois, USA (Engle et al., 2010; Table S5 and S6).

3.2.2 Temporal Variations from Diurnal Cycle to Seasonal Trends

3.2.1.1 Diurnal Variation

The predominant diurnal pattern of GOM at remote, rural, urban, and elevated sites is an increase in the morning leading to a maximum sometime between midday to late afternoon and eventually decreasing at night (Yatavelli et al., 2006; Manolopoulos et al. 2007; Abbott et al., 2008; Lyman and Gustin, 2008; Faïn et al., 2009; Rothenberg et al., 2010; Cheng et al., 2012; Fu et al., 2012a; Nair et al., 2012; Eckley et al., 2013; Gratz et al., 2013; Cole et al., 2014; Civerolo et al., 2014; Marumoto et al. 2015; Zhang et al., 2015). At a *remote* Canadian site, the ratio of the standard deviation to the daily mean of GOM for this type of diurnal pattern was 52% (Cheng et al., 2012). The GOM diurnal amplitudes varied by 35-180% across Canadian *rural* sites (Cole et al., 2014). In *urban* areas, the daytime GOM can be 2-3 folds higher than

Atmos. Chem. Phys. Discuss., doi:10.5194/acp-2016-563, 2016
Manuscript under review for journal Atmos. Chem. Phys.
Published: 21 July 2016

Atmospheric Chemistry and Physics Discussions

nighttime during spring and summer (Civerolo et al., 2014). The diurnal amplitude was larger during spring/summer than fall/winter (Peterson et al., 2009; Cheng et al., 2012; Mao and Talbot, 2012; Choi et al., 2013) and at urban sites compared to rural sites (Nair et al., 2012; Cheng et al., 2014).

In addition to this diurnal pattern, GOM was elevated throughout the day and night at a higher latitude remote site (Cole et al., 2014). A weak diurnal variation was also observed at *rural* sites (Cobbett and Van Heyst, 2007; Choi et al., 2008; Rothenberg et al., 2010), urban sites (Rothenberg et al., 2010; Civerolo et al., 2014; Xu et al., 2015), and an elevated site (Sigler et al., 2009; Mao and Talbot, 2012; Mao et al., 2012). Unlike rural sites, diurnal patterns at *urban* and *elevated* sites can appear opposite to the higher daytime diurnal pattern. Late evening increases in GOM were observed at some urban sites (Lynam and Keeler, 2005; Song et al., 2009; Gratz et al., 2013), resulting in a lower diurnal amplitude of 14% in one study (Song et al., 2009). Some high altitude sites observed higher GOM (average: 18-60 pg m^{-3}) between midnight and early morning (Swartzendruber et al., 2006; Sheu et al., 2010). By comparison, the average daytime GOM at these sites were 9.2-39 pg m^{-3}.

No predominant diurnal pattern was found for PBM, which was mostly measured using the Tekran speciation unit (2537-1135-1130). At *rural* sites, the types of diurnal patterns include, daytime/afternoon peak (Yatavelli et al., 2006; Choi et al., 2008; Rothenberg et al. 2010; Cole et al., 2014), increasing during daytime leading to a nighttime peak (Nair et al., 2012; Zhang et al., 2013), or lack of variation (Cobbett and Van Heyst, 2007; Choi et al., 2008; Rothenberg et al., 2010; Cole et al., 2014). These three patterns were also found at *urban* sites. For the higher daytime pattern, daytime PBM can be 1.5-2 times higher than nighttime during spring (Civerolo et al., 2014). In comparison, the diurnal amplitude was only 14% of the daily mean at an *urban*

Atmos. Chem. Phys. Discuss., doi:10.5194/acp-2016-563, 2016
Manuscript under review for journal Atmos. Chem. Phys.
Published: 21 July 2016

site (Song et al., 2009). At *high elevation* sites, higher daytime/afternoon (Fu et al., 2012a) and a lack of variation were observed (Sheu et al., 2010; Zhang et al., 2015).

3.2.1.2 Seasonal Variation

No predominant seasonal pattern in GOM was found at remote, rural, urban, and elevated sites. At *remote* sites, some studies observed a winter to early-spring maximum and lower concentrations during summer/fall (Manolopoulos et al., 2007; Cheng et al., 2012), whereas higher summer/fall than winter/spring concentrations were also reported (Abbott et al., 2008). In *rural* areas, the maximum concentration can occur in different seasons. The maximum GOM was found in spring and minimum in the fall at most Canadian sites (Cole et al., 2014), except for a summer maximum observed at one Canadian rural site (Eckley et al., 2013). The seasonal maxima in GOM at other *rural* sites can also occur during spring/fall (Nair et al., 2012), winter/summer (Choi et al., 2008), and summer/fall (Zhang et al., 2013). Han et al. (2014) did not observe a seasonal pattern. At *urban* sites, the maximum GOM typically occurred in warmer seasons, e.g. spring or summer (Song et al., 2009; Liu et al., 2010; Choi et al., 2013; Wang et al., 2013; Gratz et al., 2013; Civerolo et al., 2014; Han et al., 2014; Marumoto et al., 2015; Xu et al., 2015). An exception to this seasonal pattern is the higher fall and winter concentrations in northern Mississippi, USA (Jiang et al., 2013). The maximum GOM was also reported in different seasons at *elevated* sites. The maximum GOM was found sometime between fall and spring at mountain sites in China (Wan et al., 2009b; Sheu et al., 2010; Fu et al., 2012a; Zhang et al., 2015) and an elevated site in the U.S. (Sigler et al., 2009a). This contrasts the summer maximum of reactive mercury (GOM+PBM) at three elevated western U.S. sites (Weiss-Penzias et al., 2015).

Atmos. Chem. Phys. Discuss., doi:10.5194/acp-2016-563, 2016
Manuscript under review for journal Atmos. Chem. Phys.
Published: 21 July 2016

Higher PBM and total particulate Hg (TPM) during colder seasons than summer is a highly ubiquitous trend for remote, rural, urban, and elevated sites (Zielonka et al, 2005; Choi et al., 2008; Wan et al., 2009b; Liu et al., 2010; Kim et al., 2012; Gratz et al., 2013; Beldowska et al., 2012; Marumoto et al., 2015; Schleicher et al., 2015; Zhang et al., 2015). In one study, the TPM fraction was 20.2% of TGM during winter and 6.3% during summer (Zielonka et al, 2005). Beldowska et al. (2012) also observed a larger fraction of TPM during the heating season (0.1-12%) than summer (0.1-3%). However, increases in PBM also occurred during summer in a few studies (Song et al., 2009; Huang et al., 2010; Cheng et al., 2012).

3.2.3 Mechanisms Driving the Observed Temporal Variabilities

3.2.3.1 Diurnal Variations of GOM and PBM

The widespread observation of a midday to late afternoon peak in GOM at continental sites (Table 1) often coincided with meteorological parameters, such as solar radiation and temperature, and/or ozone (Yatavelli et al., 2006; Abbott et al., 2008; Wan et al., 2009a; Weiss-Penzias et al., 2009; Nair et al., 2012; Mao et al., 2012; Gratz et al., 2013; Zhang et al., 2013; Civerolo et al., 2014; Cole et al., 2014; Marumoto et al., 2015). At *high elevation* sites, GOM was also inversely correlated with relative humidity, water vapor, or dew point temperature (Swartzendruber et al., 2006; Lyman and Gustin, 2008, 2009; Weiss-Penzias et al., 2009), and in some cases GOM was not correlated with ozone (Lyman and Gustin, 2009; Peterson et al., 2009; Xu et al., 2015). These diurnal trends infer daytime *in-situ* photochemical production of GOM or entrainment of GOM from the free troposphere due to convective mixing. Increases in GOM during daytime at a rural site was attributed to local transport from urban areas as indicated by similarities in diurnal patterns between GOM, SO_2, and O_3 and a delay in the timing of the GOM maximum likely resulting from emissions transport (Rothenberg et al., 2010). Short-term

Atmos. Chem. Phys. Discuss., doi:10.5194/acp-2016-563, 2016
Manuscript under review for journal Atmos. Chem. Phys.
Published: 21 July 2016

1228 fluctuations in the diurnal pattern of GOM also suggested the influence of point sources (Rutter
1229 et al., 2008; Engle et al., 2010). Dry deposition and scavenging of GOM by dew played a role in
1230 decreasing GOM during nighttime (Liu et al., 2007; Wan et al., 2009b; Weiss-Penzias et al.,
1231 2009; Nair et al., 2012; Choi et al., 2013; Civerolo et al., 2014). The stronger diurnal amplitude
1232 during the spring/summer coincided with stronger correlations between GOM, solar radiation,
1233 temperature and O_3 (Yatavelli et al., 2006; Mao et al., 2012; Gratz et al., 2013; Zhang et al.,
1234 2013), which suggested that increased photochemical processes led to higher GOM. Large
1235 diurnal variation during summer was also potentially driven by high pressure, drier and cloud-
1236 free conditions that are conducive to the buildup of GOM in the free troposphere (Lyman and
1237 Gustin, 2009).

1238 Nighttime increases in GOM seen exclusively at *urban* and *elevated* sites (Table 1)
1239 appeared to be driven by anthropogenic emissions and the free troposphere. Nocturnal emissions
1240 and local/regional transport within the boundary layer (Lynam and Keeler, 2005; Song et al.,
1241 2009) and reduced vertical mixing in the stable nocturnal boundary layer led to higher GOM at
1242 night in *urban* areas (Gratz et al., 2013). At *high elevation* sites, katabatic winds entrained GOM
1243 from the free troposphere. In one study, GOM from the free troposphere was believed to
1244 originate from *in-situ* photochemical processes due to a strong inverse GEM-GOM correlation
1245 and a GOM/GEM slope near unity during an elevated GOM episode (Swartzendruber et al.,
1246 2006). While an anti-correlation between GEM and GOM was also found at another elevated
1247 site, Sheu et al. (2010) did not observe a complete photochemical conversion of GEM to GOM.
1248 The difference between these two *elevated* sites suggests different sources of GOM in the free
1249 troposphere. Timonen et al. (2013) found that in one type of free troposphere air mass, GEM
1250 oxidation occurred in anthropogenic plumes transported from Asia to Mt. Bachelor Observatory,

Atmos. Chem. Phys. Discuss., doi:10.5194/acp-2016-563, 2016
Manuscript under review for journal Atmos. Chem. Phys.
Published: 21 July 2016

1251 USA and converted 20% of the GEM to GOM. A second type of air mass travelling over the
1252 Pacific Ocean resulted in 100% GEM conversion to GOM likely because of GEM oxidation by
1253 bromine.

1254 The driving mechanisms behind the diurnal pattern of PBM were better explored for
1255 *urban* sites than other site categories. Frequent spikes in hourly concentrations during daytime
1256 were attributed to point sources (Rutter et al., 2008; Civerolo et al., 2014). At a valley *urban* site,
1257 higher PBM and GEM during daytime suggested similar emission sources from Hg enriched
1258 areas (Lyman and Gustin, 2009). Higher PBM during daytime in the summer could also be
1259 initiated by photochemical production of GOM followed by absorption on secondary organic
1260 aerosols (Choi et al., 2013). Diurnal patterns exhibiting nighttime increases in PBM in urban
1261 areas could be due to multiple mechanisms and sources, such as nocturnal emissions and
1262 local/regional transport within the boundary layer (Song et al., 2009), reduced vertical mixing in
1263 the stable nocturnal boundary layer (Gratz et al., 2013; Xu et al., 2015), vehicular emissions in
1264 China (Xu et al., 2015), and nighttime street food vending in Beijing (Schleicher et al. 2015).

1265 3.2.3.2 Seasonal Variations of GOM and PBM

1266 The seasonal variation characterized by higher GOM in the warm seasons (Table 1) is
1267 primarily driven by photochemical production due to increased solar radiation, O_3, and likely
1268 other atmospheric oxidants (Liu et al., 2010; Choi et al., 2013; Civerolo et al., 2014; Xu et al.,
1269 2015). Alternative reasons could be attributed to anthropogenic emissions leading to higher
1270 GOM in the summer at urban sites (Song et al., 2009; Gratz et al., 2013). Atmospheric mercury
1271 depletion events occurring at higher latitude continental sites led to higher GOM during spring
1272 (Cole et al., 2014). Free troposphere transport was a major driving mechanism for higher
1273 reactive Hg at three high elevation western U.S. sites (Weiss-Penzias et al., 2015). In one study,

Atmos. Chem. Phys. Discuss., doi:10.5194/acp-2016-563, 2016
Manuscript under review for journal Atmos. Chem. Phys.
Published: 21 July 2016

increases in GOM during fall and winter coincided with increases in traffic at a university campus when classes were in session (Jiang et al., 2013). At *elevated* sites in China, the occurrence of higher GOM between fall and spring were attributed to coal and biofuel burning (Wan et al., 2009b) and changes in the prevailing winds that advected GOM from polluted regions (Fu et al., 2012a; Zhang et al., 2015). Lower GOM during summer was due to wet deposition (Wan et al., 2009b; Sheu et al., 2010).

Several mechanisms contribute to the increase in PBM or TPM during colder seasons (Table 1) including, local/regional coal combustion and wood burning emissions, lower mixing height, less oxidation, and increased gas-particle partitioning (Song et al., 2009; Xiu et al., 2009; Liu et al., 2010; Cheng et al., 2012; Fu et al., 2012a; Kim et al., 2012; Choi et al., 2013; Gratz et al., 2013; Wang et al., 2013; Civerolo et al., 2014; Cole et al., 2014; Schleicher et al., 2015; Xu et al., 2015). Oxidized Hg tended to partition to particles during colder seasons because of lower temperatures (Rutter et al., 2007), higher relative humidity (Kim et al., 2012), and reduced volatilization of gaseous Hg (Choi et al., 2013). Similar to GOM, decreases in PBM during summer at many sites in China were due to wet deposition (Wan et al., 2009b; Schleicher et al., 2015; Xu et al., 2015; Zhang et al., 2015) and a shift to cleaner marine airflows during summer (Kim et al., 2012). Higher PBM during warm seasons may be driven by forest fire emissions (Eckley et al., 2013) and increased $PM_{2.5}$ available for GOM absorption at urban sites (Song et al., 2009; Schleicher et al., 2015).

4. Latitudinal Variation

There are a few shipboard and airborne studies that surveyed latitudinal variation of TGM/GEM (Slemr et al., 1981, 1985, 1995; Slemr and Langer, 1992; Fitzgerald et al., 1984; Lamborg et al., 1999; Temme et al., 2003a; Aspmo et al., 2006; Soerensen et al., 2010). Overall,

Atmos. Chem. Phys. Discuss., doi:10.5194/acp-2016-563, 2016
Manuscript under review for journal Atmos. Chem. Phys.
Published: 21 July 2016

the composite latitudinal distribution from studies of the past three decades showed that TGM/GEM concentrations over the ocean surface decreased from NH to SH (**Figs. 3 & 4**), with the highest concentrations (~3.5 ng m^{-3}) in northern hemispheric midlatitudes and the lowest in southern hemispheric latitudes (~0.9 ng m^{-3}). Slemr et al. (1981, 1985) found that the concentrations remained relatively constant (1.4 – 1.6 ng m^{-3}) in NH, dropped rapidly once the ship passed the ITCZ at about 12°N – 13°N latitude, with natural variability of 16%, and varied over 1.0 – 1.2 ng m^{-3} in the South Atlantic. In addition, Temme et al. (2003a) found higher variability of TGM in NH (21% vs. 8% in the southern hemisphere) suggesting the majority of Hg emissions were located in NH, refuting the hypothesis of large oceanic sources of Hg by previous work (e.g., Mason et al., 1994).

Bagnato et al. (2013) compiled a latitudinal distribution of GEM using measurement data from a number of shipboard measurement studies spanning the time period of 1980 – 2012 (**Fig. 3**) and showed a small but discernible inter-hemispheric gradient in GEM resulting from greater emissions of Hg to the atmosphere in the more industrialized NH. However, caution should be taken that global anthropogenic emissions had decreased significantly over that time period, and the trend in natural emissions (reemissions) was unknown (Slemr et al., 2010).

Tropospheric airborne measurements from INTEX-B (Talbot et al., 2007, 2008) and ARCTAS (Mao et al., 2010), spanning near the surface to 12 km altitude, suggested on average ~50 ppqv (~0.5 ng m^{-3}) increases in GEM concentrations from lower latitudes (~20 – 30 °N) to higher (60 – 90°N) latitudes in spring, while negligible latitudinal variation in summer (Fig. 2). There seemed to be distinct seasonal variation in concentrations and latitudinal gradient. It was speculated that smaller latitudinal gradient of temperature in summer likely enhanced meridional circulation resulting in smaller latitudinal variation in GEM concentration in the troposphere.

Atmos. Chem. Phys. Discuss., doi:10.5194/acp-2016-563, 2016
Manuscript under review for journal Atmos. Chem. Phys.
Published: 21 July 2016

Atmospheric Chemistry and Physics Discussions

A small gradient was measured in atmospheric GEM concentrations over the Pacific from 1.32 ng m^{-3} in 14 – 20°N latitudes to 1.15 ng m^{-3} in 1-15°S latitudes in October 2011 (Soerensen et al., 2014). Atmospheric GEM elevated in the northern part of the ITCZ was temporarily influenced by the northeastern trade wind that enhanced oceanic evasion, consistent with the largest evasion flux in that region.

5. Altitude Variation

Airborne measurements of TGM, GEM, and/or GOM have been conducted since 1977 (Seiler et al., 1980) extending from near the surface to ~12 km altitude at several geographic locations (Table S7; references therein). Tropospheric GEM, GOM, and PBM concentrations have not thus far been mapped out globally, and a general understanding is lacking on the mechanisms driving the distributions.

Early studies had conflicting reports of the vertical gradient of TGM. Seiler et al. (1980) reported vertical and hemispheric gradient in TGM, 2.7 ng m^{-3} at 1-3 km and 1.5 ng m^{-3} at 8 km altitude over the Pacific west of San Francisco, and at 8 km altitude 1.45± 0.22 ng m^{-3} and 1.08±0.36 ng m^{-3} in the northern and southern hemisphere, respectively. They attributed higher concentrations of TGM (2.4 – 2.7 ng m^{-3}) in the ITCZ to convective transport. In contrast, Slemr et al. (1985) suggested vertically well-mixed TGM in the troposphere based on their average concentration of TGM (2.24±0.51 ng m^{-3}) at 6 – 8 km altitude over central Europe being close to their NH midlatitude shipboard measurements conducted in the same study. A similar range of upper tropospheric GEM was reported by Ebinghaus et al. (2007) and elevated GEM concentrations in biomass burning plumes from the same study suggested biomass burning representing a major mercury source.

Atmos. Chem. Phys. Discuss., doi:10.5194/acp-2016-563, 2016
Manuscript under review for journal Atmos. Chem. Phys.
Published: 21 July 2016

1342 *Vertical profiles* showing nearly constant, slightly decreasing GEM with altitude were
1343 measured in more studies (Banic et al., 2003; Radke et al., 2007; Talbot et al., 2007, 2008; Mao
1344 et al., 2010). Moreover, *seasonal variation* was observed in flights from surface to 7 km over
1345 Canada with ~1.5 ng m^{-3} in summer, 1.7 ng m^{-3} in winter, 1.7 ng m^{-3} >1 km altitude and 1.2 ng
1346 m^{-3} below 1 km due to widespread MDEs over the sea ice in the springtime Arctic (Banic et al.,
1347 2003). During ARCTAS, Mao at el. (2010) found that the vertical extent of springtime Arctic
1348 MDEs varied from meters to 1 km depending on the thickness of the surface inversion layer.
1349 Over the West Pacific near the Californian coastline, it was found that GEM decreased
1350 distinctly with altitude above relatively constant concentrations from the surface to ~ 3–4 km
1351 altitude, associated with a marked decrease in GEM under stratospherically influenced
1352 conditions, and it was hypothesized that the upper troposphere/lower stratosphere (UTLS) was a
1353 Hg sink region (Radke et al., 2007). Depleted GEM in stratospheric air was observed repeatedly
1354 by Talbot et al. (2007, 2008) during INTEX-B flights at ~ 12 km altitude over the Pacific
1355 Northwest, near Honolulu, HI and Anchorage, AK, USA as well as over the western US near the
1356 Pacific coast. Coupled with Murphy et al. (1998, 2006)'s findings of enrichment of PBM in
1357 lower stratospheric aerosols, Talbot et al. (2007) hypothesized that GEM depletion was caused
1358 by fast oxidation of GEM by abundant halogen radicals and O_3 in that region and estimated a
1359 lifetime of 2 and 0.5 days for 100 ppqv GEM oxidized by O_3 and Br, respectively. Talbot et al.
1360 (2007) suggested that stratospheric intrusion could be a source of tropospheric Hg if PBM was to
1361 be transformed back to gaseous Hg.
1362 In the atmosphere of East Asia, Friedli et al. (2004) was the first to report Hg GEM
1363 concentrations from sea level to ~7 km altitude under the influence of continental export from
1364 East China, showing concentrations at all altitudes higher than the global background, with the

Atmos. Chem. Phys. Discuss., doi:10.5194/acp-2016-563, 2016
Manuscript under review for journal Atmos. Chem. Phys.
Published: 21 July 2016

largest 6.3 ng m^{-3} in an industrial plume mostly from coal combustion and at times from other sources including dust storms, biomass burning, and volcanic eruption.

Unlike measurements from the studies aforementioned, Swartzendruber et al. (2008) found that layer-averaged GEM concentrations increasing with altitude from 1.30±0.084 ng m^{-3} in 0 – 0.5 km altitude to 1.52±0.182 ng m^{-3} in the highest layer 5.5 – 6.5 km altitude over the Pacific Northwest over 13 April – 16 May 2006. The higher GEM concentrations above 2.5 km were associated with long range transport of Asian pollution based on the positive GEM-CO correlation and back trajectories.

Upper air GOM concentrations were first measured in spring by Lindberg et al. (2002) at 1000 m (exterior to the boundary layer) and 100 m altitude (within the boundary layer) immediately northeast of Point Barrow. Six aircraft surveys consistently showed that GOM concentrations decreased from an average 70 to 20 to 2 pg m^{-3} from 5 to 100 to 1000 m altitude, supporting the hypothesis that the Hg oxidation reactions occurred in the near-surface boundary layer driven by halogen compounds derived from sea-salt aerosols.

In recent years, more studies found that higher GOM concentrations in higher altitudes were attributed to lack of depositional loss, lower temperature, and/or more abundant Br radicals (Sillman et al., 2007; Lyman and Jaffe, 2011; Brooks et al., 2014; Gratz et al., 2015; Shah et al., 2016). Sillman et al. (2007) reported GOM concentrations measured in Florida varying from 10 to 230 pg m^{-3} increasing with height. They reproduced observed free tropospheric GOM using CMAQ (Bullock and Brehme, 2002) with GEM being oxidized primarily in gas-phase by O_3 and OH, the latter being dominant, and found anticorrelation between GEM and GOM under the dominance of photochemistry while positive correlation directly from emissions. Lyman and Jaffe (2011) found enhanced GOM concentrations of ~450 pg m^{-3} and depleted GEM in one

Atmos. Chem. Phys. Discuss., doi:10.5194/acp-2016-563, 2016
Manuscript under review for journal Atmos. Chem. Phys.
Published: 21 July 2016

stratospheric intrusion case, further speculated that the stratosphere was depleted in total Hg and enriched in GOM, and suggested that stratospheric intrusion could be a source of GOM to the troposphere. Near Tullahoma, TN, USA the highest GOM concentrations (200 – 500 pg m^{-3}) from flights over a year were observed always at 2 – 4.5 km altitude in 0 – 6 km vertical profiles with a strong *seasonal variation* with a wintertime minimum and a summertime maximum (Brooks et al., 2014). In the same study, limited PBM measurements exhibited similar levels to GOM at all altitudes.

In a most recent field campaign NOMADSS, the highest Hg(II) concentrations, 300–680 pg m^{-3} were observed in dry (RH<35 %) and clean air masses during two flights over Texas at 5–7 km altitude and off the North Carolina coast at 1–3 km (Gratz et al., 2015; Shah et al., 2016). Gratz et al. (2015) found, using back trajectories, that a segment of air masses with elevated GOM averaged at 0.266±0.038 ng m^{-3} and ranging over 0.182 – 0.347 ng m^{-3} at 7 km altitude over Texas originated from the upper troposphere of the Pacific High. It was speculated that the stable, dry conditions of large scale anticyclones resulted in a lack of GOM removal by wet deposition or in-cloud reduction and were thus ideal for GOM accumulation. They demonstrated that elevated BrOx could persist and that sufficient GOM could be produced during long-range transport in the Pacific upper troposphere. Their sensitivity analysis suggested a range of 8 – 13 days required to produce the observed GOM. Shah et al. (2016), using GEOS-Chem with tripled bromine radical concentrations or a faster oxidation rate constant for GEM + Br, simulated 1.5–2 times higher modeled Hg(II) concentrations and improved agreement with the observations, and suggested that the subtropical anticyclones are significant global sources of Hg(II).

6. Summary and Recommendations

Atmos. Chem. Phys. Discuss., doi:10.5194/acp-2016-563, 2016
Manuscript under review for journal Atmos. Chem. Phys.
Published: 21 July 2016

Atmospheric Chemistry and Physics Discussions

1411 This review summarized the general characteristics in GEM, GOM, and PBM
1412 concentrations in the MBL, over land, from low to high latitudes, and from the surface to the
1413 upper troposphere, and further the factors driving such variabilities based on a great wealth of
1414 research in the literature. The Key points are summarized below.

1415 1. For TGM/GEM in the MBL, diurnal variation mostly featured noon to afternoon minimums
1416 due probably to in situ oxidation of GEM in the MBL in most oceanic regions, while in a few
1417 studies, on TGM over the Atlantic and the equatorial Pacific Ocean, the opposite pattern was
1418 observed with daytime maximums and attributed to enhanced oceanic evasion linked to
1419 enhanced photoreduction and biological activity. Seasonal to annual variation was generally
1420 characterized as higher (lower) concentrations in colder (warmer) months, which was largely
1421 thought to be caused by less (more) loss via oxidation in colder (warmer) months. Long term
1422 trends have been identified in three environments, Mace Head, Ireland, Canadian midlatitude
1423 sites, and Cape Point, South Africa, and varied over different time periods, speculated to be
1424 associated with changing anthropogenic and natural emissions as well as possibly redox
1425 chemistry.
1426 2. For MBL GOM, diurnal variation was generally characterized with noon to afternoon peaks
1427 and nighttime low values, most likely driven by daytime GEM photooxidation involving
1428 reactive halogens. Seasonal variation was often observed with higher concentrations in
1429 spring and summer and lower in fall and winter, largely attributed to GEM photooxidation as
1430 often supported by correlation of GOM with solar radiation and BrO. In one study
1431 springtime maximums were also linked to biological activity and in a few studies annual
1432 minimums were associated with scavenging by precipitation. No long term trends have been
1433 reported for oceanic regions.

Atmos. Chem. Phys. Discuss., doi:10.5194/acp-2016-563, 2016
Manuscript under review for journal Atmos. Chem. Phys.
Published: 21 July 2016

3. For MBL PBM, no consistent diurnal and seasonal variation has been identified in most studies, and only two studies reported seasonal variation with higher concentrations in fall/winter associated with anthropogenic emissions. Results from one study showed no consistent diurnal variation in Tekran measurements, but found a clear diurnal cycle with maximums at noon and minimums before sunrise using 10-stage impactor measurements.
4. For continental TGM/GEM, higher concentrations were found at urban sites than remote, rural, and elevated sites. This result is unbiased by elevated TGM/GEM from Asian sites. The predominant diurnal pattern was an early morning minimum and afternoon maximum, opposite to that at urban sites. Diurnal patterns at surface sites were thought to be driven by surface and local emissions, boundary layer dynamics, Hg photochemistry, dry deposition, and sequestering by dew. At elevated sites, mountain-valley winds appeared to be important drivers of the diurnal cycle. Seasonal variations were influenced by fossil fuel emissions for winter heating, surface emissions, and monsoons in Asia. At background sites, long-term declines in TGM are partially attributed to lower anthropogenic Hg emissions.
5. For continental GOM, concentrations were higher at elevated sites. However, this result may be biased by a large proportion of high elevation studies from China where speciated atmospheric mercury are typically elevated. The predominant diurnal pattern was a noon to mid-afternoon maximum and nighttime minimum, except for nighttime increases at urban and elevated sites. The driving mechanisms of the diurnal variations were suggested to include in situ photochemical production, dry deposition, and scavenging by dew. Entrainment of GOM from the free troposphere was believed to contribute to nighttime increases at some elevated sites. No predominant seasonal pattern in GOM was found, except for higher concentrations in the spring/summer at urban sites. Photochemical

Atmos. Chem. Phys. Discuss., doi:10.5194/acp-2016-563, 2016
Manuscript under review for journal Atmos. Chem. Phys.
Published: 21 July 2016

production driven by strong solar radiation and atmospheric oxidants, free tropospheric transport, anthropogenic emissions, and increased wet deposition during summer appeared to be factors affecting the GOM seasonal pattern.

6. For continental PBM or TPM, no predominant diurnal pattern was found. Increase in PBM or TPM was prevalent during colder seasons and are driven by local/regional coal combustion and wood burning emissions, lower mixing height, reduced oxidation, and increased gas-particle partitioning.
7. TGM/GEM over the ocean surface decreased from NH to SH with the highest concentrations (~3.5 ng m^{-3}) in northern hemispheric midlatitudes and the lowest in southern hemispheric latitudes (~0.9 ng m^{-3}), as shown in the composite latitudinal distribution derive from studies of the past three decades. This interhemispheric gradient was believed to suggest the majority of Hg emissions in NH, refuting the hypothesis of large oceanic sources of Hg by previous work. However, in other studies the largest oceanic source was found in the equatorial region. Airborne measurement of TGM suggested distinct seasonal variation in concentrations and latitudinal gradient, a ~50 ppqv (~0.5 ng m^{-3}) increases in GEM concentrations from ~20°N – 30 °N to 60°N – 90°N latitudes in spring and negligible latitudinal variation in summer. It was speculated that smaller latitudinal gradient of temperature in summer likely enhanced meridional circulation resulting in smaller latitudinal variation in GEM concentration in the troposphere.
8. Nearly constant, slightly decreasing GEM with altitude were shown in airborne measurements in some regions, and depleted GEM was found in air masses under stratospheric influence. Abundant GOM has been suggested, but only a handful of studies have conducted measurements of GOM in the free troposphere showing concentrations of

Atmos. Chem. Phys. Discuss., doi:10.5194/acp-2016-563, 2016
Manuscript under review for journal Atmos. Chem. Phys.
Published: 21 July 2016

Atmospheric Chemistry and Physics Discussions

hundreds of pg m^{-3}, particularly in the area of Pacific High.

There remain several outstanding unresolved questions and issues regarding our understanding of the mechanisms controlling observed spatiotemporal variations in atmospheric Hg, as listed follows.

1. Global distributions of tropospheric TGM/GEM, GOM, and PBM remain lacking despite nearly two decades of extensive monitoring and modeling studies. Speciated atmospheric mercury in the continental boundary layer have been monitored in various regions of the northern hemisphere, including in Asia, Europe and North America, and in different remote, rural, urban, and high elevation environments; yet measurements remain scarce at inland locations in the southern hemisphere. In the MBL, most observations have been obtained via shipboard measurements with a few exceptions as ground-based on islands, and subsequently the global coverage was limited in space and time. As a result, the diurnal variation to long-term trends derived from such data suggested composite information instead of instantaneous variation. This limitation inevitably impedes the advancement of our understanding of the factors controlling observed significant variation in atmospheric Hg concentrations. In this vein, it is therefore of paramount importance to have long-term monitoring of atmospheric Hg continued in time and expanded in space, particularly over oceans perhaps utilizing innovative platforms and at high altitudes, which certainly demands technological breakthroughs in instrumentation.
2. GEM oxidation is one of the main driving mechanisms of the diurnal and seasonal variations of TGM/GEM and GOM. However, which oxidants are involved in the photochemical reactions that could reproduce the diurnal and seasonal variations of GOM remain largely unknown/uncertain, due to the lack of upper air measurements and speciated GOM

Atmos. Chem. Phys. Discuss., doi:10.5194/acp-2016-563, 2016
Manuscript under review for journal Atmos. Chem. Phys.
Published: 21 July 2016

measurements, to a great extent a result of inadequate technologies, and a thorough understanding of chemical reactions in atmospheric Hg transformation. Studies such as Chand et al. (2008) estimated GOM concentrations using the reaction of GEM + OH alone, and Sillman et al. (2007) reproduced observed GOM concentrations over Florida using CMAQ with gas-phase oxidation of GEM by O_3 and OH only. However, the reactions of GEM+ O_3 and GEM + OH have been subject to debate between theoretical and experimental studies, as no mechanism consistent with thermochemistry has been proposed (Pal and Ariya, 2004; Calvert and Lindberg, 2005; Subir et al., 2011; Ariya et al., 2015). It was speculated that GEM oxidation in the MBL and the upper troposphere was possibly largely Br-initiated (Holmes et al., 2009; Gratz et al., 2015; Shah et al., 2016). This indicated that even if a model reproduced observed concentrations of GOM, the chemistry in the model was not necessarily correct. So far, most chemical transport models have largely focused on reproducing annual and monthly variations in TGM/GEM (Lei et al., 2013; Song et al., 2015), with large discrepancies between model simulations and surface measurements of GOM and PBM (Zhang et al., 2012; Kos et al., 2012) . Future atmospheric modeling studies need to focus more on reproducing the observed diurnal and seasonal variations using different Hg photochemistry scenarios. Measurement studies need to include other oxidants besides ozone (and BrO in limited number of studies) in the analysis of diurnal variation. Again, this boils down to the most urgent need of fundamental understanding of the chemistry driving atmospheric Hg cycling.

3. Mountain-valley atmospheric patterns appeared to be very common at elevated sites and conducive to the entrainment of GOM from the free troposphere at night. Yet, the nighttime increase in GOM did not seem to be widespread among elevated sites, with some sites

Atmos. Chem. Phys. Discuss., doi:10.5194/acp-2016-563, 2016
Manuscript under review for journal Atmos. Chem. Phys.
Published: 21 July 2016

observing a GOM minimum at night. It implies spatial variability in GOM in the free troposphere that warrants further study. Another related question is the degree of influence the free troposphere has on surface GOM in the absence of katabatic winds. The use of ozone and water vapor as tracers of the free troposphere may not be ideal considering abundant ozone and water vapor near the surface.

4. The higher summer TGM seasonal pattern was found to be more common among continental sites impacted by surface emissions, whereas the seasonal TGM pattern characterized by higher winter/spring concentrations tended to occur at sites affected by regional emissions related to winter heating. Thus, it is important that studies on temporal variabilities broaden their scope to include an analysis of source-receptor relationships.
5. No definitive diurnal patterns in PBM measurements were found at MBL and continental sites when measurements were collected using the Tekran speciation system. However, impactor measurements in the MBL showed clearly-defined diurnal variation with daily maximums at around noon and minimums before sunrise. PBM measurements need to include particles of all size, as the current Tekran instruments could only measure PBM <2.5 μm.

Acknowledgements

The authors acknowledge the field technicians, students and/or researchers for collection of speciated atmospheric mercury data that are summarized and discussed in this review paper.

Atmos. Chem. Phys. Discuss., doi:10.5194/acp-2016-563, 2016
Manuscript under review for journal Atmos. Chem. Phys.
Published: 21 July 2016

Atmospheric Chemistry and Physics Discussions

1549 **Table Caption**

1550 Table 1: Summary of predominant temporal patterns of speciated atmospheric mercury at
1551 continental sites in the northern hemisphere
1552

1553 **Figure Captions**

1554 Figure 1. Mean and ranges of TGM/GEM (a), GOM (b), and PBM (c) concentrations, estimated
1555 from the values in the literature as shown in Tables S1 – S3, over the Atlantic, Indian, Pacific,
1556 seas over the West Pacific (denoted as Pacific-Seas, only TGM/GEM in this category), seas in
1557 the Mediterranean region (denoted as Mediterranean), Arctic, and Antarctica Ocean. The solid
1558 black squares represent the mean value and the lowest whisker the minimum and the largest the
1559 maximum concentration in the region.
1560
1561 Figure 2. Median and range in TGM/GEM, GOM and PBM by site category (a) and by
1562 geographical region (b). Bar graph represents the median and error bar represents the maximum,
1563 estimated from the values in the literature as shown in Tables S4 – S6.
1564
1565 Figure 3. Compiled values for several marine/oceanic environmental systems. GEM over the
1566 Augusta basin is in red open circles. (Based on the figure from Bagnato et al., 2013)
1567
1568 Figure 4. GEM (ppqv) from the INTEX-B in spring 2006 and ARCTAS in spring and summer
1569 2008 (Data sources: Talbot et al., 2007, 2008; Mao et al., 2010).
1570

1571

Atmos. Chem. Phys. Discuss., doi:10.5194/acp-2016-563, 2016
Manuscript under review for journal Atmos. Chem. Phys.
Published: 21 July 2016

Atmospheric Chemistry and Physics Discussions

References

Abbott, M. L., Lin, C. J., Martian, P., and Einerson, J. J.: Atmospheric mercury near Salmon Falls creek reservoir in southern Idaho, Appl. Geochem., 23(3), 438-453, 2008.

Angot, H., M. Barret1, O. Magand, M. Ramonet, and A. Dommergue, A 2-year record of atmospheric mercury species at a background Southern Hemisphere station on Amsterdam Island, Atmos. Chem. Phys., 14, 11461–11473, 2014.

Ariya, P. A., Amyot, M., Dastoor, A., Deeds, D., Feinberg, A., Kos, G., Poulain, A., Ryjkov, A., Semeniuk, K., Subir, M., and Toyota, K.: Mercury physicochemical and biogeochemical transformation in the atmosphere and at atmospheric interfaces: a review and future directions, Chem. Rev., 115, 3760–3802, doi:10.1021/cr500667e, 2015.

Aspmo, K., C. Temme, T. Berg, C. Ferrari, P.-A. Gauchard, X. Fain, and G. Wibetoe, Mercury in the atmosphere, snow, and melt water ponds in the North Atlantic Ocean during Arctic Summer, Environ. Sci. Technol., 40(13), 4083 – 4089, 2007.

Bagnato, E., M. Sproverie, M. Barra, The sea–air exchange of mercury (Hg) in the marine boundary layer of the Augusta basin (southern Italy): Concentrations and evasion flux, Chemosphere, 93, 2024–2032, 2013.

Banic, C. M., S. T. Beauchamp, R. J. Tordon, W. H. Schroeder, A. Steffen, K. A. Anlauf, and H. K. T. Wong, Vertical distribution of gaseous elemental mercury in Canada, J. Geophys. Res., 108(D9), 4264, doi:10.1029/2002JD002116, 2003.

Beldowska, M., D. Saniewska, L. Falkowska, and A. Lewandowska, Mercury in particulate matter over Polish zone of the southern Baltic Sea, Atmos. Environ., 46, 397-404, 2012.

Berg, T., Pfaffhuber, K. A., Cole, A. S., Engelsen, O., and Steffen, A.: Ten-year trends in atmospheric mercury concentrations, meteorological effects and climate variables at Zeppelin, Ny-Ålesund, Atmos. Chem. Phys., 13(13), 6575-6586, 2013.

Brooks, S. X. Ren, M. Cohen, W. T. Luke, P. Kelley, R. Artz, A. Hynes, W. Landing, and B. Martos, Airborne Vertical Profiling of Mercury Speciation near Tullahoma, TN, USA, *Atmos.*, *5*, 557-574; doi:10.3390/atmos5030557, 2014.

Brown, R. J., Goddard, S. L., Butterfield, D. M., Brown, A. S., Robins, C., Mustoe, C. L., and McGhee, E. A.: Ten years of mercury measurement at urban and industrial air quality monitoring stations in the UK, Atmos. Environ., 109, 1-8, 2015.

Brunke, E. G., Labuschagne, C., Ebinghaus, R., Kock, H.H., Slemr, F. Gaseous elemental mercury depletion events observed at Cape Point during 2007 and 2008, Atmos. Chem. Phys. 10, 1121-1131, 2010.

1612 Bullock, O. R. and Brehme, K. A.: Atmospheric mercury simulation using the CMAQ model:
1613 formulation description and analysis of wet deposition results, *Atmos. Environ.*, *36*(13), 2135-
1614 2146, 2002.
1615
1616 Calvert, J. G. and Lindberg, S. E.: Mechanisms of mercury removal by O3 and OH in the
1617 atmosphere, Atmos. Environ., *39*(18), 3355-3367, 2005.
1618
1619 Chand, D., et al. (2008), Reactive and particulate mercury in the Asian marine boundary layer,
1620 Atmos. Environ., 28, 7988–7996, doi:10.1016/j.atmosenv.2008.06.048.
1621
1622 Chen, L., Liu, M., Xu, Z., Fan, R., Tao, J., Chen, D., Zhang, D., Xie, D. and Sun, J.: Variation
1623 trends and influencing factors of total gaseous mercury in the Pearl River Delta—A highly
1624 industrialised region in South China influenced by seasonal monsoons, Atmos. Environ., 77,
1625 757-766, 2013.
1626
1627 Chen, L., Y. Zhang, D. J. Jacob, A. L. Soerensen, J. A. Fisher, H.M. Horowitz, E. S. Corbitt, and
1628 X. Wang (2015), A decline in Arctic Ocean mercury suggested by differences in decadal trends
1629 of atmospheric mercury between the Arctic and northern midlatitudes, Geophys. Res. Lett., 42,
1630 6076–6083, doi:10.1002/2015GL064051.
1631
1632 Cheng, I., Zhang, L., Blanchard, P., Dalziel, J., Tordon, R., Huang, J., and Holsen, T. M.:
1633 Comparisons of mercury sources and atmospheric mercury processes between a coastal and
1634 inland site, J. Geophys. Res. Atmos., 118(5), 2434-2443, 2013.
1635
1636 Cheng, I., Zhang, L., Blanchard, P., Graydon, J. A., and St. Louis, V. L.: Source-receptor
1637 relationships for speciated atmospheric mercury at the remote Experimental Lakes Area,
1638 northwestern Ontario, Canada, Atmos. Chem. Phys., 12(4), 1903-1922, 2012.
1639
1640 Cheng, I., Zhang, L., Mao, H., Blanchard, P., Tordon, R., and Dalziel, J.: Seasonal and diurnal
1641 patterns of speciated atmospheric mercury at a coastal-rural and a coastal-urban site, Atmos.
1642 Environ., 82, 193-205, 2014.
1643
1644 Choi, E. M., Kim, S. H., Holsen, T. M., and Yi, S. M.: Total gaseous concentrations in mercury
1645 in Seoul, Korea: local sources compared to long-range transport from China and Japan. Environ.
1646 Pollut., 157(3), 816-822, 2009.
1647
1648 Choi, H. D., Holsen, T. M., and Hopke, P. K.: Atmospheric mercury (Hg) in the Adirondacks:
1649 Concentrations and sources, Environ. Sci. Technol., 42(15), 5644-5653, 2008.
1650
1651 Choi, H. D., Huang, J., Mondal, S., and Holsen, T. M.: Variation in concentrations of three
1652 mercury (Hg) forms at a rural and a suburban site in New York State, Sci. Total Environ., 448,
1653 96-106, 2013.

1654 Ci, Z. J., Zhang, X. S., Wang, Z. W., Niu, Z. C., Diao, X. Y., Wang, S. W., Distribution and air-
1655 sea exchange of mercury (Hg) in the Yellow Sea, Atmos. Chem. Phys., 11, 2881–2892, doi:
1656 10.5194/acp-11-2881-2011, 2011.

1657 Civerolo, K. L., Rattigan, O. V., Felton, H. D., Hirsch, M. J., and DeSantis, S.: Mercury wet
1658 deposition and speciated air concentrations from two urban sites in New York State: Temporal
1659 patterns and regional context, Aerosol Air Qual. Res., 14(7), 1822-1837, 2014.
1660
1661 Cobbett, F. D., and Van Heyst, B. J.: Measurements of GEM fluxes and atmospheric mercury
1662 concentrations (GEM, RGM and Hgp) from an agricultural field amended with biosolids in
1663 Southern Ont., Canada (October 2004–November 2004), Atmos. Environ., 41(11), 2270-2282,
1664 2007.
1665
1666 Cole, A. S., A. Steffen, K. A. Pfaffhuber, T. Berg, M. Pilote, L. Poissant, R. Tordon, and H.
1667 Hung (2013), Ten-year trends of atmospheric mercury in the high Arctic compared to Canadian
1668 sub-Arctic and mid-latitude sites, Atmos. Chem. Phys., 13, 1535–1545, doi:10.5194/acp-13-
1669 1535-2013.
1670
1671 Cole, A. S., Steffen, A., Eckley, C. S., Narayan, J., Pilote, M., Tordon, R., Graydon, J. A., St.
1672 Louis, V.L., Xu, X., and Branfireun, B. A.: A survey of mercury in air and precipitation across
1673 Canada: patterns and trends, Atmosphere, 5(3), 635-668, 2014.

1674 Dastoor, A. P., and D. A. Durnford, Arctic Ocean: is it a sink of a source of atmospheric mercury?
1675 Environ. Sci. Technol., 48, 1707−1717, 2014.

1676 De More, S. J., J. E. Patterson, D. M. Bibby, Baseline atmospheric mercury studies at Ross
1677 Island, Antarctica, Antarctic Sci., 5(3), 323-326, 1993.

1678 Dibble, T. S., Zelie, M. J., and Mao, H.: Thermodynamics of reactions of ClHg and BrHg
1679 radicals with atmospherically abundant free radicals, Atmos. Chem. Phys., *12*(21), 10271-10279,
1680 2012.
1681
1682 Driscoll, C. T., Mason, R. P., Chan, H. M., Jacob, D. J., and Pirrone, N.: Mercury as a global
1683 pollutant: sources, pathways, and effect, Environ. Sci. Technol., *47*(10), 4967-4983, 2013.
1684
1685 Ebinghaus, R., and F. Slemr, Aircraft measurements of atmospheric mercury over southern and
1686 eastern Germany, Atmos. Environ., 34, 895-903, 2000.
1687
1688 Ebinghaus, R., F. Slemr, C.A.M. Brenninkmeijer, P. van Velthoven, A. Zahn,M.Hermann, D. A.
1689 O'Sullivan, and D. E. Oram (2007), Emissions of gaseous mercury from biomass burning in
1690 South America in 2005 observed during CARIBIC flights, Geophys. Res. Lett., 34, L08813,
1691 doi:10.1029/2006GL028866.
1692
1693 Ebinghaus, R., Jennings, S. G., Kock, H. H., Derwent, R. G., Manning, A. J., and Spain, T. G.:
1694 Decreasing trends in total gaseous mercury observations in baseline air at Mace Head, Ireland
1695 from 1996 to 2009, Atmos. Environ., 45(20), 3475-3480, 2011.
1696
1697 Ebinghaus, R., Kock, H. H., Coggin, AM, Spain, TG, Jennings, SG, Temme, C., Long term
1698 measurements of atmospheric mercury at Mace Head, Irish west coast, between 1995 and 2001.
1699 Atmos. Environ., 36, 5267 – 76, 2002a.

1700
1701 Ebinghaus, R., Kock, H. H., Temme, C., Einax, J. W., Löwe, A. G., Richter, A., Burrows, J. P.,
1702 Schroeder, W. H., Antarctic springtime depletion of atmospheric mercury, Environ. Sci.
1703 Technol., 36, 1238-1244, 2002b.
1704
1705 Eckley, C.S., Parsons, M.T., Mintz, R., Lapalme, M., Mazur, M., Tordon, R., Elleman, R.,
1706 Graydon, J.A., Blanchard, P. and St. Louis, V.: Impact of closing Canada's largest point-source
1707 of mercury emissions on local atmospheric mercury concentrations, Environ. Sci. Technol.,
1708 47(18), 10339-10348, 2013.
1709
1710 Engle, M. A., Tate, M. T., Krabbenhoft, D. P., Schauer, J. J., Kolker, A., Shanley, J. B., and
1711 Bothner, M. H.: Comparison of atmospheric mercury speciation and deposition at nine sites
1712 across central and eastern North America, J. Geophys. Res. Atmos., 115(D18), 2010.
1713
1714 Faïn, X., Obrist, D., Hallar, A. G., Mccubbin, I., and Rahn, T.: High levels of reactive gaseous
1715 mercury observed at a high elevation research laboratory in the Rocky Mountains, Atmos. Chem.
1716 Phys., 9(20), 8049-8060, 2009.
1717
1718 Feddersen, D. M., Talbot, R., Mao, H., and Sive, B. C.: Size distribution of particulate mercury
1719 in marine and coastal atmospheres, Atmos. Chem. Phys., *12*(22), 10899-10909, 2012.
1720
1721 Fisher, J. A., D. J. Jacob, A. L. Soerensen, H. M. Amos, E. S. Corbitt, D. G. Streets, Q. Wang, R.
1722 M. Yantosca, and E. M. Sunderland (2013), Factors driving mercury variability in the Arctic
1723 atmosphere and ocean over the past 30 years, Global Biogeochem. Cycles, 27, 1226–1235,
1724 doi:10.1002/2013GB004689.
1725
1726 Fisher, J. A., Jacob, D. J., Soerensen, A. L., Amos, H. M., Steffen, A. & Sunderland, E. M.:
1727 Riverine source of Arctic Ocean mercury inferred from atmospheric observations. Nature
1728 Geoscience, 5(7), 499-504, 2012
1729
1730 Fitzgerald, W.F.: Is mercury increasing in the atmosphere? The need for an atmospheric mercury
1731 network (AMNET). Water, Air and Soil Pollut., 80, 245-254, 1995.
1732
1733 Fitzgerald, W.F., Gill, G.A., Kim, J.P., 1984. An Equatorial Paci"c source of atmospheric ercury.
1734 Science, 224, 597-599.
1735
1736 Fitzgerald, W.F., Mason, R.P., 1996. The global mercury cycle: oceanic and anthropogenic
1737 aspects. In: Baeyens, W., Ebinghaus, R., Vasiliev, O. (Eds.), Global and Regional Mercury
1738 Cycles: Sources, Fluxes and Mass Balances. NATO ASI Series 2. Environment, vol. 21. Kluwer
1739 Ac. Pub., Dordrecht, pp. 85-108.
1740
1741 Fostier, A. H. and Michelazzo, P. A.: Gaseous and particulate atmospheric mercury
1742 concentrations in the Campinas Metropolitan Region (Sao Paulo State, Brazil), J. Brazilian
1743 Chem. Soc., 17(5), 886-894, 2006.
1744

1745 Friedli, H. R., L. F. Radke, R. Prescott, P. Li, J.-H. Woo, and G. R. Carmichael (2004), Mercury
1746 in the atmosphere around Japan, Korea, and China as observed during the 2001 ACE-Asia field
1747 campaign: Measurements, distributions, sources, and implications, J. Geophys. Res., 28, D19S25,
1748 doi:10.1029/2003JD004244.
1749
1750 Fu, X. W., Feng, X., Dong, Z. Q., Yin, R. S., Wang, J. X., Yang, Z. R., and Zhang, H.:
1751 Atmospheric gaseous elemental mercury (GEM) concentrations and mercury depositions at a
1752 high-altitude mountain peak in south China, Atmos. Chem. Phys., 10(5), 2425-2437, 2010.
1753
1754 Fu, X. W., Feng, X., Liang, P., Zhang, H., Ji, J., and Liu, P.:Temporal trend and sources of
1755 speciated atmospheric mercury at Waliguan GAW station, Northwestern China, Atmos. Chem.
1756 Phys., 12(4), 1951-1964, 2012a.
1757
1758 Fu, X. W., Feng, X., Shang, L. H., Wang, S. F., and Zhang, H.: Two years of measurements of
1759 atmospheric total gaseous mercury (TGM) at a remote site in Mt. Changbai area, Northeastern
1760 China, Atmos. Chem. Phys., 12, 4215-4226, doi:10.5194/acp-12-4215-2012, 2012b.
1761
1762 Fu, X. W., Zhang, H., Yu, B., Wang, X., Lin, C.-J., and Feng, X. B.: Observations of
1763 atmospheric mercury in China: a critical review, Atmos. Chem. Phys., 15, 9455-9476,
1764 doi:10.5194/acp-15-9455-2015, 2015.
1765
1766 Fu, X., Feng, X., Wang, S., Rothenberg, S., Shang, L., Li, Z., and Qiu, G.: Temporal and spatial
1767 distributions of total gaseous mercury concentrations in ambient air in a mountainous area in
1768 southwestern China: Implications for industrial and domestic mercury emissions in remote areas
1769 in China, Sci. Total Environ., 407(7), 2306-2314, 2009.
1770
1771 Fu, X., Feng, X., Zhang, G., Xu, W., Li, X., Yao, H., Liang, P., Li, J., Sommar, J., Yin, R., and
1772 Liu, N.: Mercury in the marine boundary layer and seawater of the South China Sea:
1773 Concentrations, sea/air flux, and implication for land outflow, J. Geophys. Res., 115, D06303,
1774 doi:10.1029/2009JD012958, 2010.
1775
1776 Fu, X., Feng, X., Zhu, W., Wang, S., and Lu, J.: Total gaseous mercury concentrations in
1777 ambient air in the eastern slope of Mt. Gongga, South-Eastern fringe of the Tibetan plateau,
1778 China, Atmos. Environ., 42(5), 970-979, 2008.
1779
1780 Gay, D. A., Schmeltz, D., Prestbo, E., Olson, M., Sharac, T., and Tordon, R.: The Atmospheric
1781 Mercury Network: measurement and initial examination of an ongoing atmospheric mercury
1782 record across North America, Atmos. Chem. Phys., 13(22), 11339-11349, 2013.
1783 Geoscience, 5(7), 499-504.
1784
1785 Gratz, L. E., Ambrose, J.L., Jaffe, D.A., Shah, V., Jaeglé, L., Stutz, J., Festa, J., Spolaor, M., Tsai,
1786 C., Selin, N.E. and Song, S: Oxidation of mercury by bromine in the subtropical Pacific free
1787 troposphere, Geophys. Res. Lett., 42, 10,494–10,502, doi:10.1002/2015GL066645, 2015.
1788

1789 Gratz, L. E., Keeler, G. J., Marsik, F. J., Barres, J. A., and Dvonch, J. T.: Atmospheric transport
1790 of speciated mercury across southern Lake Michigan: Influence from emission sources in the
1791 Chicago/Gary urban area, Sci. Total Environ., 448, 84-95, 2013.
1792
1793 Hall, C.B., Mao, H., Ye, Z., Talbot, R., Ding, A., Zhang, Y., Zhu, J., Wang, T., Lin, C.J., Fu, C.
1794 and Yang, X.: Sources and Dynamic Processes Controlling Background and Peak Concentrations
1795 of TGM in Nanjing, China, Atmosphere, 5(1), 124-155, 2014.
1796
1797 Han, Y. J., Kim, J. E., Kim, P. R., Kim, W. J., Yi, S. M., Seo, Y. S., and Kim, S. H.: General
1798 trends of atmospheric mercury concentrations in urban and rural areas in Korea and
1799 characteristics of high-concentration events, Atmos. Environ., 94, 754-764, 2014.
1800
1801 Hedgecock I. M., and N. Pirrone, Chasing quicksilver: modeling the atmospheric lifetime of Hg0
1802 (g) in the marine boundary layer at various latitudes. Environ. Sci. Technol., 38, 69–76, 2004.
1803
1804 Hedgecock, I. M., G. A. Trunfio, N. Pirrone, and F. Sprovieri (2005), Mercury chemistry in the
1805 MBL: Mediterranean case and sensitivity studies using the AMCOTS (Atmospheric Mercury
1806 Chemistry over the Sea) model, Atmos. Environ., 39, 7217– 7230.
1807
1808 Hedgecock, I. M., N. Pirrone, F. Sprovieri, and E. Pesenti (2003), Reactive gaseous mercury in
1809 the marine boundary layer: Modelling and experimental evidence of its formation in the
1810 Mediterranean region, Atmos. Environ., 37, suppl. 1, S41– S49.
1811
1812 Huang, J., Choi, H. D., Hopke, P. K., and Holsen, T. M.: Ambient mercury sources in Rochester,
1813 NY: results from principle components analysis (PCA) of mercury monitoring network data,
1814 Environ. Sci. Technol., 44(22), 8441-8445, 2010.
1815
1816 Holmes, C. D., Jacob, D. J., and Yang, X.: Global lifetime of elemental mercury against
1817 oxidation by atomic bromine in the free troposphere, Geophys. Res. Lett., *33*, *L20808*,
1818 doi:10.1029/2006GL027176, 2006.
1819
1820 Holmes, C. D., Jacob, D. J., Mason, R. P., and Jaffe, D. A.: Sources and deposition of reactive
1821 gaseous mercury in the marine atmosphere, Atmos. Environ., *43*(14), 2278-2285, 2009.
1822
1823 Hynes, A. J., Donohoue, D. L., Goodsite, M. E., and Hedgecock, I. M.: Our current
1824 understanding of major chemical and physical processes affecting mercury dynamics in the
1825 atmosphere and at the air-water/terrestrial interfaces, Pirrone, N. and Mason, R. (Eds.), In
1826 Mercury fate and transport in the global atmosphere (pp. 427-457). Springer U.S., 2009.
1827
1828 Jiang, Y., Cizdziel, J. V., and Lu, D.: Temporal patterns of atmospheric mercury species in
1829 northern Mississippi during 2011–2012: Influence of sudden population swings, Chemosphere,
1830 93(9), 1694-1700, 2013.

1831 Kang, H, and Z. Xie, Atmospheric mercury over the marine boundary layer observed during the
1832 third China Arctic Research Expedition, J. Environ. Sci., 23(9), 1424–1430, 2011.

1833 Kim, J. and Fitzgerald, W.: Gaseous mercury profiles in the tropical Pacific Ocean, Geophys.
1834 Res. Lett., *15*(1), 40-43, 1988.

1835 Kim, K. H., Yoon, H. O., Brown, R. J., Jeon, E. C., Sohn, J. R., Jung, K., Park, C. G., and Kim, I.
1836 S.: Simultaneous monitoring of total gaseous mercury at four urban monitoring stations in Seoul,
1837 Korea, Atmos. Res., 132, 199-208, 2013.
1838
1839 Kim, P. R., Han, Y. J., Holsen, T. M., and Yi, S. M.: Atmospheric particulate mercury:
1840 Concentrations and size distributions, Atmos. Environ., 61, 94-102, 2012.
1841
1842 Kolker, A., Olson, M. L., Krabbenhoft, D. P., Tate, M. T., and Engle, M. A.: Patterns of mercury
1843 dispersion from local and regional emission sources, rural Central Wisconsin, USA, Atmos.
1844 Chem. Phys., 10(10), 4467-4476, 2010.
1845
1846 Kos G., Ryzhkov A., Dastoor A., Narayan J., Steffen A., Ariya P.A., and Zhang L., 2013.
1847 Evaluation of discrepancy between measured and modelled oxidized mercury species.
1848 Atmospheric Chemistry and Physics, 13, 4839-4863.
1849
1850 Kotnik, J., Sprovieri, F., Ogrinc, N., Horvat, M., and Pirrone, N.: Mercury in the Mediterranean,
1851 part I: spatial and temporal trends, *Environ. Sci. Pollut. Res.*, *21*(6), 4063-4080, 2014.
1852
1853 Lamborg, C. H., K. R. Rolfhus, and W. F. Fitzgerald, The atmospheric cycling and air-sea
1854 exchange of mercury species in the south and equatorial Atlantic Ocean, Deep Sea Res., Part II,
1855 46, 957– 977, 1999.
1856
1857 Lan, X., Talbot, R., Castro, M., Perry, K., and Luke, W.: Seasonal and diurnal variations of
1858 atmospheric mercury across the US determined from AMNet monitoring data, Atmos. Chem.
1859 Phys., 12(21), 10569-10582, 2012.
1860
1861 Lan, X., Talbot, R., Laine, P., Lefer, B., Flynn, J., and Torres, A.: Seasonal and diurnal
1862 variations of total gaseous mercury in urban Houston, TX, USA, Atmosphere, 5(2), 399-419,
1863 2014.
1864
1865 Laurier, F. J. G., R. P. Mason, L. Whalin, and S. Kato, Reactive gaseous mercury formation in
1866 the North Pacific Ocean's marine boundary layer: A potential role of halogen chemistry, J.
1867 Geophys. Res., 108(D17), 4529, doi:10.1029/2003JD003625, 2003.
1868
1869 Laurier, F., and R. Mason, Mercury concentration and speciation in the coastal and open ocean
1870 boundary layer, J. Geophys. Res., 112, D06302, doi:10.1029/2006JD007320.
1871
1872 Lei, H., Liang, X.-Z., Wuebbles, D. J., and Tao, Z.: Model analyses of atmospheric mercury:
1873 present air quality and effects of transpacific transport on the United States, Atmos. Chem. Phys.,
1874 13, 10807-10825, doi:10.5194/acp-13-10807-2013, 2013.
1875

1876 Li, J., Sommar, J., Wängberg, I., Lindqvist, O., and Wei, S. Q.: Short-time variation of mercury
1877 speciation in the urban of Göteborg during GÖTE-2005, Atmos. Environ., 42(36), 8382-8388,
1878 2008.
1879
1880 Li, Z., Xia, C., Wang, X., Xiang, Y., and Xie, Z.: Total gaseous mercury in Pearl River Delta
1881 region, China during 2008 winter period, Atmos. Environ., 45(4), 834-838, 2011.
1882
1883 Lindberg, Lindberg, S. E. et al. Dynamic oxidation of gaseous mercury in the Arctic troposphere
1884 at polar sunrise. Environ. Sci. Tech. 36, 1245-1256, 2002.
1885
1886 Liu, B., Keeler, G. J., Dvonch, J. T., Barres, J. A., Lynam, M. M., Marsik, F. J., and Morgan, J.
1887 T.: Temporal variability of mercury speciation in urban air. Atmos. Environ., 41(9), 1911-1923,
1888 2007.
1889
1890 Liu, B., Keeler, G. J., Dvonch, J. T., Barres, J. A., Lynam, M. M., Marsik, F. J., and Morgan, J.
1891 T.: Urban–rural differences in atmospheric mercury speciation, Atmos. Environ., 44(16), 2013-
1892 2023, 2010.
1893
1894 Lyman, S. N. and Gustin, M. S.: Speciation of atmospheric mercury at two sites in northern
1895 Nevada, USA, Atmos. Environ., 42(5), 927-939, 2008.
1896
1897 Lyman, S. N., and D. A. Jaffe, Formation and fate of oxidized mercury in the upper troposphere
1898 and lower stratosphere, Nature Geosci., DOI: 10.1038/NGEO1353, 2011.
1899
1900 Lyman, S. N., and Gustin, M. S.: Determinants of atmospheric mercury concentrations in Reno,
1901 Nevada, USA, Sci. Total Environ., 408(2), 431-438, 2009.
1902
1903 Lynam, M. M. and Keeler: Automated speciated mercury measurements in Michigan, Environ.
1904 Sci. Technol., 39(23), 9253-9262, 2005.
1905
1906 Malcolm, E. G.; Keeler, G. J.; Landis, M. S. The effects of the coastal environment on the
1907 atmospheric mercury cycle. *J. Geophys. Res.* 2003, *108*, article no. 4357.
1908
1909 Manolopoulos, H., Schauer, J. J., Purcell, M. D., Rudolph, T. M., Olson, M. L., Rodger, B., and
1910 Krabbenhoft, D. P.: Local and regional factors affecting atmospheric mercury speciation at a
1911 remote location. J. Environ. Eng. Sci., 6(5), 491-501, 2007.
1912
1913 Mao, H., Talbot, R. W., Sigler, J. M., Sive, B. C., and Hegarty, J. D.: Seasonal and diurnal
1914 variations of Hg over New England, Atmos. Chem. Phys., 8(5), 1403-1421, 2008.
1915
1916 Mao, H. and Talbot, R.: Speciated mercury at marine, coastal, and inland sites in New England–
1917 Part 1: Temporal variability, Atmos. Chem. Phys., 12(11), 5099-5112, 2012.
1918
1919 Mao, H., Talbot, R., Hegarty, J., and Koermer, J.: Speciated mercury at marine, coastal, and
1920 inland sites in New England–Part 2: Relationships with atmospheric physical parameters, Atmos.
1921 Chem. Phys., 12(9), 4181-4206, 2012.

Mao, H., Talbot, R. W., Sive, B. C., Kim, S. Y., Blake, D. R., and Weinheimer, A. J.: Arctic mercury depletion and its quantitative link with halogens, *J. Atmos. Chem.*, *65*(2-3), 145-170, 2010.

Marumoto, K., Hayashi, M., and Takami, A.: Atmospheric mercury concentrations at two sites in the Kyushu Islands, Japan, and evidence of long-range transport from East Asia, Atmos. Environ., 117, 147-155, 2015.

Mason, R. P., and G.-R. Sheu, Role of the ocean in the global mercury cycle, Global Biogeochem. Cycles, 16(4), 1093, 10.1029/2001GB001440, 2002.

Mason, R. P.; Lawson, N. M.; Sheu, G.-R. Mercury in the Atlantic Ocean: factors controlling air-sea exchange of mercury and its distribution in the upper waters. *Deep-Sea Res. II.*, *48*, 2829-2853, 2001.

Mason, R.P., Fitzgerald, W.F., Morel, F.M., 1994. The biogeochemical cycling of elemental mercury: anthropogenic influences, Geochimica et Cosmochimica Acta, 58, 3191–3198.

Mason, R.P., Fitzgerald, W.F., Vandal, G.M., 1992. The sources of mercury in Equatorial Pacific rain. Journal of Atmospheric Chemistry 14, 489-500.

Mazur, M., Mintz, R., Lapalme, M., and Wiens, B.: Ambient air total gaseous mercury concentrations in the vicinity of coal-fired power plants in Alberta, Canada, Sci. Total Environ., 408(2), 373-381, 2009.

Moore, C., D. Obrist, M. Luria, Atmospheric mercury depletion events at the Dead Sea: Spatial and temporal aspects, Atmos. Environ., 69, 231-239, 2013.

Müller, D., Wip, D., Warneke, T., Holmes, C. D., Dastoor, A., and Notholt, J.: Sources of atmospheric mercury in the tropics: continuous observations at a coastal site in Suriname, Atmos. Chem. Phys., 12, 7391–7397, doi:10.5194/acp-12-7391-2012, 2012.

Murphy, D. M., Thomson, D. S., and Mahoney, M. J.: In situ measurements of organics, meteoritic material, mercury, and other elements in aerosols at 5 to 19 kilometers, *Science*, *282*(5394), 1664-1669, 1998.

Murphy, D. M., Hudson, P. K., Thomson, D. S., Sheridan, P. J., and Wilson, J. C.: Observations of mercury-containing aerosols, Environ. Sci. Technol., *40*(10), 3163-3167, 2006.

Nair, U. S., Wu, Y., Walters, J., Jansen, J., and Edgerton, E. S.: Diurnal and seasonal variation of mercury species at coastal-suburban, urban, and rural sites in the southeastern United States, Atmos. Environ., 47, 499-508, 2012.

1967 Nguyen, D. L., Kim, J. Y., Shim, S. G., and Zhang, X. S.: Ground and shipboard measurements
1968 of atmospheric gaseous elemental mercury over the Yellow Sea region during 2007–2008.
1969 Atmos. Environ., 45(1), 253-260, 2011.
1970
1971 Obrist, D., E. Tas, M. Peleg, V. Matveev, X. Faïn, D. Asaf, and M. Lur, Bromine-induced
1972 oxidation of mercury in the mid-latitude atmosphere, Nature Geosci., 4, 22 – 26, 2011.
1973
1974 Obrist, D., Hallar, A. G., McCubbin, I., Stephens, B. B., and Rahn, T.: Atmospheric mercury
1975 concentrations at Storm Peak Laboratory in the Rocky Mountains: Evidence for long-range
1976 transport from Asia, boundary layer contributions, and plant mercury uptake, Atmos. Environ.,
1977 42(33), 7579-7589, 2008.
1978
1979 Pal, B. and Ariya, P. A.: Gas-phase HO-initiated reactions of elemental mercury: kinetics,
1980 product studies, and atmospheric implications, Environ. Sci. Technol., 38, 5555–5566, 2004.
1981
1982 Parsons, M. T., McLennan, D., Lapalme, M., Mooney, C., Watt, C., and Mintz, R.: Total gaseous
1983 mercury concentration measurements at Fort McMurray, Alberta, Canada, Atmosphere, 4(4),
1984 472-493, 2013.
1985
1986 Peterson, C., Gustin, M., and Lyman, S.: Atmospheric mercury concentrations and speciation
1987 measured from 2004 to 2007 in Reno, Nevada, USA, Atmos. Environ., 43(30), 4646-4654, 2009.
1988
1989 Pfaffhuber, K. A., Berg, T., Hirdman, D., and Stohl, A.: Atmospheric mercury observations from
1990 Antarctica: seasonal variation and source and sink region calculations, Atmos. Chem. Phys., 12,
1991 3241–3251, doi:10.5194/acp-12-3241-2012, 2012.
1992
1993 Pirrone, N., Ferrara, R., Hedgecock, I.M., Kallos, G., Mamane, Y., Munthe, J., Pacyna, J.M.,
1994 Pytharoulis, I., Sprovieri, F., Voudouri, A. and Wangberg, I.: Dynamic processes of atmospheric
1995 mercury over the Mediterranean region, Atmos. Environ. , 37(S1), 21–40, 2003.
1996
1997 Pongratz, R., and K. Heumann, Production of methylated mercury, lead, and cadmium by marine
1998 bacteria as a significant natural source for atmospheric heavy metals in polar regions,
1999 Chemosphere, 39, 89– 102, 1999.
2000
2001 Prestbo, E.M. 1997. Mercury speciation in the boundary layer and free troposphere advected to
2002 South Florida: Phase I - Reconnaissance. Report to the Florida Department of Environmental
2003 Protection, Tallahassee. Frontier Geosciences, Seattle, WA.
2004
2005 Radke, L. F., H. R. Friedli, and B. G. Heikes (2007), Atmospheric mercury over the NE Pacific
2006 during spring 2002: Gradients, residence time, upper troposphere lower stratosphere loss, and
2007 long-range transport, J. Geophys. Res., 112, D19305, doi:10.1029/2005JD005828.
2008
2009 Rothenberg, S. E., McKee, L., Gilbreath, A., Yee, D., Connor, M., and Fu, X.: Evidence for
2010 short-range transport of atmospheric mercury to a rural, inland site, Atmos. Environ., 44(10),
2011 1263-1273, 2010.
2012

2013 Rutter, A. P., and Schauer, J. J.: The effect of temperature on the gas–particle partitioning of
2014 reactive mercury in atmospheric aerosols, Atmos. Environ., 41(38), 8647-8657, 2007.
2015
2016 Rutter, A. P., Schauer, J. J., Lough, G. C., Snyder, D. C., Kolb, C. J., Von Klooster, S., Rudolf,
2017 T., Manolopoulos, H., and Olson, M. L.: A comparison of speciated atmospheric mercury at an
2018 urban center and an upwind rural location. J. Environ. Monit., 10(1), 102-108, 2008.
2019
2020 Rutter, A.P., Snyder, D. C., Stone, E.A., Schauer, J.J., Gonzalez-Abraham, R., Molina, L.T.,
2021 Márquez, C., Cárdenas, B. and Foy, B.D.: In situ measurements of speciated atmospheric
2022 mercury and the identification of source regions in the Mexico City Metropolitan Area, Atmos.
2023 Chem. Phys., 9(1), 207-220, 2009.
2024
2025 Sander, R.; Keene, W. C.; Pszenny, A. A. P.; Arimoto, R.; Ayers, G. P.; Baboukas, E.; Cainey, J.
2026 M.; Crutzen, P. J.; Duce, R. A.; Honninger, G.; Huebert, B. J.; Maenhaut, W.; Mihalopoulos, N.;
2027 Schleicher, N. J., Schäfer, J., Blanc, G., Chen, Y., Chai, F., Cen, K., and Norra, S.: Atmospheric
2028 particulate mercury in the megacity Beijing: Spatio-temporal variations and source
2029 apportionment, Atmos. Environ., 109, 251-261, 2015.
2030
2031 Schroeder, W. H., Anlauf, K. G., Barrie, L. A., Lu, J. Y., Steffen, A., Schneeberger, D. R., and
2032 Berg, T. : Arctic springtime depletion of mercury, Nature, 394, 331-332, 1998.
2033
2034 Schroeder, W. H., and Munthe, J.: Atmospheric mercury—an overview, Atmos. Environ., *32*(5),
2035 809-822, 1998.

2036 Seiler, W., C. Eberling, and G. Slemr, Global distribution of gaseous mercury in the troposphere,
2037 Pageoph, 118, 964 – 974, 1980.

2038 Selin, N. E., D. J. Jacob, R. J. Park, R. M. Yantosca, S. A. Strode, L. Jaegle, and D. Jaffe (2007),
2039 Chemical cycling and deposition of atmospheric mercury: Global constraints from observations,
2040 J. Geophys. Res., 112, D02308, doi:10.1029/2006JD007450.
2041
2042 Shah, V., et al., Origin of oxidized mercury in the summertime free troposphere over the
2043 southeastern US, Atmos. Chem. Phys., 16, 1511–1530, 2016.
2044
2045 Sheu, G. R., Lin, N. H., Wang, J. L., Lee, C. T., Yang, C. F. O., and Wang, S. H.: Temporal
2046 distribution and potential sources of atmospheric mercury measured at a high-elevation
2047 background station in Taiwan, Atmos. Environ., 44(20), 2393-2400, 2010.
2048
2049 Sheu, G.-R., and R. P. Mason (2001), An examination of methods for the measurements of
2050 reactive gaseous mercury in the atmosphere, Environ. Sci. Technol., 35, 1209–1216.
2051
2052 Sheu, G.-R., and R. P. Mason (2004), An examination of the oxidation of elemental mercury in
2053 the presence of halide surfaces, J. Atmos. Chem., 48, 107–130.
2054

2055 Sheu, G.-R., Speciation and distribution of atmospheric mercury: Significance of reactive
2056 gaseous mercury in the global mercury cycle, Ph.D. thesis, 170 pp., Univ. of Md., College Park,
2057 2001.
2058
2059 Sigler, J. M., Mao, H., and Talbot, R.: Gaseous elemental and reactive mercury in Southern New
2060 Hampshire, Atmos. Chem. Phys., 9(6), 1929-1942, 2009a.
2061
2062 Sigler, J. M., Mao, H., Sive, B., and Talbot, R., Oceanic Influence on Atmospheric Mercury at
2063 Coastal and Inland Sites: A Springtime Nor'easter in New England, *Atmos. Chem. Phys.*,
2064 *9*, 4023-4030, 2009b.
2065
2066 Sillman, S., Marsik, F. J., Al-Wali, K. I., Keeler, G. J., and Landis, M. S.: Reactive mercury in
2067 the troposphere: Model formation and results for Florida, the northeastern United States, and the
2068 Atlantic Ocean, *J. Geophys. Res. Atmos.*, *112*(D23305), doi:10.1029/2006JD008227, 2007.
2069
2070 Siudek, P., Frankowski, M., and Siepak, J.: Atmospheric particulate mercury at the urban and
2071 forest sites in central Poland, Environ. Sci. Pollut. Res., 23(3), 2341-2352, 2016.
2072
2073 Slemr, F., Angot, H., Dommergue, A., Magand, O., Barret, M., Weigelt, A., Ebinghaus, R.,
2074 Brunke, E.-G., Pfaffhuber, K. A., Edwards, G., Howard, D., Powell, J., Keywood, M., and Wang,
2075 F.: Comparison of mercury concentrations measured at several sites in Southern Hemisphere,
2076 submitted to Atmos. Chem. Phys., 15, 3125–3133, 2015.
2077
2078 Slemr, F., Brunke, E.-G., Ebinghaus, R., Kuss, J., Worldwide trend of atmospheric mercury since
2079 1995. Atmos. Chem. Phys., 11, 4779-4787, 2011.
2080
2081 Slemr, F., E.-G. Brunke, C. Labuschagne, and R. Ebinghaus (2008), Total gaseous mercury
2082 concentrations at the Cape Point GAW station and their seasonality, Geophys. Res. Lett., 35,
2083 L11807, doi:10.1029/2008GL033741.

2084 Slemr, F., G. Schuster, W. Seiler, Distribution, speciation, and budget of atmospheric mercury, J.
2085 Atmos. Chem., 3(4), 407-434, 1985.

2086 Slemr, F., Trends in atmospheric mercury concentrations over the Atlantic ocean and the Wank
2087 summit, and the resulting constraints on the budget of atmospheric mercury, in "*Global and*
2088 *Regional Mercury Cycles: Sources, Fluxes and Mass Balances"*, eds. W. Bayyens, R. Ebinghaus,
2089 and O. Vasiliev, NATO-ASI-Series, Vol. 21, pp 33-84, Kluwer Academic Publishers, Dordrecht,
2090 The Netherlands, 1996.

2091 Slemr, F., W. JunkermannR, .W. H. Schmidt, and R. Sladkovic, Indication of change in global
2092 and regional trends of atmospheric mercury concentrations, Geophys. Res. Lett., 22(16), 2143-
2093 2146, 1995.
2094
2095 Slemr, F. and Langer, E.: Increase in global atmospheric concentrations of mercury inferred from
2096 measurements over the Atlantic Ocean, *Nature* **355**, 434 – 437, 1992.

2097 Slemr, F., W. Seiler, and G. Schuster, Latitudinal distribution of mercury over the Atlantic
2098 Ocean, J. Geophys. Res., 86, C2, 1159-1166, 1981.

2099 Soerensen, A. L., D. J. Jacob, D. G. Streets, M. L. I. Witt, R. Ebinghaus, R. P. Mason, M.
2100 Andersson, and E.M. Sunderland (2012), Multi-decadal decline of mercury in the North Atlantic
2101 atmosphere explained by changing subsurface seawater concentrations, Geophys. Res. Lett., 39,
2102 L21810, doi:10.1029/2012GL053736.
2103
2104 Soerensen, A. L., H. Skov, D. J. Jacob, B. T. Soerensen, M. S. Johnson, Global Concentrations
2105 of Gaseous Elemental Mercury and Reactive Gaseous Mercury in the Marine Boundary Layer,
2106 Environ Sci Technol., 44(19), 7425-30. doi: 10.1021/es903839n, 2010.
2107
2108 Sommar, J., M. E. Anersson, and H.-W. Jacobi, Circumpolar measurements of speciated mercury,
2109 ozone and carbon monoxide in the boundary layer of the Arctic Ocean, Atmos. Chem. Phys., 10,
2110 5031–5045, 2010.
2111
2112 Song, S., Selin, N. E., Soerensen, A. L., Angot, H., Artz, R., Brooks, S., Brunke, E.-G., Conley,
2113 G., Dommergue, A., Ebinghaus, R., Holsen, T. M., Jaffe, D. A., Kang, S., Kelley, P., Luke, W.
2114 T., Magand, O., Marumoto, K., Pfaffhuber, K. A., Ren, X., Sheu, G.-R., Slemr, F., Warneke, T.,
2115 Weigelt, A., Weiss-Penzias, P., Wip, D. C., and Zhang, Q.: Top-down constraints on
2116 atmospheric mercury emissions and implications for global biogeochemical cycling, Atmos.
2117 Chem. Phys., 15, 7103-7125, doi:10.5194/acp-15-7103-2015, 2015.
2118
2119 Song, X., Cheng, I., and Lu, J.: Annual atmospheric mercury species in downtown Toronto,
2120 Canada, J. Environ. Monit., 11(3), 660-669, 2009.
2121
2122 Sprovieri, F. and Pirrone, N., Spatial and temporal distribution of atmospheric mercury species
2123 over the Adriatic Sea, Environ. Fluid Mech., 8, 117–128, doi:10.1007/s10652-007-9045-4, 2008.
2124
2125 Sprovieri, F., I. M. Hedgecock, and N. Pirrone, An investigation of the origins of reactive
2126 gaseous mercury in the Mediterranean marine boundary layer, Atmos. Chem. Phys., 10, 3985–
2127 3997, 2010a.
2128
2129 Sprovieri, F., N. Pirrone, I. M. Hedgecock, M. S. Landis, and R. K. Stevens, Intensive
2130 atmospheric mercury measurements at Terra Nova Bay in Antarctica during November and
2131 December 2000, J. Geophys. Res., 107(D23), 4722, doi:10.1029/2002JD002057, 2002.

2132 Sprovieri, F., N. Pirrone, K. Gärfeldt, and J. Sommar, Mercury measurements in the marine
2133 boundary layer along a 6000 km cruise path around the Mediterranean Sea, Atmos. Environ., 37
2134 suppl., S63-S71, 2003.

2135 Sprovieri, F., Pirrone, N., Ebinghaus, R., Kock, H., and Dommergue, A.: A review of worldwide
2136 atmospheric mercury measurements, Atmos. Chem. Phys., 10(17), 8245-8265, 2010b.
2137

2138 Stamenkovic, J., Lyman, S., and Gustin, M. S.: Seasonal and diel variation of atmospheric
2139 mercury concentrations in the Reno (Nevada, USA) airshed, Atmos. Environ., 41(31), 6662-
2140 6672, 2007.
2141
2142 Steffen, A., Douglas, T., Amyot, M., Ariya, P., Aspmo, K., Berg, T., Bottenheim, J., Brooks, S.,
2143 Cobbett, F., Dastoor, A. and Dommergue, A.: A synthesis of atmospheric mercury depletion
2144 event chemistry in the atmosphere and snow, Atmos. Chem. Phys., 8(6), 1445-1482, 2008.
2145
2146 Steffen, A., Bottenheim, J., Cole, A., Douglas, T.A., Ebinghaus, R., Friess, U., Netcheva, S.,
2147 Nghiem, S., Sihler, H. and Staebler, R.: Atmospheric mercury over sea ice during the OASIS-
2148 2009 campaign, Atmos. Chem. Phys., 13, 7007–7021, 2013.
2149
2150 Strode, S. A., L. Jaegle, N. E. Selin, D. J. Jacob, R. J. Park, R. M. Yantosca, R. P. Mason, and F.
2151 Slemr (2007), Air-sea exchange in the global mercury cycle, Global Biogeochem. Cycles, 21,
2152 GB1017, doi:10.1029/2006GB002766.
2153
2154 Subir, M., Ariya, P. A., and Dastoor, A. P.: A review of uncertainties in atmospheric modeling of
2155 mercury chemistry I. Uncertainties in existing kinetic parameters – fundamental limitations and
2156 the importance of heterogeneous chemistry, Atmos. Environ., 45, 5664–5676, 2011.

2157 Swartzendruber, P. C., D. Chand, D. A. Jaffe, J. Smith, D. Reidmiller, L. Gratz, J. Keeler, S.
2158 Strode, L. Jaegle, and R. Talbot (2008), Vertical distribution of mercury, CO, ozone, and aerosol
2159 scattering coefficient in the Pacific Northwest during the spring 2006 INTEX-B campaign, J.
2160 Geophys. Res., 113, D10305, doi:10.1029/2007JD009579.
2161
2162 Swartzendruber, P.C., Jaffe, D.A., Prestbo, E.M., Weiss-Penzias, P., Selin, N.E., Park, R., Jacob,
2163 D.J., Strode, S. and Jaegle, L.: Observations of reactive gaseous mercury in the free troposphere
2164 at the Mount Bachelor Observatory, J. Geophys. Res. Atmos., 111(D24301),
2165 doi:10.1029/2006JD007415, 2006.
2166
2167 Talbot, R., H. Mao, E. Scheuer, J. Dibb, and M. Avery (2007), Total Depletion of Hg° in the
2168 Upper Troposphere - Lower Stratosphere, *Geophys. Res. Lett.*, 34, L23804,
2169 doi:10.1029/2007GL031366.
2170
2171 Talbot, R., H. Mao, E. Scheuer, J. Dibb, M. Avery, E. Browell, G. Sachse, S. Vay, D. Blake, G.
2172 Huey, and H. Fuelberg (2008), Factors influencing the large-scale distribution of Hg° in the
2173 Mexico City area and over the North Pacific, *Atmos. Chem. Phys. 8*, 2103-2114.
2174
2175 Temme, C., F. Slemr, R. Ebinghaus, J.W. Einax, Distribution of mercury over the Atlantic Ocean
2176 in 1996 and 1999–2001, Atmos. Environ., 37, 1889–1897, 2003a.
2177
2178 Temme, C., J.W. Einax , R. Ebinghaus, and W. H. Schroeder, Measurements of mercury species
2179 at a coastal site in the Antarctic and over the South Atlantic Ocean in the polar summer, Environ.
2180 Sci. Technol., 37, 1, 22 – 31, 2003b.
2181

2182 Timonen, H., J. L. Ambrose, and D. A. Jaffe, Oxidation of elemental Hg in anthropogenic and
2183 marine airmasses, Atmos. Chem., Phys., 13, 2827–2836, 2013.
2184
2185 Tseng, C.M., C.S. Liu, and C. Lamborg (2012) Seasonal changes in gaseous elemental mercury
2186 in relation to monsoon cycling over the northern South China Sea, *Atmospheric Chemistry and*
2187 *Physics*, 12, 7341-7350.
2188
2189 Turekian, V. C.; Van Dingenen, R. Inorganic bromine in the marine boundary layer: a critical
2190 review, *Atmos. Chem. Phys*., *3*, 1301-1336, 2003.
2191
2192 UNEP, Global Mercury Assessment 2013: Sources, Emissions, Releases and Environmental
2193 Transport. UNEP Chemicals Branch, Geneva, Switzerland, 2013.
2194
2195 Valente, R. J., Shea, C., Humes, K. L., and Tanner, R. L.: Atmospheric mercury in the Great
2196 Smoky Mountains compared to regional and global levels, Atmos. Environ., 41(9), 1861-1873,
2197 2007.
2198
2199 Wan, Q., Feng, X., Lu, J., Zheng, W., Song, X., Han, S., and Xu, H.: Atmospheric mercury in
2200 Changbai Mountain area, northeastern China I. The seasonal distribution pattern of total gaseous
2201 mercury and its potential sources, Environ. Res., 109(3), 201-206, 2009a.
2202
2203 Wan, Q., Feng, X., Lu, J., Zheng, W., Song, X., Li, P., Han, S. and Xu, H., Atmospheric mercury
2204 in Changbai Mountain area, northeastern China II. The distribution of reactive gaseous mercury
2205 and particulate mercury and mercury deposition fluxes, Environ. Res., 109(6), 721-727, 2009b.
2206
2207 Wang, F., A. Saiz-Lopez, A. S. Mahajan,, J. C. Gómez Martín,, D. Armstrong, M. Lemes, T.
2208 Hay, and C. Prados-Roman, Enhanced production of oxidised mercury over the tropical Pacific
2209 Ocean: a key missing oxidation pathway, Atmos. Chem. Phys., 14, 1323–1335, 2014。
2210
2211 Wang, Y., Huang, J., Hopke, P. K., Rattigan, O. V., Chalupa, D. C., Utell, M. J., and Holsen, T.
2212 M.: Effect of the shutdown of a large coal-fired power plant on ambient mercury species,
2213 Chemosphere, 92(4), 360-367, 2013.
2214
2215 Weigelt, A., Ebinghaus, R., Manning, A. J., Derwent, R. G., Simmonds, P. G., Spain, T. G.,
2216 Jennings, S. G., and Slemr, F.: Analysis and interpretation of 18 years of mercury observations
2217 since 1996 at Mace Head at the Atlantic Ocean coast of Ireland, Atmos. Environ. 100, 85–93,
2218 2015.
2219
2220 Weiss-Penzias, P. S., E. J. Williams, B. M. Lerner, T. S. Bates, C. Gaston, K. Prather, A.
2221 Vlasenko, and S. M. Li (2013), Shipboard measurements of gaseous elemental mercury along the
2222 coast of Central and Southern California. J. Geophys. Res. Atmos., 118, 208–219,
2223 doi:10.1029/2012JD018463.
2224
2225 Weiss-Penzias, P., Amos, H.M., Selin, N.E., Gustin, M.S., Jaffe, D.A., Obrist, D., Sheu, G.R.
2226 and Giang, A.: Use of a global model to understand speciated atmospheric mercury observations
2227 at five high-elevation sites, Atmos. Chem. Phys., 15(3), 1161-1173, 2015.

Weiss-Penzias, P., D. A. Jaffe, A. McClintick, E. M. Presbo, and M. S. Landis, Gaseous elemental mercury in the Marine Boundary Layer: Evidence for rapid removal in anthropogenic pollution, Environ. Sci. Technol., 3755 – 3763, 37, 2003.

Weiss-Penzias, P., Gustin, M. S., and Lyman, S. N.: Observations of speciated atmospheric mercury at three sites in Nevada: Evidence for a free tropospheric source of reactive gaseous mercury, J. Geophys. Res. Atmos., 114(D14), 2009.

Weiss-Penzias, P., Jaffe, D., Swartzendruber, P., Hafner, W., Chand, D., and Prestbo, E.: Quantifying Asian and biomass burning sources of mercury using the Hg/CO ratio in pollution plumes observed at the Mount Bachelor Observatory, Atmos. Environ., 41(21), 4366-4379, 2007.

Weiss-Penzias, P.S., Gay, D.A., Brigham, M.E., Parsons, M.T., Gustin, M.S. and ter Schure, A.: Trends in mercury wet deposition and mercury air concentrations across the US and Canada. Sci. Total Environ., in press, 2016.

Williston, S. H. *(*1968*),* Mercury in the atmosphere, J. Geophys. Res., *73(*22*),* 7051–7055, *doi:*10.1029/JB073i022p07051.

Witt, M. L. I., Mather, T. A., Baker, A. R., De Hoog, J. C. M., and Pyle, D. M.: Atmospheric trace metals over the south-west Indian Ocean: total gaseous mercury, aerosol trace metal concentrations and lead isotope ratios, Mar. Chem., 121, 2–16, 2010.

Witt, M. L. I., Meheran, N., Mather, T. A., De Hoog, J. C. M., and Pyle, D. M.: Aerosol trace metals, particle morphology and total gaseous mercury in the atmosphere of Oxford, UK, Atmos. Environ., 44(12), 1524-1538, 2010.

Xia, C., Z. Xie, and L. Sun, Atmospheric mercury in the marine boundary layer along a cruise path from Shanghai, China to Prydz Bay, Antarctica, Atmos. Environ., 44, 1815-1821, 2010.

Xiu, G., Cai, J., Zhang, W., Zhang, D., Büeler, A., Lee, S., Shen, Y., Xu, L., Huang, X. and Zhang, P.: Speciated mercury in size-fractionated particles in Shanghai ambient air, Atmos. Environ., 43(19), 3145-3154, 2009.

Xu, L., Chen, J., Yang, L., Niu, Z., Tong, L., Yin, L., and Chen, Y.: Characteristics and sources of atmospheric mercury speciation in a coastal city, Xiamen, China, Chemosphere, 119, 530-539, 2015.

Xu, X. and Akhtar, U. S.: Identification of potential regional sources of atmospheric total gaseous mercury in Windsor, Ontario, Canada using hybrid receptor modeling, Atmos. Chem. Phys., 10(15), 7073-7083, 2010.

Xu, X., Akhtar, U., Clark, K., and Wang, X.: Temporal variability of atmospheric total gaseous mercury in Windsor, ON, Canada, Atmosphere, 5(3), 536-556, 2014.

2274 Yang, Y., Chen, H., and Wang, D.: Spatial and temporal distribution of gaseous elemental
2275 mercury in Chongqing, China, Environ. Monit. Assess., 156(1-4), 479-489, 2009.
2276
2277 Yatavelli, R. L., Fahrni, J. K., Kim, M., Crist, K. C., Vickers, C. D., Winter, S. E., and Connell,
2278 D. P.: Mercury, PM 2.5 and gaseous co-pollutants in the Ohio River Valley region: Preliminary
2279 results from the Athens supersite, Atmos. Environ., 40(34), 6650-6665, 2006.
2280
2281 Yu, J. et al., High variability of atmospheric mercury in the summertime boundary layer through
2282 the central Arctic Ocean. Scientific Reports, 4, 6091, DOI:10.1038/srep06091, 2014.
2283
2284 Zhang, H., Fu, X. W., Lin, C.-J., Wang, X., and Feng, X. B.: Observation and analysis of
2285 speciated atmospheric mercury in Shangri-La, Tibetan Plateau, China, Atmos. Chem. Phys., 15,
2286 653-665, doi:10.5194/acp-15-653-2015, 2015.
2287
2288 Zhang L., Blanchard P., Johnson D., Dastoor A., Ryzhkov A., Lin C.-J., Vijayaraghavan K., Gay
2289 D., Holsen T.M., Huang J., Graydon J.A., St. Louis V.L., Castro M.S., Miller E.K., Marsik F.,
2290 Lu J., Poissant L., Pilote M., and Zhang K.M., 2012. Assessment of modelled mercury
2291 deposition over the Great Lakes region. Environmental Pollution, 161, 272-283.
2292
2293 Zhang, L., Wang, S. X., Wang, L., and Hao, J. M.: Atmospheric mercury concentration and
2294 chemical speciation at a rural site in Beijing, China: implications of mercury emission sources,
2295 Atmos. Chem. Phys., 13(20), 10505-10516, 2013.
2296
2297 Zhang, Y., Jacob, D.J., Horowitz, H.M., Chen, L., Amos, H.M., Krabbenhoft, D.P., Slemr, F., St.
2298 Louis, V.L. and Sunderland, E.M.: Observed decrease in atmospheric mercury explained by
2299 global decline in anthropogenic emissions, Proceed. Natl, Acad. Sci., 113(3), 526-531, 2016.
2300
2301 Zhu, J., Wang, T., Talbot, R., Mao, H., Hall, C.B., Yang, X., Fu, C., Zhuang, B., Li, S., Han, Y.
2302 and Huang, X.: Characteristics of atmospheric total gaseous mercury (TGM) observed in urban
2303 Nanjing, China, Atmos. Chem. Phys., 12(24), 12103-12118, 2012.
2304
2305 Zielonka, U., Hlawiczka, S., Fudala, J., Wängberg, I., and Munthe, J.: Seasonal mercury
2306 concentrations measured in rural air in Southern Poland: Contribution from local and regional
2307 coal combustion, Atmos. Environ., 39(39), 7580-7586, 2005.
2308
2309
2310
2311
2312
2313
2314
2315
2316
2317
2318

Atmos. Chem. Phys. Discuss., doi:10.5194/acp-2016-563, 2016
Manuscript under review for journal Atmos. Chem. Phys.
Published: 21 July 2016

Atmospheric Chemistry and Physics Discussions

2319 Table 1: Summary of predominant temporal patterns of speciated atmospheric mercury at
2320 continental sites in the northern hemisphere

	Diurnal variation	Seasonal variation
TGM/GEM		
Rural	Daytime maximum, nighttime minimum	Winter-spring maximum and summer-fall minimum
Urban	Nighttime maximum, daytime minimum	No predominant pattern
High elevation	Daytime maximum, nighttime minimum	Winter-spring maximum and summer-fall minimum
GOM		
Rural	Midday to late afternoon maximum, nighttime minimum	No predominant pattern
Urban		Spring or summer maximum
High elevation	*Exception: nighttime maximum at urban and elevated sites	No predominant pattern
PBM		
Rural	No predominant pattern	Maximum during heating season
Urban	No predominant pattern	Maximum during heating season *Exception: summer maximum
High elevation	No predominant pattern	Maximum during heating season

2321
2322

Atmos. Chem. Phys. Discuss., doi:10.5194/acp-2016-563, 2016
Manuscript under review for journal Atmos. Chem. Phys.
Published: 21 July 2016

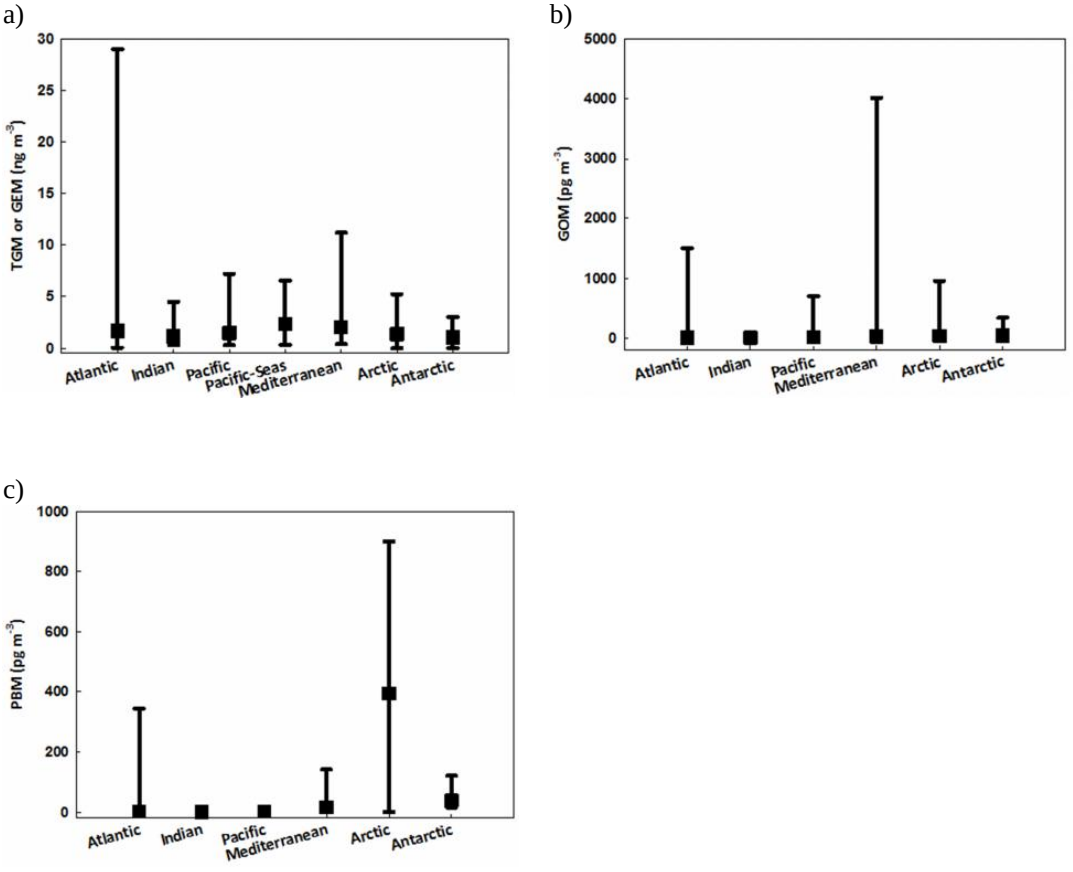

Figure 1. Mean and ranges of TGM/GEM (a), GOM (b), and PBM (c) concentrations, estimated from the values in the literature as shown in Tables S1 – S3, over the Atlantic, Indian, Pacific, seas over the West Pacific (denoted as Pacific-Seas, only TGM/GEM in this category), seas in the Mediterranean region (denoted as Mediterranean), Arctic, and Antarctica Ocean. The solid black squares represent the mean value and the lowest whisker the minimum and the largest the maximum concentration in the region.

Atmos. Chem. Phys. Discuss., doi:10.5194/acp-2016-563, 2016
Manuscript under review for journal Atmos. Chem. Phys.
Published: 21 July 2016

Atmospheric Chemistry and Physics Discussions

2329
2330

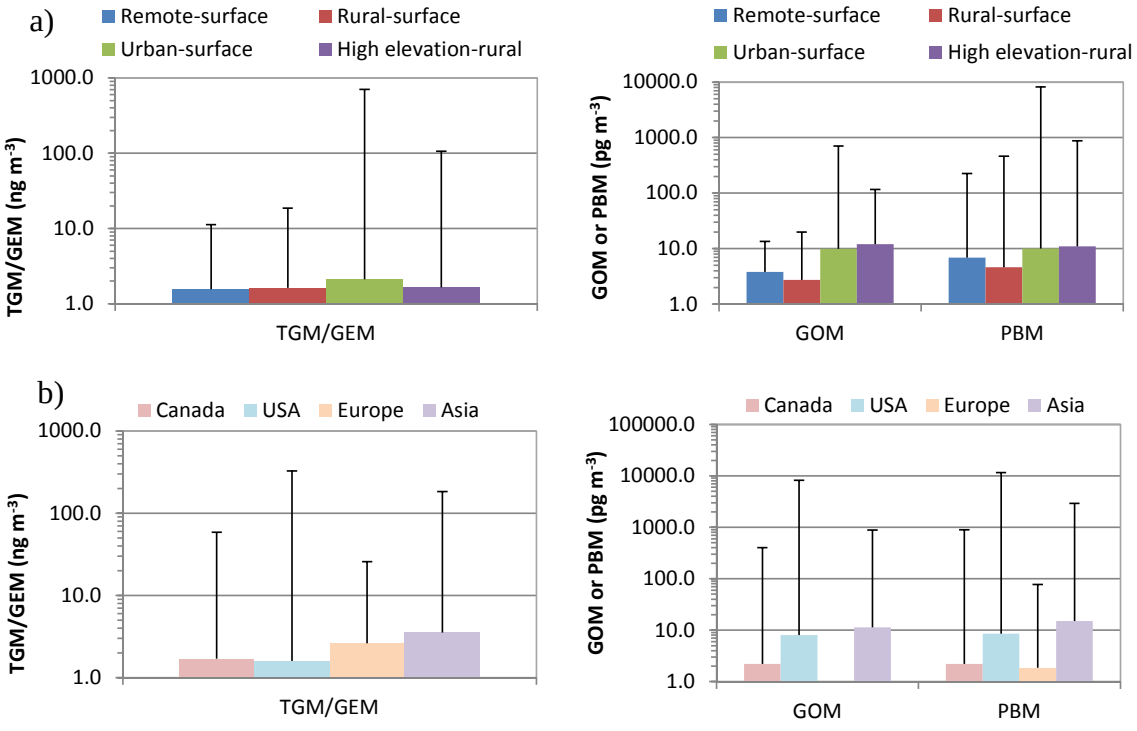

2331
2332
2333
2334
2335

2336 Figure 2. Median and range in TGM/GEM, GOM and PBM by site category (a) and by
2337 geographical region (b). Bar graph represents the median and error bar represents the maximum,
2338 estimated from the values in the literature as shown in Tables S4 – S6.

2339
2340
2341
2342

Atmos. Chem. Phys. Discuss., doi:10.5194/acp-2016-563, 2016
Manuscript under review for journal Atmos. Chem. Phys.
Published: 21 July 2016

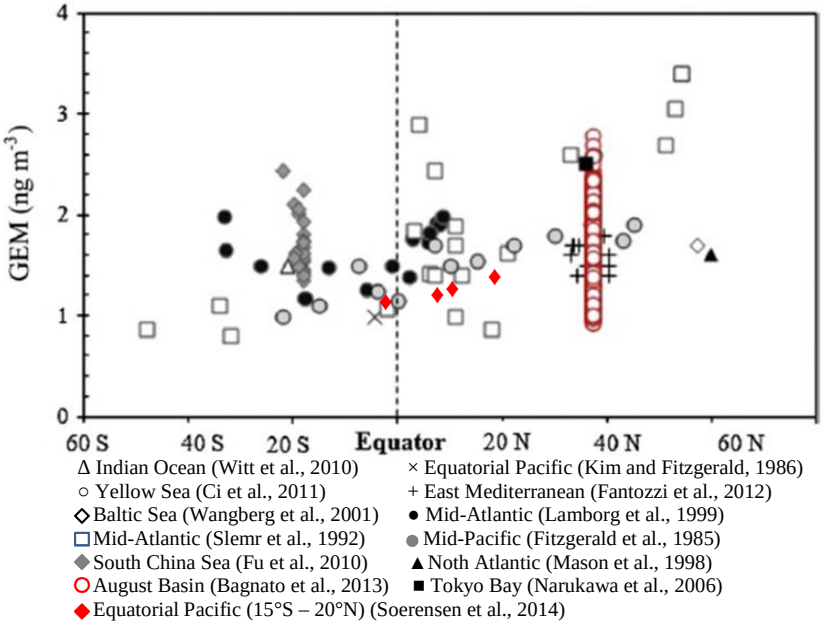

Figure 3. Compiled values for several marine/oceanic environmental systems. GEM over the Augusta basin is in red open circles. (Based on the figure from Bagnato et al., 2013)

Atmos. Chem. Phys. Discuss., doi:10.5194/acp-2016-563, 2016
Manuscript under review for journal Atmos. Chem. Phys.
Published: 21 July 2016

2373
2374
237

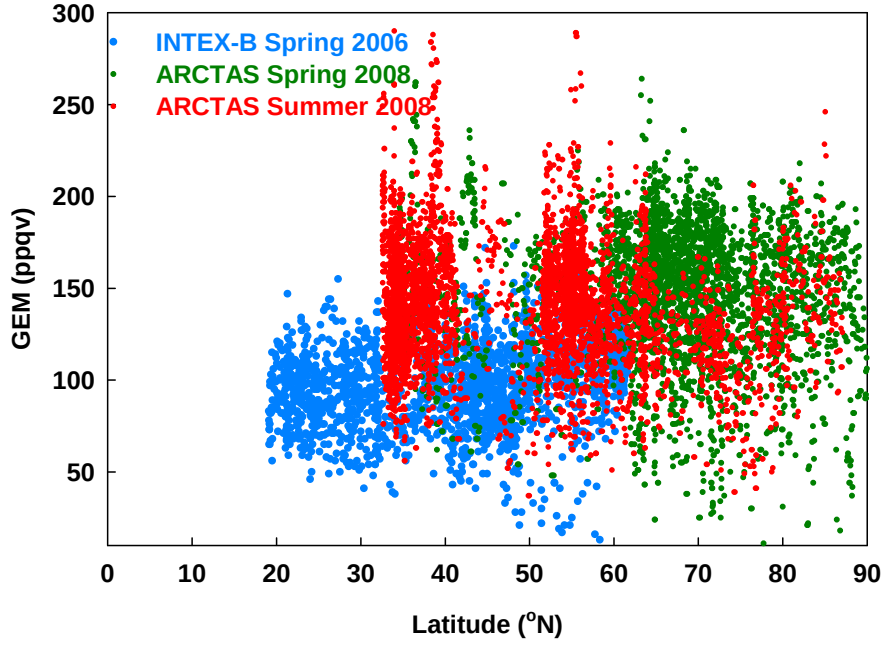

Figure 4. GEM (ppqv) from the INTEX-B in spring 2006 and ARCTAS in spring and summer 2008 (Data sources: Talbot et al., 2007, 2008; Mao et al., 2010).